NASA TECHNICAL TRANSLATION

NASA TT F-15,662

LIGHT SCATTERING IN SEAWATER. EXPERIMENTAL RESULTS AND THEORETICAL APPROACH

André Morel

Translation of "Diffusion de la lumiere par les eaux de mer. Resultats experimentaux et approche theorique," in Optics of the Sea (Interface and In-water Transmission and Imaging), Advisory Group for Aerospace Research and Development, Neuilly-sur-Seine, France, AGARD LS-61, August 1973, pp. 3.1-1 to 3.1-76

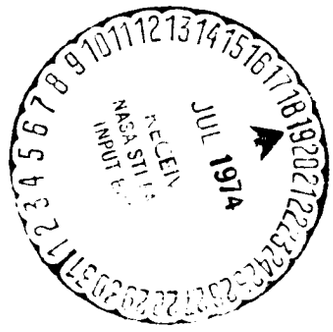

NATIONAL AERONAUTICS AND SPACE ADMINISTRATION
WASHINGTON, D.C. 20546
JULY 1974

(NASA-TT-F-15662) LIGHT SCATTERING IN SEAWATER. EXPERIMENTAL RESULTS AND THEORETICAL APPROACH (Kanner (Leo) Associates) 153 p HC $10.75 CSCL 20F

N74-28133

Unclas
G3/23 42719

STANDARD TITLE PAGE

1. Report No.	2. Government Accession No	3 Recipient's Catalog No.
NASA TT F-15,662		

4. Title and Subtitle	5. Report Date
LIGHT SCATTERING IN SEAWATER. EXPERIMENTAL RESULTS AND THEORETICAL APPROACH	July 1974
	6. Performing Organization Code

7. Author(s)	8. Performing Organization Report No.
André Morel, University of Paris, Physical Oceanography Laboratory, Center of Oceanographic Research, Villefranche	10. Work Unit No.

9. Performing Organization Name and Address	11. Contract or Grant No.
Leo Kanner Associates, P.O. Box 5187 Redwood City, California 94063	NASw-248
	13. Type of Report and Period Covered
12. Sponsoring Agency Name and Address	Translation
NATIONAL AERONAUTICS AND SPACE ADMINISTRATION, WASHINGTON, D.C. 20546	14. Sponsoring Agency Code

15. Supplementary Notes

Translation of "Diffusion de la lumiere par les eaux de mer. Resultats experimentaux et approche theorique," in Optics of the Sea (Interface and In-water Transmission and Imaging), Advisory Group for Aerospace Research and Development, Neuilly-sur-Seine, France, AGARD LS-61, August 1973, pp. 3.1-1 to 3.1-76.

16. Abstract The general shape of the scattering indicatrix for seawater is discussed with attention to possible variations at mean angles and the special case of small angles. The respective roles of molecular and particle scattering are examined separately throughout the discussion, since seawater must be considered an optically disturbed medium. The influence of wavelength on the indicatrix, scattering selectivity, and variations in the rate of polarization are also examined. For purposes of simplification, a detailed discussion of scattering by particles is based on the assumption of spherical particle shape. This is followed by a discussion of scattering by a system of polydispersed spherical particles. An attempt is made to determine the most rational numerical values to be assigned to the various factors influencing the phenomenon. The influence of the exponent of the law of distribution and that of the index of refraction on the indicatrix are analyzed, and rational values are assigned to these factors. The roles of various classes of particles, according to size, are compared and the dependence of scattering on the spectrum is analyzed.

17. Key Words (Selected by Author(s))	18. Distribution Statement
	Unclassified - Unlimited

19. Security Classif. (of this report)	20. Security Classif. (of this page)	21. No. of Pages	22. Price
Unclassified	Unclassified	151	

Foreword

There has always been increasing practical motivation for study of light scattering in seawater, despite the fact that this field sometimes seems to be merely speculative. Overall, this phenomenon reflects a characteristic of seawater which is essential from the standpoint of sedimentology or geochemistry, or again, biology: the concentration of particulate matter in suspension. Scattering is actually a spatial redistribution of energy which does not proceed by chance, but rather in conformity with a law which precisely describes the "scattering indicatrix." Determination of this factor, in conjunction with its theoretical interpretation, permits the possibility of obtaining information on the particles and their properties which will complement that obtained with somewhat greater difficulty by direct observation.

In addition, all problems of oceanographic optics, including the propagation, or more generally, the radiative transfer of radiation, and the destruction of contrasts, that is, of images -- whether treated experimentally or theoretically -- all these problems imply a knowledge of the index of diffusion. Some cases involve the influence of properties such as backscattering or scattering, on the other hand, in the vicinity of the direction of propagation, which are difficult to evaluate by simple experimentation; in these cases, theoretical analysis may be of equal or even greater value.

The following text is divided into three principal parts. The first deals solely with experimental findings, while the second indicates how theory may be used and how it is expressed. Finally, the third part deals conjointly with the experimental and theoretical results and is directed toward their interpretation and application.

In order to simplify the text itself, definitions and certain numerical aspects of the computations performed on a computer are dealt with in two appendices. Similarly, to avoid overburdening the bibliography, references to original works relating to those designated under the theories of Rayleigh, Rayleigh-Gans and Mie have been omitted. All these references are in effect replaced by a single entry: the now-classical work by H.C. Van de Hulst (1957), which encompasses them all.

Note: Each figure is given two numbers, the first being I, II or III, depending on whether it appears in the first, second or third part. Equations are numbered only in the second part, again with two figures, the first being 1, 2 or 3, depending on whether they appear in Chapter 1, 2 or 3 of this part.

Table of Contents

Part 1

Introduction

1. Scattering Indicatrix of Seawater

1.1. General Shape
1.2. Possible Variations at Mean Angles
1.3. Case of Small Angles ($\theta < 30°$)

2. Role of Molecular Scattering

2.1. Review of Useful Values for Water and Seawater
2.2. Relative Importance of Molecular Scattering

3. Particle Scattering Indicatrix

3.1. Results
3.2. Adoption of a "Typical" Particle Indiactrix

4. Influence of Wavelength

4.1. Variations in the Shape of the Indicatrix
4.2. Scattering Selectivity
4.2.1. Volume Scattering Functions
4.2.2. Total Scattering Coefficient

5. Polarization

5.1. Results
5.2. Variability of Rate of Polarization at 90°

6. Relationships between Scattering Coefficients

Part 2

Introduction

1. States of Polarization and Scattering

1.1. Description of State of Polarization by Stokes Parameters
1.2. Scattering Matrices

2. Scattering by a Spherical Particle

2.1. Formulation of the Mie Theory
2.1.1. The Functions π_n, τ_n and a_n, b_n

2.1.2. The Intensity Functions $i_1(\theta)$ and $i_2(\theta)$
2.2. Numerical Results and Interpretation
2.2.1. The Functions $i_T(\theta)\alpha^{-4}$
2.2.2. Rayleigh Scattering Range
2.2.3. Rayleigh-Gans Approximation
2.2.4. Approximation by Diffraction Theory
2.2.5. Role of Refraction and Reflection
2.2.6. General Remarks on the Asymmetry of the Indicatrix
2.2.7. Total Scattering Coefficient. Efficiency Factor
2.2.8. Efficiency Factor and Intensity at 0°. Limiting Values (Diffraction)
2.2.9. Van de Hulst Approximation
2.2.10. Efficiency Factor in the Rayleigh and Rayleigh-Gans Ranges

3. Scattering by a System of Polydispersed Particles

3.1. Calculation of Scattering Properties
3.1.1. Scattering Indicatrix for a Given Number of Particles
3.1.2. Mean Efficiency Factor
3.1.3. Normalized Indicatrix
3.2. Predictions of Results of Computation
3.2.1. Convergence Conditions: INfluence of the Upper Limit on the Indicatrix
3.2.2. Role of Small Particles: Influence of the Lower Size Limit on the Indicatrix
3.2.3. Total Scattering; Influence of Limits on Computations
3.2.4. Summary Dealing with Range of Validity of Calculations
3.2.5. Extension of Distribution Laws Differing from the Junge Law

Part 3

Introduction

1. Theoretical Variations in the Indicatrix

1.1. Influence of the Exponent of the Law of Distribution on the Indicatrix
1.2. Influence of the Index of Refraction on the Indicatrix
1.3. Conclusions To Be Drawn from Theoretical Variations in the Indicatrix

2. Interpretation of Observations and Applications

2.1. Application of Criteria to the Index and the Exponent of the Law of Distribution. Ratio of Angular Coefficients

2.2. Relationships between $\beta(45°)$ or $\beta(90°)$ and b
2.3. Characteristic Properties of Coefficients $\beta(4°)$ and $\beta(6°)$
2.4. Rational Values for Index of Refraction and Exponent of Law of Distribution
2.4.1. Comparison of Indicatrices
2.4.2. Initial Observation on Rational Limits of Distribution

3. Other Conclusions and Applications of Theoretical Computations

3.1. Different Roles of Various Classes of Particles
3.1.1. Case of Total Scattering
3.1.2. Case of Angular Scatte Coefficients
3.1.3. Specific Case of the Angle 0°
3.2. Dependence of Scattering on the Spectrum
3.2.1. General Case: Selectivity in the Case of an Unlimited Junge Distribution
3.2.2. Modification in the Case of Non-Unlimited Distribution
3.2.3. Shape of Indicatrix and Wavelength
3.3. Polarization
3.3.1. Influence of Limits and Interpretation
3.3.2. Conclusions; Second Observation on the Value of the Limits
3.4. Relationships between Scattering and Particle Content
3.4.1. General Observation on Possible Variations in the Mean Efficiency Factor $\bar{Q}$
3.4.2. Examples of Application

Conclusion

Appendix 1: Definitions, followed by Principal Symbols Used

Appendix 2: Computation Procedure and Adaptation to Computer

1. Calculation of Individual Indicatrices by Mie Theory
2. Computation for Polydispersed Systems

References

LIGHT SCATTERING IN SEAWATER.
EXPERIMENTAL RESULTS AND THEORETICAL APPROACH

André Morel
University of Paris, Physical Oceanography Laboratory,
Center of Oceanographic Research, Villefranche-sur-Mer

/3.1-4*

Introduction

The propagation of light radiation in any medium other than a vacuum is accompanied by two phenomena which determine the attenuation of the flux: absorption and scattering. The energy absorbed is converted into heat, or may be partially re-emitted by fluorescence or the Raman effect, but with a change in wavelength. The scattered energy, on the other hand, is not transformed, but is merely dispersed in space. If the medium is "optically pure," scattering is provoked by the molecules themselves and by them alone. In "disturbed" mediums, scattering of particles in suspension is added to the molecular scattering. Even in its purest state, seawater behaves as an optically disturbed medium for visible radiation; as a result, it will be necessary to examine the respective roles of molecular scattering and particle scattering with reference to each problem considered, whether it concerns the total scattering coefficient or the volume scattering function, the shape of the indicatrix, selectivity, or polarization.

All the useful definitions are given in Appendix 1.

1. Scattering Indicatrix of Seawater

1.1. General Shape

During the same year (1963), N.G. Jerlov and S.Q. Duntley independently made systematic reviews of the scattering indicatrix measurements for seawater which had been performed so far. The results compared by these investigators were obtained with different devices, some operating in situ and others necessitating sampling and decanting of the sample; some made use of white light and others of filtered radiation (blue, blue-green, green, yellow); moreover, the results concerned water with extremely diverse characteristics as to turbidity and origin (Pacific Ocean, Atlantic Ocean, English Channel, China Sea, and even lakes). Reaching identical conclusions at the end of this comparison, N.G. Jerlov and S.Q. Duntley noted the very significant fact illustrated by Fig. I.1: all the measurements are in agreement for angles less than 90°, thus showing that the shape

*Numbers in the margin indicate pagination in the foreign text. Hereafter, only the final digit(s) -- i.e. after the dash -- will be indicated.

of the scattering indicatrix varies little from one type of seawater to the next and is extremely asymmetrical in all cases. For angles greater than 90° greater dispersion may be noted. In another connection, the angle at which scattering is minimal varies from approximately 100° to 130° depending on the case, the minimum itself being more or less marked.

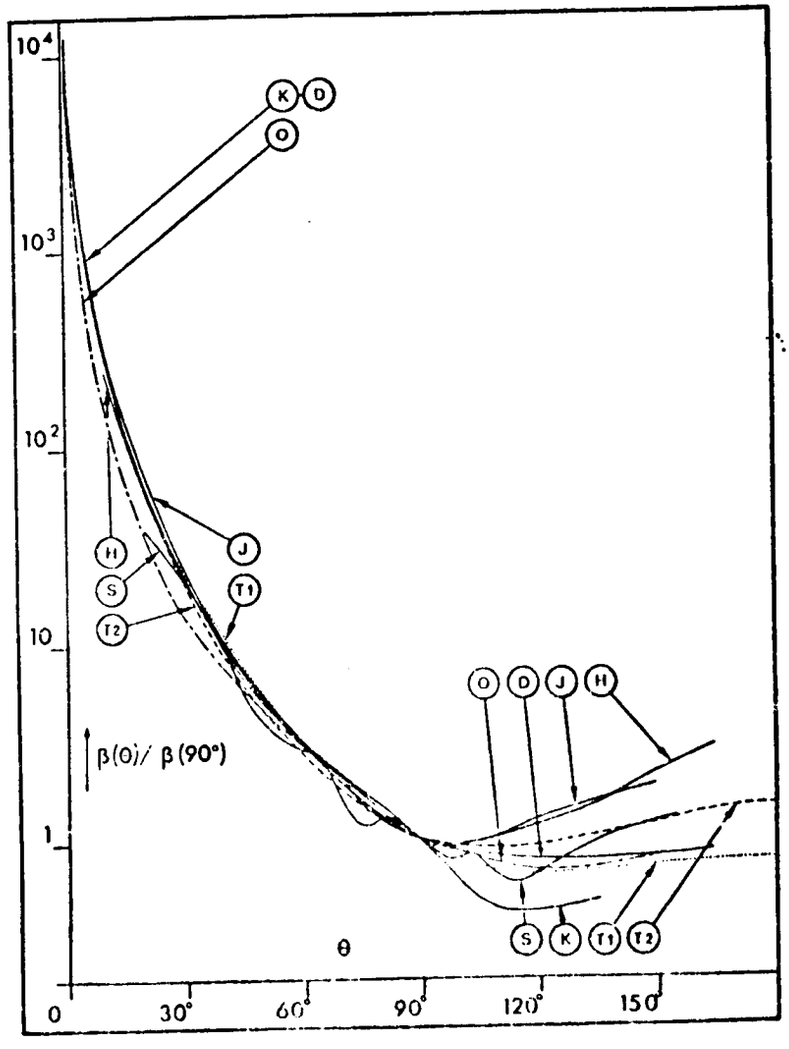

Fig. I.1. Scattering indicatrices obtained by various investigators, normalized to 90°.
H: E.O. Hulburt (1945), Chesapeake Bay;
K: M. Kozlianinov (1957), China Sea;
S: T. Sasaki (1960), Japanese trench;
J: N.G. Jerlov (1961), Atlatic (Madeira);
[Caption continued on following page.]

Fig. I.1, continued:

T_1/T_2: J.E. Tyler (1961), Pacific (San Diego);
D: S.Q. Duntley (1963), Lake Winnipesakee;
O: Y.E. Otchakovski (1965), Mediterranean

It should be noted that the measurements made by Pickard and Giovando (1960) on water which may afford a special case (fjord of British Columbia) diverge considerably from the overall results, the increase toward small angles being more marked. The measurements made by Sasaki et al. (1960) also diverge from the other findings to some degree since they reveal slight undulations. Mankovsky et al. (1970) have also detected such special characteristics. In a very general manner, however, subsequent analyses have consistently confirmed the broad tendencies drawn from an examination of these initial measurements. /5

1.2. Possible Variations at Mean Angles ($\theta > 30°$)

In reality, a large number of tests performed on water of much more varied type from the standpoint of clearness have revealed that the shape of the indicatrix for seawater may vary considerably within the range of mean angles. Figure I.2 gives an example (the curves are normalized to 90°, since it is also necessary to show changes in shape without bringing the magnitude of the indicatrix into play). Without giving a large number of examples, Fig. I.2 roughly summarizes the variations in the indicatrix which may occur within this range of angles. Curve 3 shows the most symmetrical shape which could be observed, corresponding to extremely pure deep water (identical shapes have been obtained below 1000 or 2000 meters both in the Eastern Mediterranean -- laboratory team, 1969 -- and in the Madeira region); curve 2 is an intermediate curve which is frequently observed with reference to the "blue" surface water of oceans; and curve 1 is the predominant curve for a number of types of surface water and coastal waters. The asymmetry is slightly more marked for the waters of the Baltic Sea (Station 2, G. Kullenberg (1967), $b_{525} = 0.76_{m-1}$). Curve 5, based on measurements made by T.J. Petzold (1972) falls between cases 2 and 3.

Systematic analysis of the shape of the indicatrix leads to the following conclusion: between the two extreme cases shown, that is, from the extremely asymmetrical shapes such as that of curve 1 to the most symmetrical shape, that of curve 3, the various intermediate shapes for the indicatrix are not randomly distributed. The tendency toward symmetry actually occurs /6

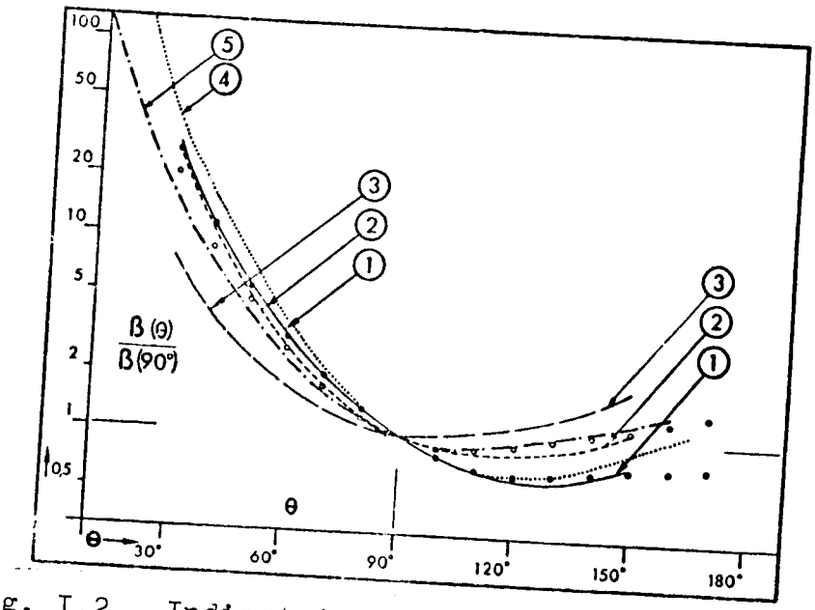

Fig. I.2. Indicatrices normalized to 90°.
1. English channel (surface, Roscoff, 6/29/63, $b > 0.6$ m^{-1}, $\lambda = 546$ nm);
2. Mediterranean (surface, Villefranche Bay, 11/16/63, $b \sim 0.1$ m^{-1}, $\lambda = 546$ nm);
3. Mediterranean (1500 m, Tyrrhenian Sea, 7/21/64, $b \sim 0.015$ m^{-1}, $\lambda = 546$ nm); (see also A. Morel, 1965);
4. Baltic Sea (5 m, Station 2, 6/13/67, $b = 0.76$ m^{-1}, $\lambda = 525$ nm, G. Kullenberg, 1967);
5. Atlantic (1500 m, Tongue of the Ocean, 7/13/71, $b = 0.037$ m^{-1}, $\lambda = 510$ nm, T.J. Petzold, 1972).

Black points and circles stations,1 and 2 respectively (T_1 and T_2 of the preceding figure.) (Pacific, J.E. Tyler, 1961).

gradually, to the degree that the scattering capability of the water decreases, and thus to the degree that the volume functions decrease in absolute value. With a satisfactory approximation, and taking experimental uncertainty into account, this orderly arrangement of indicatrices was checked by tests of more than 150 samples taken from widely separated areas (English Channel, Atlantic Ocean, Mediterranean Ocean, Indian Ocean). The most marked irregularities (for such irregularities did occur)pertained almost exclusively to backscattering (more precisely, $\theta > 120°$). This gradual transformation is also illustrated (Fig. I.3) by the approximately regular variation in the ratio of asymmetry $\beta(45°)/\beta(135°)$. This ratio decreases from a neighboring value

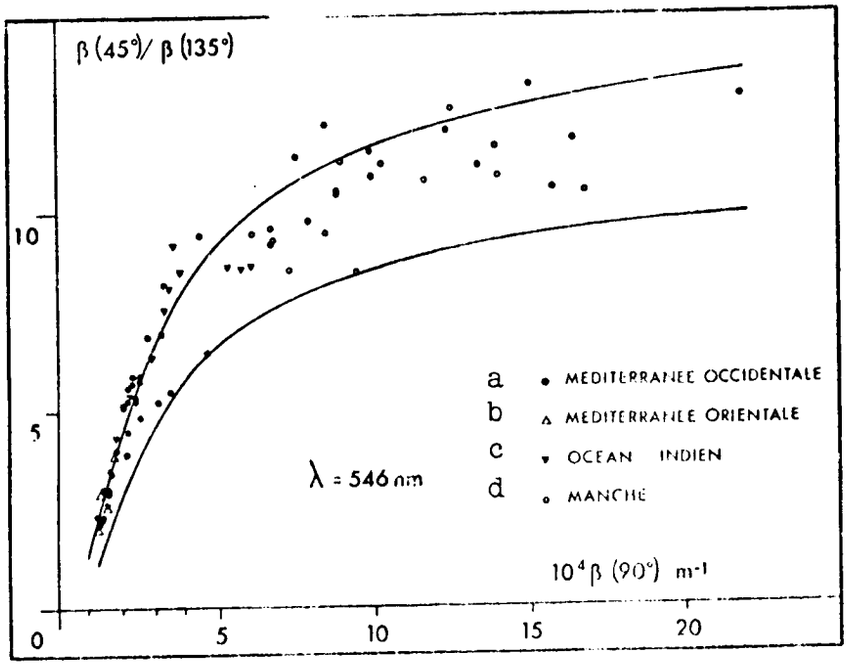

Fig. I.3. $\beta(45°)/\beta(135°)$ ratio characterizing the asymmetry of the indicatrix for seawater, expressed as a function of $\beta(90°)$ for various types of seawater (λ = 546 nm). From the expression relating $\beta(\theta)$ to $\beta(90°)$, this ratio can easily be found to be:

$$\frac{\beta(45)}{\beta(135)} = \frac{R(45)\ (\beta(90) + \text{Const}}{R(135)\ (\beta(90) + \text{Const}}$$

and varies with $\beta(90)$ according to a hyperbolic law. Two hyperbolas are plotted on the basis of the average values (upper curve) or extreme values (lower curve) assigned to R(45) and R(135).

Key: a. Western Mediterranean
b. Eastern Mediterranean
c. Indian Ocean
d. English Channel

on the order of 12 to reach values as low as 2 when the water changes from an extremely scattered state to extreme clearness. In Fig. I.3 and in all subsequent cases the unit indicated for the volume functions is m^{-1}, and not m^{-1} steradian^{-1}, as it should more properly be stated (this expression remains understood and was omitted for convenience).

Since turbid waters show relatively similar and extremely asymmetrical indicatrices, since only "clear" waters result in varied and more symmetrical shapes, it is logical to attribute this change at least partially to the more or less sizable role of molecular scattering. The effect of this factor

must be known in order to proceed to a study of the residual variations, which themselves would thus be attributed solely to the particles.

This point may be studied in a simple manner without the additional necessity of knowing the characteristic values for molecular scattering (A. Morel, 1965). By using the indices p and o to designate the respective parts attributable to scattering of particles and of the water itself, it is possible to break down the volume scattering functions at θ and at 90°:

$$\beta(\theta) = \beta_p(\theta) + \beta_o(\theta) \qquad \beta(90) = \beta_p(90) + \beta_o(90)$$

and from this to formulate the equation:

$$\beta(\theta) - \beta_o(\theta) = \frac{\beta_p(\theta)}{\beta_p(90)} \left(\beta(90) - \beta_o(90)\right)$$

If for various samples $\beta(\theta)$ is used as a function of $\beta(90)$, the distribution of experimental points can be found to occur generally in linear fashion. This means that the equation $\beta_p(\theta)/\beta_p(90) = R(\theta)$ is relatively constant on a first approximation and characterizes scattering by the particles alone. It should be added that if the linearity is unchanged for water with a high scattering capability, this line should pass through a figurative point corresponding to optically pure water, with the coordinates $\beta_o(\theta) - \beta_o(90)$ (the value for $\beta_o(90)$ may be estimated indirectly and approximately in this way). Figure I.4 shows examples of this procedure.

Computation of regression[1] reveals that the correlation coefficient, which is high for small angles (greater than 0.96), is considerably lower for large angles (0.86 at 150°), thus showing that sizable variations occur only in the particle indicatrix and not in that for seawater (water + particles). On the other hand, the values for the average gradients, that is, the various values for $R(\theta)$, are not significantly different for the three lengths considered. Using $R(\theta)$ as a function of θ, one obtains a representation of the "mean" indicatrix for the particles alone (see Figs. I.6, I.9 and III.7 in Part 3). Indicatrices for turbid water do actually tend toward this form of maximum asymmetry; examples borrowed from V.W. Reese and /7

[1] Performed for λ = 546 nm at a maximum for 112 values and for λ = 436 and 366 nm at a maximum for 26 values (36 values for the specific angles 45 and 135°). Some points diverge very considerably from the linear configuration. Usually, but not necessarily, these correspond to coastal samples which are probably loaded with terrigeneous particles. No systematic study of these deviations has been made so far.

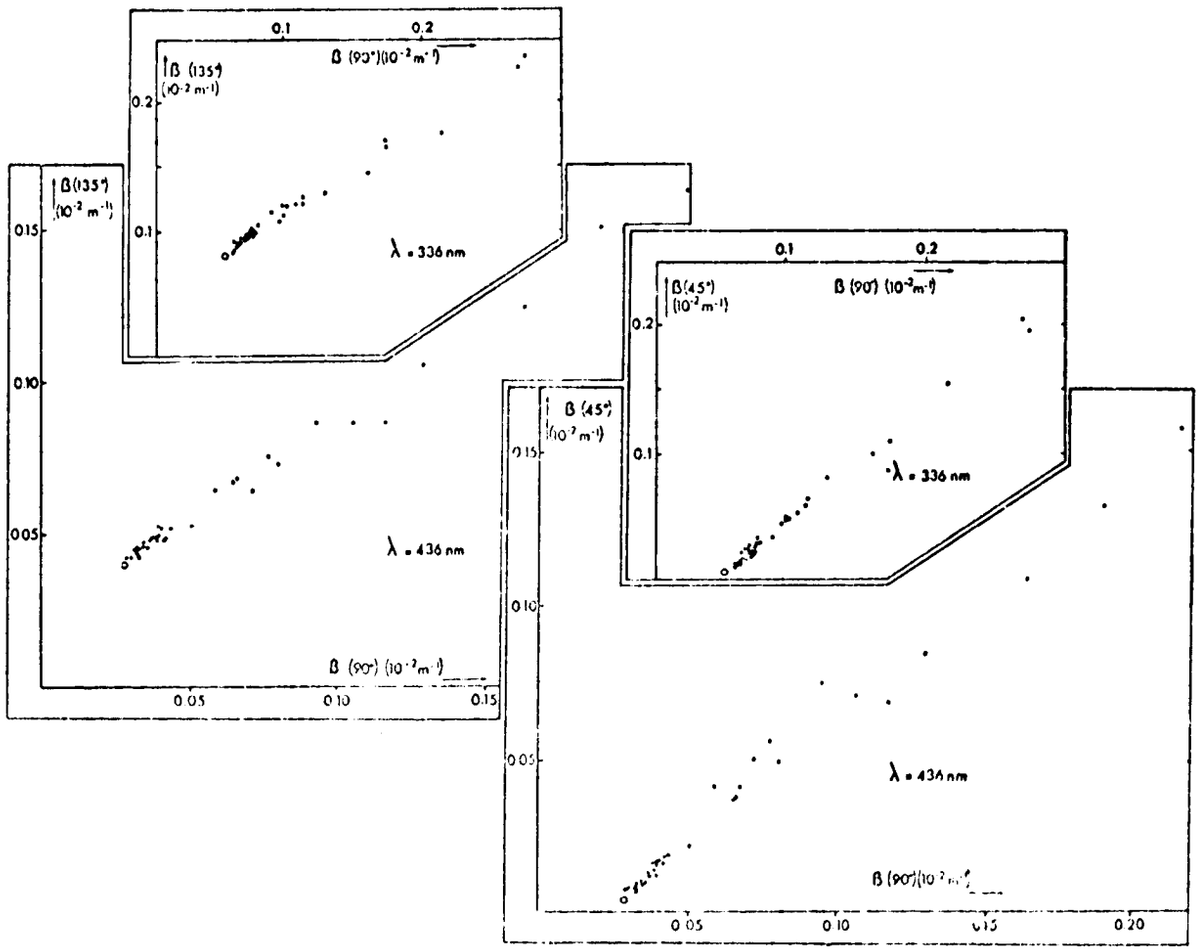

Fig. I.4. Points representing various samples obtained for wavelengths 436 and 366 nm and two angles θ, 45° and 135°, using β(θ) as a function of β(90). These figures complement those previously given for λ = 546 nm (A. Morel, 1965). They deal with various types of seawater: seven samples from the English Channel, 15 from the Mediterranean (eastern and western), five from the Atlantic (Madeira region), and nine from the Indian Ocean (Madagascar region). The circles represent optically pure water (cf. Section 2.1).

S.P. Tucker (1970) are an excellent illustration from this standpoint (cf. Fig. I.6). Two observations should be made with respect to to this curve: due to the fact that it is a mean curve, there are some special cases which it represents very imperfectly, and in addition, in this mean, particles present in turbid water are favored to some extent (since the computed R(θ) equations are extremely dependent on the most highly separated points corresponding to water with the highest scattering capability). These points will be re-examined later (Section 3.1).

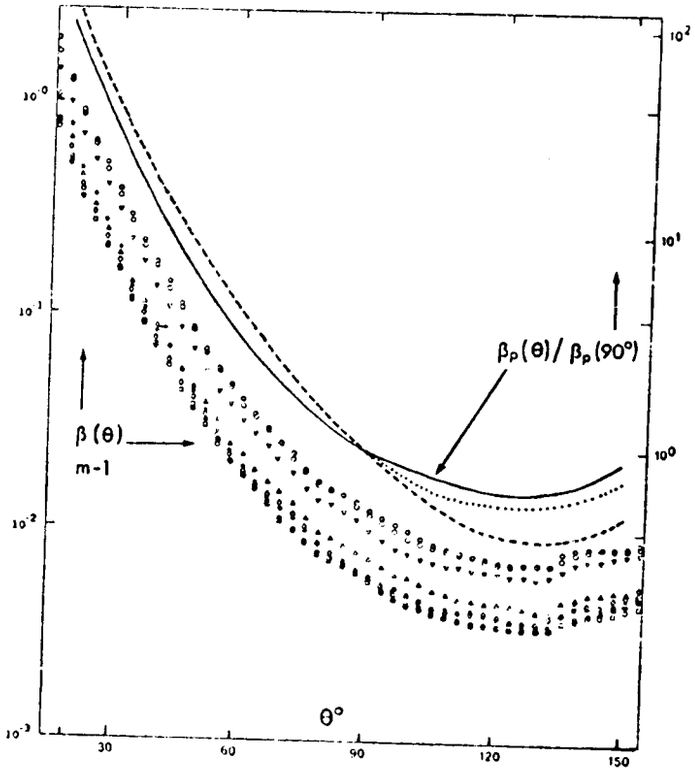

Fig. I.6. Scattering indicatrices determined by J.W. Reese and S.P. Tucker (1970) at depths of between 1 and 15 meters in San Diego Bay on 6/30/1967. The attenuation coefficient C is greater than 1.70 m-1; the absolute values may be read on the scale at the left. With the scale at the right, the "mean" particle index (A. Morel, 1965), normalized to 90°, is plotted in an unbroken line; the broken and dotted lines show particle indicatrices computed from the measurements made by T.J. Petzold (1972) for the same two stations noted previously, respectively Station 8 (Atlantic) and 5 (Pacific).

1.3. Case of Small Angles ($\theta < < 30°$)

Given the extremely high values assumed by the seawater indicatrix in this range of angles (Fig. I.1), molecular scattering plays only a negligible role here (since it varies with the angle only by a ratio of less than 2; cf. Section 2.1 below). Figure I.5 shows a few examples of indicatrices in this small angle range. Two of them are mean curves, that obtained by D. Bauer and A. Morel (1967) from 58 measurements taken in the English Channel and the Mediterranean (at wavelength 550 nm), and that of F. Nyffeler (1969-1970) computed from 66 measurements taken in the Mediterranean (in situ at wavelengths 455, 559 and 599 nm using the previously mentioned device and in vitro at wavelengths 488.0 and 632.8 nm). In general, it may be noted that this part of the indicatrix does not vary greatly (cf. above references), and also that the influence of the wavelength, which is not detected, is slight, if it exists at all. There is satisfactory agreement among these various findings, especially if one considers that for measurements as delicate as these, systematic error and error due to the experimental device used are probably inevitable. Thus the slight incurvation and decrease in gradient

toward 3° to 1° shown by some curves seems to manifest such an instrumental effect. Indeed, the recent measurements made by R. Morrison (1970) and T.J. Petzold (1972) using the equipment of the Visibility Laboratory at Scrips Institute show that the increase in $\beta(\theta)$, which approximately follows a law of $\theta^{-1.6}$ between 10° and 1°, is extended to angles less than 1°. This rapid increase is precisely the most notable finding revealed by these recent measurements; the volume function is found to gain nearly two orders of magnitude between 1° and 0.1°. As will be seen later on (Part 3, Section 3.1.3), even the value of these coefficients is probably not independent of the scale under consideration (or, if one prefers, the scattering volume considered, which, depending on its size, permits or does not permit a particle to be considered as a scattering center cf. 3.1.1, 3.1.3, Part 3).

2. Role of Molecular Scattering

2.1. Review of Useful Values for Water and Seawater

/8

Measurements performed on seawater optically purified by repeated filtration have furnished the value of volume scattering functions for molecular scattering. An attempt was made to confirm these values by additionally performing measurements on artificial seawater, on sodium chloride solutions (which are easier to purify than natural seawater) and also on pure water prepared in this instance by evaporation in a vacuum (A. Morel, 1966, 1968a). The scattering indicatrices obtained for these solutions and the water itself are in effect completely symmetrical (which may constitute a criterion for optical purity) and obey Rayleigh's theoretical law (actually a version of this law modified to take into account the anisotropic quality of the water molecules, which produces partial depolarization), that is:

$$\beta_o(\theta) = \beta_o(90°)(1 + p_{90} \cos^2\theta),$$

p_{90} being the rate of polarization at 90°, whose experimental value is 0.84, corresponding to the value 0.09 for the depolarization factor δ [δ is the ratio $(1-p)/(1+p)$]. In the case of water, the absolute values for the coefficient $\beta_o(90)$ obtained at five wavelengths are in satisfactory agreement with several other experimental findings (at 546 and 436 nm), and also with those which may be computed by density fluctuation theory. A detailed review of these problems has recently been made (A. Morel, 1973b), from which has been drawn the following table, giving the theoretical values for $\beta_o(90)$ and b_o (total scattering coefficient) at intervals of 25 nm for optically pure water and seawater.

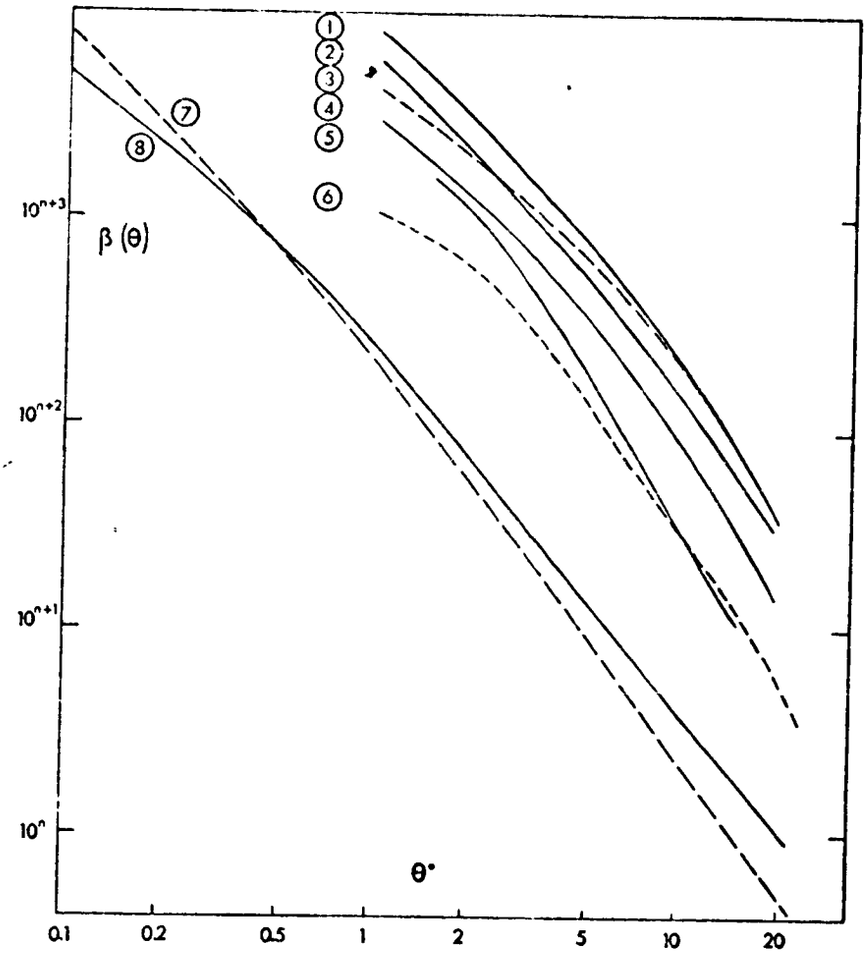

Fig. I.5. Scattering indicatrix at small angles (the two scales are logarithmic). The positioning of the curves in relation to each other is arbitrary.
1: S.Q. Duntley (1963);
2: Y.E. Otchakovski (1965);
3: M. Kozlianinov (1957);
4: G. Kullenberg (1968);
5: D. Bauer, A. Morel (1967);
6: F. Nyffeler (1970);
7 and 8: T.J. Petzold (1972), Station 5 (Pacific) and Station 8 (Atlantic), respectively; that is, respectively, the most scattered water (b = = 0.27 m^{-1}) and the clearest water (b = 0.037 m^{-1})considered by this investigator (aside from port water.

It may be noted that if an attempt is made to express the molecular scattering of water (or seawater) as an exponential function, the best expression is $\lambda^{-4.32}$. The fact that the exponent differs from 4 arises basically from the dispersion of the indicatrix.

TABLE I. THEORETICAL VALUES FOR $\beta_o(90)$ AND b_o AS A FUNCTION OF WAVELENGTH. THE OTHER VOLUME FUNCTIONS $\beta_o(\theta)$ MAY BE DEDUCED FROM $\beta_o(90)$ BY MEANS OF THE EXPRESSION BELOW. INTEGRATION OF THIS SAME EXPRESSION OVER THE ENTIRE SPACE, WHICH LEADS TO $b = \frac{8M}{3} \beta_o(90) \frac{2+\delta}{1+\delta}$, MAKES IT POSSIBLE TO COMPUTE b_o (δ IS ASSUMED TO BE EQUAL TO 0.09). /9

	λ (nm)	350	375	400	425	450	475	500	525	550	575	600
water	$\beta_{90}(10^{-4}m^{-1})$	6.47	4.80	3.63	2.80	2.18	1.73	1.38	1.12	0.93	0.78	0.68
	b $(10^{-4}m^{-1})$	103.5	76.8	58.1	44.7	34.9	27.6	22.2	17.9	14.9	12.5	10.9
sea-water S=35/35‰	$\beta_{90}(10^{-4}m^{-1})$	8.41	6.24	4.72	3.63	2.84	2.25	1.80	1.46	1.21	1.01	0.88
	b $(10^{-4}m^{-1})$	134.5	99.8	75.5	58.1	45.4	35.9	28.8	23.3	19.3	16.2	14.1

Scattering is highest for solutions, since in this case an additional term is added, explained by fluctuations in concentration. This term may be computed, at least for dilute and ideal solutions, from the molecular weight of the solute and the increment in the indicatrix produced by its presence. In this way measurements performed on sodium chloride solutions can be interpreted and subsequently will furnish a term of comparison for the values relative to seawater. Thus seawater shows values 6% higher than those of a sodium chloride solution with the same chloride ion concentration, and 30% greater than the values for water.

2.2. Relative Importance of Molecular Scattering

Given the marked asymmetry of the particle indicatrix, molecular scattering is especially likely to play a significant role for the tail end, especially where the indicatrix is at a minimum, toward 120 or 140°. When the water is turbid, the relative influence of molecular scattering obviously becomes negligible at any angle; inversely, for clear water it may be of interest to determine what the maximum influence might be (at least with the measurements available, with the understanding that the possibility of the existence of clearer water is in no way excluded).

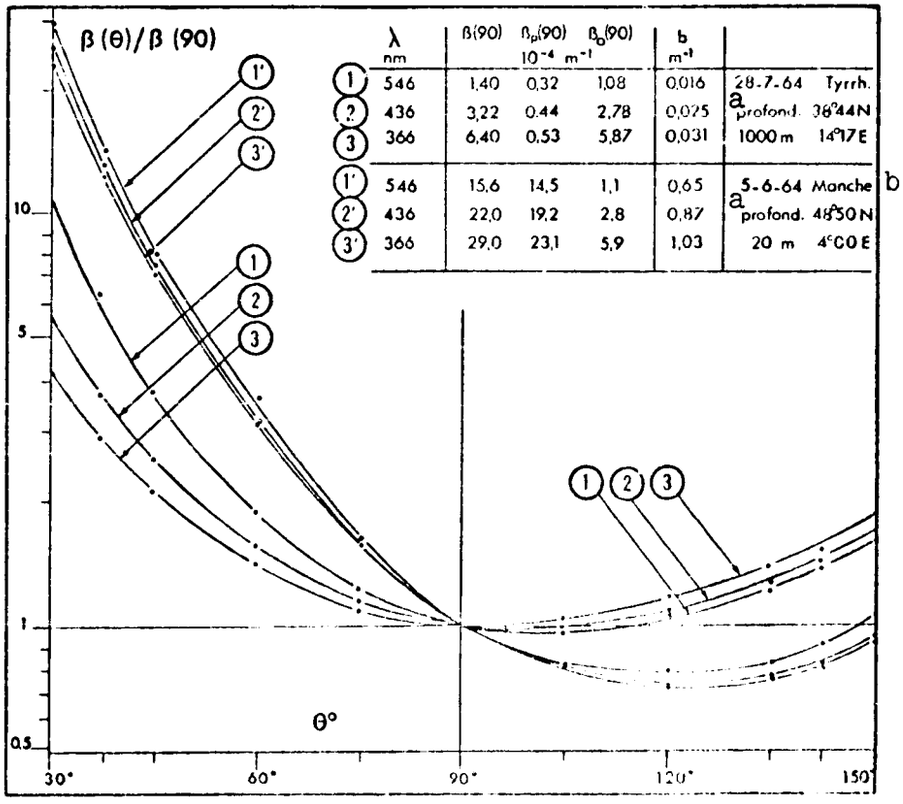

Fig. I.7. Indicatrices normalized to 90°. Measurements performed at three wavelengths on one sample of turbid seawater (English Channel) and on another very clear sample (Tyrrhenian Sea).

Key: a. Depth
b. English Channel

The curve in Fig. I.2 or curves 1, 2 and 3 in Fig. I.7 are /10 representative examples of deep clear water. In this connection, it is possible at each angle to form the ratio[2] $\beta_o(\theta)/\beta(\theta)$ of the molecular scattering to the scattering (total) observed for one of these typical cases (that of Fig. I.7), where the indicatrix is determined at three wavelengths. One thus obtains the ratios

[2] Rather than using the theoretical values given in Table I, experimental values obtained in tests of purified seawater (A. Morel, 1968) were used to form this ratio; these values were slightly lower (approximately 10%). This was deemed preferable since measurements of both the purified water and the sample were performed with the same device and under the same conditions; uncertainty in regard to the absolute values is eliminated in the ratio.

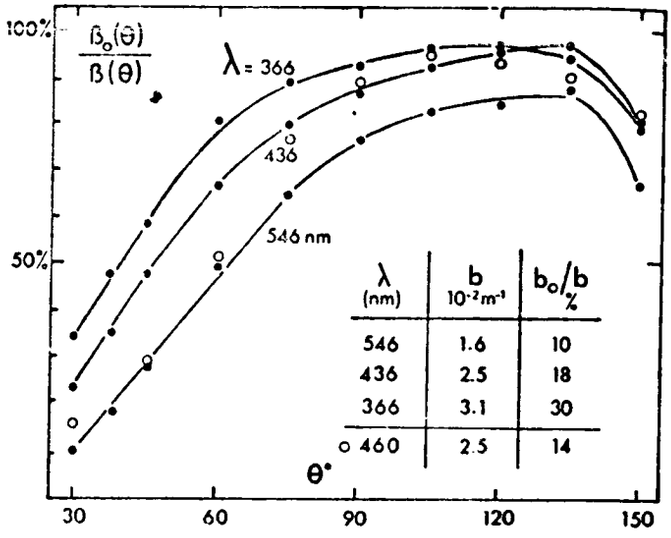

λ (nm)	b $10^{-2}m^{-1}$	b_o/b %
546	1.6	10
436	2.5	18
366	3.1	30
o 460	2.5	14

Fig. I.8. Relative importance of molecular scattering as a function of angle. The curves, representing three wavelengths, are based on the sample from the Tyrrhenian Sea (cf. Fig. I.7). The small circles are deduced from the measurements made by G. Kullenberg (1968) in the Sargasso Sea (10 m) at wavelength 460 nm.

used in Fig. I.8 as a function of the scattering angle. Due to the pronounced selectivity of molecular scattering, the relative importance of the latter increases as the wavelength decreases, and in all cases it is at an effective maximum for angles between 90° and 140°. The total molecular scattering coefficient b_o can thus be compared to the coefficient b of the sample (computed from $\beta(30°)$, cf. Section 6). In the case of this extremely pure water, the ratio b_o/b would increase 10% for λ = 546 nm and 30% for λ = 366 nm. It should be added that similar results have also been obtained in the Eastern Mediterranean (laboratory team, 1969) and in the Atlantic in the Madeira region, generally at depths greater than 1000 m, while analogous values may be deduced from the measurements made by G. Kullenberg (1968) at only 10 meters, but in the Sargasso Sea, providing definitive proof of the high purity of the waters of this sea.

3. Particle Scattering Indicatrix

3.1. Results

A "mean" indicatrix was obtained by an indirect procedure, which, it should be recalled, is probably more representative of the particles present in turbid water (Section 1.2). The particle indicatrices may be determined, case by case, by subtracting[3]

[3] Here again problems arise in attempting to analyze clear water. On the basis of the statements which have just been made, the part $\beta_o(\theta)$ to be subtracted is preponderant for mean angles. Thus the experimental uncertainty in regard to $\beta(\theta)$ actually is carried over integrally to $\beta_p(\theta)$, resulting in relatively sizable error. As a result, the tail end of the indicatrix obtained appears to be more variable than it actually is, despite the fact that a few aberrant indicatrices have been set aside.

the volume functions $\beta_o(\theta)$. For the three wavelengths indicated, Fig. I.9 shows the range containing all the particle indicatrices computed in this way (112 for λ = 546 nm, of which 26 correspond to measurements taken at the three wavelengths 546, 436 and 366 nm). Only the tail ends for the wavelength 436 nm are completely plotted as an example.

Figure I.6 furnishes another illustration, the computations being made on the basis of the measurements taken by T.J. Petzold (1972), which have already been shown (Figs. I.2 and I.5); two indicatrices were chosen, corresponding respectively to the clearest water (1500 m, Atlantic) and to the most turbid oceanic water (coastal,California). After deduction of the part attributable to molecular scattering, the indicatrices obtained were plotted conjointly as a mean indicatrix.

Without being more specific, in view of the uncertainty in the case of clear water, it seems that in this type of water indicatrix for suspended particulate matter generally has a very marked minimum, frequently followed by a rapid increase toward 150°. The mean indicatrix, shown as a dotted line in these figures, is virtually identical to the curve representing the lower limit of range for angles greater than 90°; for angles less than 90°, this indicatrix is appreciably in this center of the range.

3.2. Adoption of a "Typical" Particle Indicatrix /12

Knowledge of the particle indicatrix is indispensable in solving a large number of problems, both those dealing with the relationships between scattering properties and suspended matter content of the water, and those dealing with the visibility of immersed objects or the propagation of daylight or artificial light. Study of the asymptotic system of submarine luminances (L. Prieur, A. Morel, 1971), or more generally, all problems linked to radiative transfer, reveals this necessity. For these computations or for these previsional models, it is useful to have available a "typical" particle indicatrix, that is, one constituting a satisfactory approximation. For this purpose, the "mean curve" obtained between 30 and 150° may be used and combined with the mean curve for angles between 1.5° and 14°. A connection between these two parts was made earlier (D. Bauer, A. Morel, 1967) by using the measurements made by N.G. Jerlov (1961), which were performed to a limit of 10°. The measurements subsequently performed by F. Nyffeler (1969-1970) between 1° and 25° have shown that this interpolation was correct. Under these conditions, the scattering coefficients for this "typical" indicatrix are as follows:

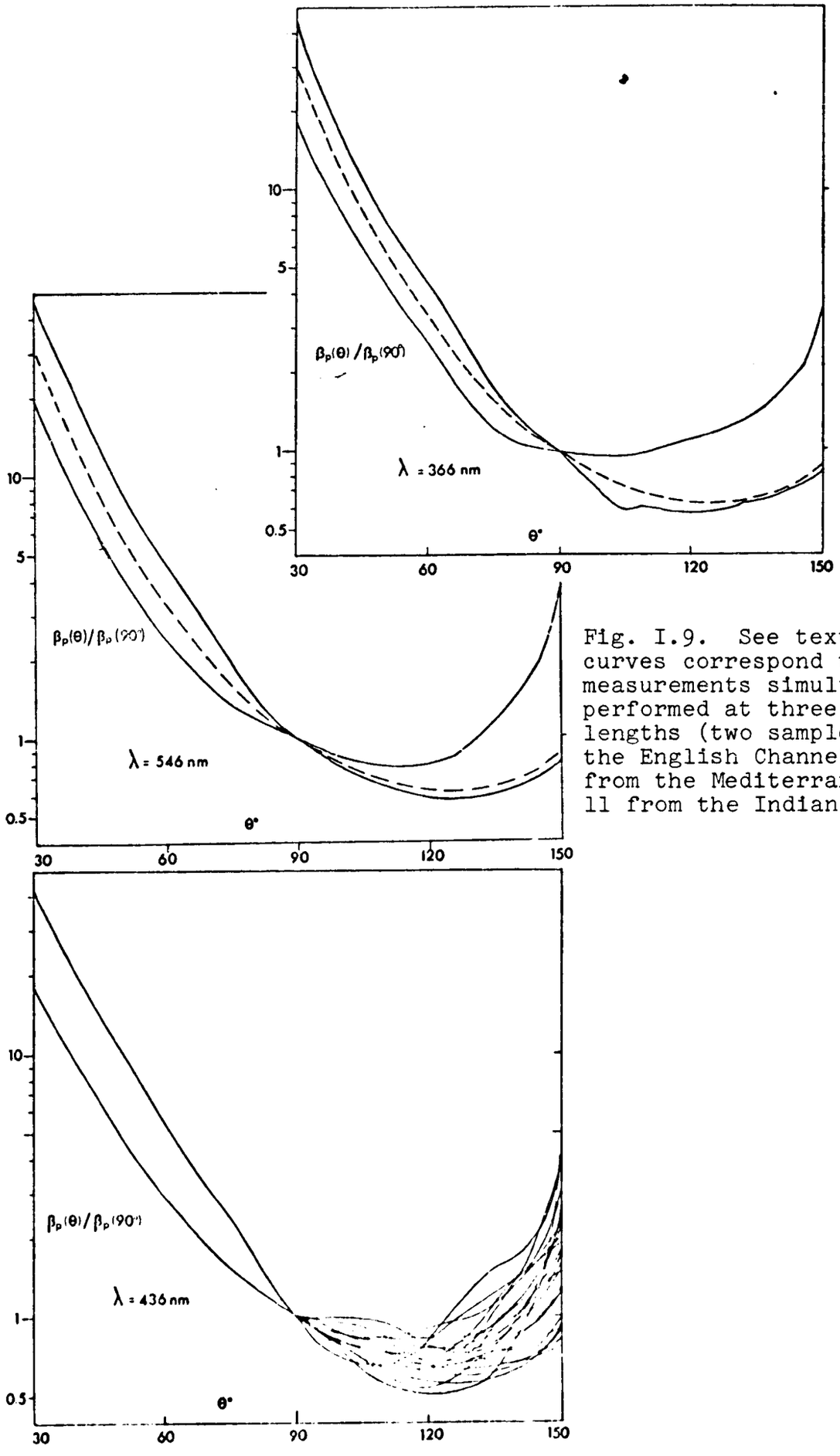

Fig. I.9. See text. These curves correspond to 26 measurements simultaneously performed at three wavelengths (two samples from the English Channel, 13 from the Mediterranean and 11 from the Indian Ocean).

TABLE II. "TYPICAL" PARTICLE INDICATRIX.

First column: volume functions normalized to 90°. Second column: normalized coefficients $\bar{\beta}(\theta)$, that is, normalized with respect to the integral yielding b (cf. Appendix 1). For this computation of the integral an exponential extrapolation of type $\beta(\theta) = \exp(-k\theta)$ was performed, between 1 and 10°. This yielded a value for the integral between 0 and 1°, equal to 9.7% of the total integral between 0 and 180°.* This value may be low, in view of the results obtained by T.J. Petzold (1972). This investigator computes as between 0.1° and 1° the values constituting 20 to 30% of the final value for the integral (0-180°). Last columns: polarized components (cf. Section 5), perpendicular ($\bar{\beta}_1$) and parallel ($\bar{\beta}_2$) to the scattering plane, computed from the rate of polarization:

$$p(\theta) = \frac{\bar{\beta}_1(\theta) - \bar{\beta}_2(\theta)}{\beta_1(\theta) + \beta_2(\theta)} = \frac{\bar{\beta}_1(\theta) - \bar{\beta}_2(\theta)}{\bar{\beta}(\theta)}$$

the values for $p(\theta)$ used are shown in Fig. I.13. The "typical" indicatrix is shown graphically in Fig. III.7 (Part 3).

θ°	$\frac{\beta(\theta)}{\beta(90)}$	$\bar{\beta}(\theta)$
(1)	34400	77.5
1.5	26100	58.8
2	19100	43.0
3	8500	19.2
4	4750	10.7
5	2990	6.7
6	1920	4.32
7	1300	2.93
8	915	2.06
9	670	1.42
10	500	1.12
12	314	0.71
14	224	0.505
16	168	0.378
18	130	0.298
20	102	0.230
22	75	0.169
24	58	0.130
26	47	0.106
28	38	0.0856

θ°	$\frac{\beta(\theta)}{\beta(90)}$	$\bar{\beta}(\theta)$ x10³	$\bar{\beta}_1(\theta)$ x10³	$\bar{\beta}_2(\theta)$ x10³
30	31.4	70.7	77.5	65.0
45	8.50	19.1	23.3	14.7
60	3.41	7.68	11.2	4.2
75	1.61	3.63	6.1	1.15
90	≡ 1	2.25	4.00	0.50
105	0.74	1.67	2.82	0.50
120	0.65	1.46	2.15	0.75
135	0.65	1.46	1.87	1.05
150	0.87	1.96	2.18	1.75
(165)	0.17	3.8		

*The value of the total integral is 444 if $\beta(90)$ is assumed to be identical to 1. An error was overlooked when these computations were first presented (A. Morel, 1968), the indicated value being $444/\pi$ rather than 444. The coefficients of the relationships between $\beta(\theta)$ and b were in error in the same equation (cf. correction, 1970). Possible variations in the indicatrix, particularly in the forward part, result in possible variations estimated at ±17% of the integral (cf. Sections 2.2 and 2.3, Part 3).

It should be emphasized that by its very nature, a typical indicatrix of this sort is nothing more than a mean which is judged to be satisfactory. It is precisely the variability about this mean which will be used during the theoretical interpretation (Part 3, Section 2) to find data on the nature of the particles (more exactly, their indicatrix, as well as on the law governing their distribution.

4. Influence of Wavelength

The qualitative aspect of the problem, that is, the influence on the shape of the indicatrix, should be distingushed from the quantitative aspect, that is, the influence on the magnitude of the scattering phenomenon.

4.1. Variations in the Shape of the Indicatrix

Actually, this question has been implicitly examined above. To give a brief summary of the main points: when the water is clear, the indicatrix, which is already relatively symmetrical, becomes more so if the wavelength decreases, due to the increasing role of molecular scattering, which is highly selective. On the other hand, for turbid water the shape of the indicatrix remains virtually unmodified by the change in wavelength, thus indicating that the molecular scattering is negligible, and that in addition the particle indicatrix is virtually insensitive to this factor. Figure I.7 gives examples of these two cases.

After molecular scattering has been subtracted, the shape of the particle indicatrix effectively varies with the wavelength; it was not possible to show any systematic law for this variation.[4] On the average, when normalized to 90° the indicatrices are virtually the same, as shown by Fig. I.9. The measurements made by N. Nyffeler (1970) also indicate an absence of marked influence in the small angle range. /13

[4]This was true in the case of our measurements, at least, since Hinzpeter (1962) notes that the indicatrix is less asymmetrical at 400 nm than it is at 700 nm; this probably is a particle indicatrix, since these results were obtained for the turbid waters of the Baltic Sea.

4.2. Scattering Selectivity

4.2.1. Volume Scattering Functions

On the other hand, when molecular scattering is subtracted, it appears that $\beta_p(\theta)$ (considered as an absolute value in this instance) varies systematically with the wavelength, increasing slightly as the wavelength decreases. Figure I.10 shows variations in the ratios of $\beta_p(\theta,\lambda)$ to $\beta_p(\theta,546)$ as a function of θ, when the value of λ is 436 or 366 nm. For reasons which have already been indicated, the ratios are better defined at small angles, since the variability of the indicatrix at large angles results in an increase in the standard deviation. Analogous results have been obtained with Atlantic water (for $\theta = 30°$ and λ = 436 and 546 nm), which have been presented elsewhere (A. Morel, 1970). J. R. Zaneveld and H. Pak (1973) have used measurements taken at 45°; the ratio of the scattering coefficients to wavelengths of 436 and 546 nm respectively varies approximately from 1.10 to 1.45 according to these investigators. (These do not seem to be coefficients relative to single particles, but directly measured coefficients, and thus the ratio may be slightly affected.)

Indirect method. A precise although indirect method (A. Morel, 1967) also makes it possible to determine selectivity for a given angle. This method has been used for five wavelengths (578, 546, 436, 405 and 366 nm) for a large number of values at 90° (Fig. I.11), and for a lesser number at 30°, nevertheless furnishing appreciably identical results, taking the confidence factor into account (Fig. I.12). This method is based on the following principle: if the measurements are performed using optically pure benzene as a reference, the scattering selectivity of a sample may be determined from the scattering selectivity of benzene, experimentally known and theoretically computed. In practice the procedure may be as follows: taking r as the ratio of the scattering coefficient of the sample to that of benzene (for an identical angle θ, which is not written for purposes of simplification), for λ = = 546 nm one has $r(546) = r_o(546) + r_p(546)$, and for all other wavelengths: $r(\lambda) = r_o(\lambda) + r_p(\lambda)$, functions o and p denoting, as above, the part attributable to pure water and that attributable to the particles: below b the indicatrix represents benzene. To state this explicitly:

/14

$$r_{(546)} = \frac{\beta_o(546) + \beta_p(546)}{\beta_b(546)}$$

and assuming that when the wavelength is changed, each scattering coefficient is multiplied by a specific coefficient k, that is by K_o, K_p and K_b respectively, one may write:

$$r(\lambda) = \frac{K_o \beta_o(546) + K_p \beta_p(546)}{K_b \beta_b(546)} = \frac{K_o}{K_b} r_o(546) + \frac{K_p}{K_b} r_p(546),$$

and finally, reintroducing r(546), one obtains:

$$r(\lambda) = \text{Const} + \frac{K_p}{K_b} (r(546) - r_o(546))$$

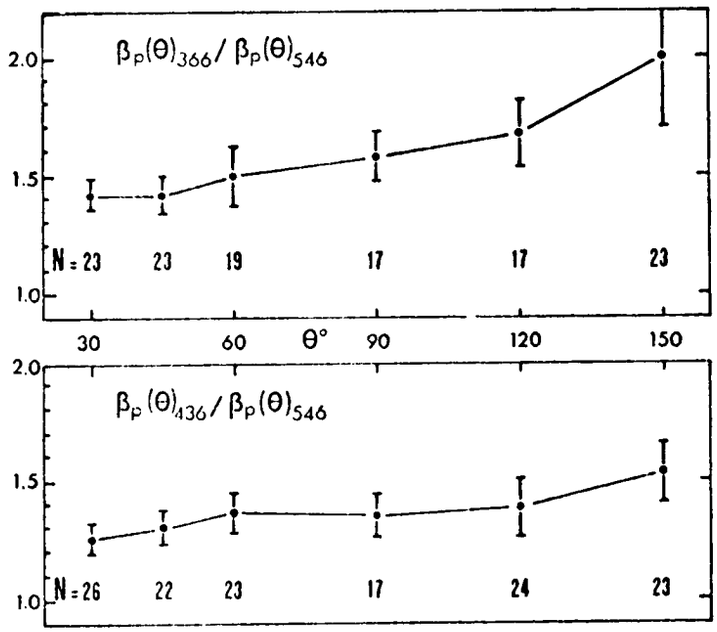

Fig. I.10. Ratios of $\beta_p(\theta,\lambda)$ to $\beta_p(\theta,546)$ given as a function of , with λ = 436 and 366 nm; the unbroken line represents the average value; the vertical line corresponds to the standard deviation computed for N measurements; the values for N are indicated. The maximum for N is 26, corresponding to 26 samples on which measurements were performed for three wavelengths in turn (see caption to Fig. I.9).

If the scattering selectivity of the particles was nil (K_p = 1), one would obtain a linear equation between $r(\lambda)$ and r(546), the gradient being the inverse of the value for K_b.[5] In actuality, by making $r(\lambda)$ a function of r(546) for each sample, one obtains approximately linear forms, but different gradients for $1/K_b$, which thus make it possible to evaluate K_p. These values, obtained for θ = 90° and θ = 30°, are given as a function of the wavelength in Fig. I.12, and are compared to the curves corresponding to $\lambda^{-0.8}$ and $\lambda^{-1.2}$ selectivities; it should be noted that they are very close to the values obtained directly by the first method.

[5]The values for K_b characterizing the scattering selectivity
[note continued on following page]

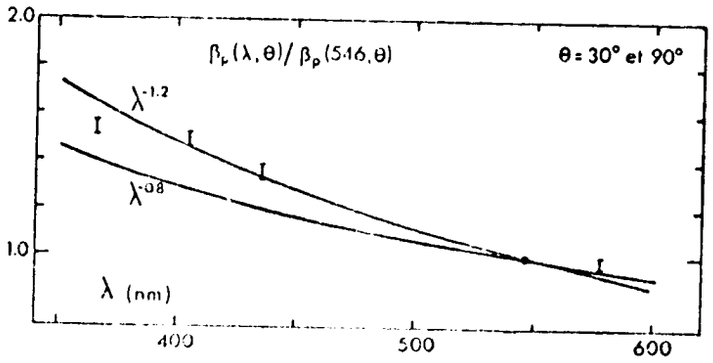

Fig. I.12. Results obtained by the method illustrated by the preceding figure, dealing with the scattering selectivity of particles (at 30° and 90°). The vertical lines correspond to the standard deviation for the values, and the curves correspond to the laws indicated.

4.2.2. Total Scattering Coefficient /15

Apparently there has been no systematic direct measurement of b at several wavelengths for a single sample or at identical locations and depths. Conclusions -- which are, moreover, relatively controversial -- may be drawn only by hypothetical means. If the shape of the particle indicatrix may be considered insensitive to wavelength, the selectivity found for various angles (which roughly corresponds to a λ^{-1} law) is related to the total coefficient b by an integral. This was the theory set forth by J.R. Zaneveld and N. Pak (1973), for example, and it is probably well founded.

Another hypothesis consists in assuming that in the attenuation due to the particles, the scattering factor is heavily preponderant[6] over the absorption factor. This is the theory

---

[5](cont'd) of benzene which were used are as follows (A. Morel, 1966):

λ nm	578	546	436	405	366
K_b	0.79	1	2.78	3.88	6.36

[6]This hypothesis is probably partially inaccurate for some bands of the spectrum in the case of highly colored particles; it does seem to be realistic, however, as can be shown in an approximate manner by the following experiment: when a spectrophotometer is used to determine the spectrum of a seawater sample in relation to a filtered sample of the same water, the particles simultaneously serve as scattering and absorbing centers. The same particles, collected on a filter with the same diameter as the tank, will act primarily as absorbing centers if the filter has been "brightened" by the oil used for immersion (the reference consists of an unused filter brightened in the same way; C. Yentsh method, 1957). Now, none of the measurements made in this manner were comparable to those made in the preceding experiment, unless a volume at least 20 times greater than that of the tank is filtered. This shows that scattering has a heavy influence on absorption. The approximations made: a spectrophotometer does not measure c, but an intermediate term between c and a, and the particles on the filters still have a scattering effect. These approximations tend in the same direction and reinforce the conclusion.

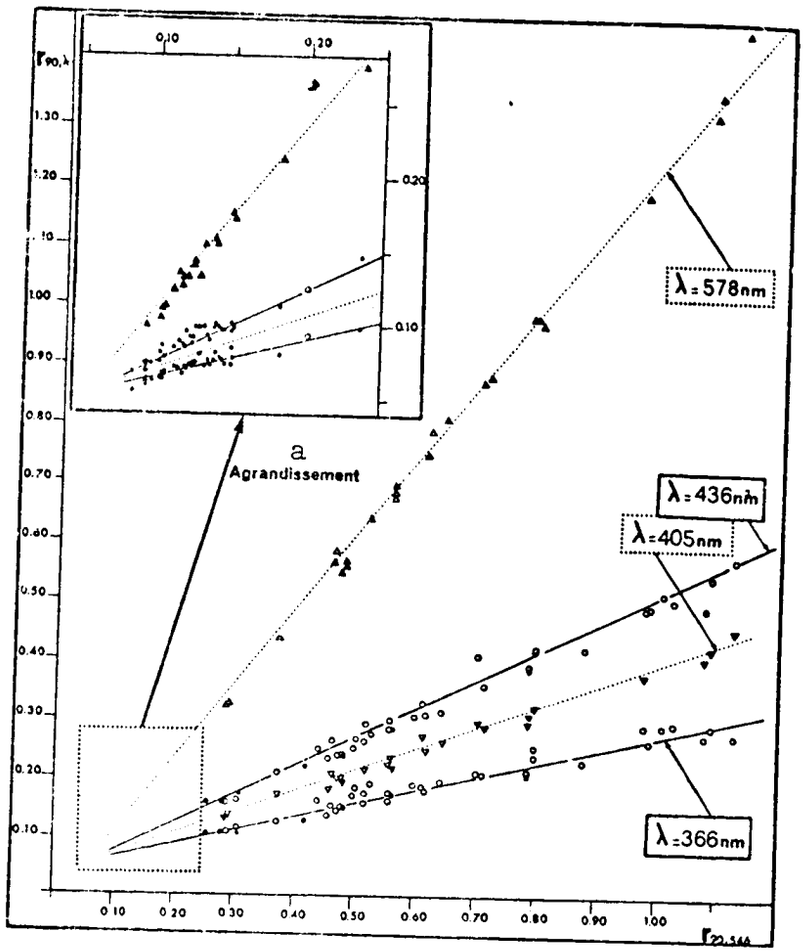

Fig. I.11. r(90,λ) given as a function of r(90,546) for various samples (see text). The open symbols correspond to measurements taken in the English Channel, and the solid symbols to measurements taken in the Mediterranean.

Key: a. Enlargement

espoused by W.V. Burt in 1955. If dispersion is observed for the attenuation coefficient c, virtually no part of this phenomenon may be attributed to the coefficient b. W.V. Burt interprets in this way measurements performed with a spectrophotometer and spectra obtained corresponding to exponential laws ranging from approximately λ^{-1} to λ^{-2}.

5. Polarization

5.1. Results

H. Hinzpeter (1962) was apparently the first to show that the angular distribution of the rate of polarization of natural incident light is very appreciably symmetrical on either side of 90°, with a maximum value at this angle on the order of 0.40 to 0.65 (slightly lower at 700 nm than at 400 nm), and values on the order[7] of 0.10 at 30 and 150°. G.F. Beardsley (1968) has measured polarization in all possible configurations, with combinations of polarizer and quarter-wave plate simultaneously on the incident and scattered beams. In this way it is possible to determine, for various angles, the 16 components of the matrix to be applied to the four Stokes parameters characterizing the incident wave (cf. Eq. (1.12), Part 2). The values for this matrix are low for non-diagonal components, which should theoretically be nil if the particles are spheres. However, the strongly diagonal nature of the experimental matrix shows that assimulation by spheres constitutes a satisfactory approximation (cf. 1.2, Part 2).

With natural incident light, the variation of the rate of polarization with the angle θ is approximately symmetrical, as shown by Fig. I.13, which gives on the left an average curve corresponding to five measurements made on water from the English Channel and three on relatively turbid water[8] from the Mediterranean (Villefranche Bay). The maximum and minimum values observed at 90° (60% and 79%) are represented by the vertical line. The dotted curve corresponds to the curve determined for optically pure water (A. Morel, 1966), with $p(90°) = 84\%$. The righthand part of this figure shows the curves obtained by G.F. Beardsley (1968) (with the exception of that obtained at the "Atlantic 4" station); these show that the maximum rate (at 90°) cannot exceed 50%, and in addition that the angular dependence would be more complex in the 20-40° zone.

---

[7] For the extremely turbid waters of the Baltic Sea.

[8] Measurements of clear water, from which the influence of molecular scattering must also be subtracted in order to compute the polarization due to the particles alone, are subject to caution due to the loss of sensitivity attendant on positioning of an analyzer. The eight measurements used here deal with water with an adequate scattering capability ($b > 1\ m^{-1}$), for which the influence of molecular scattering may be discounted.

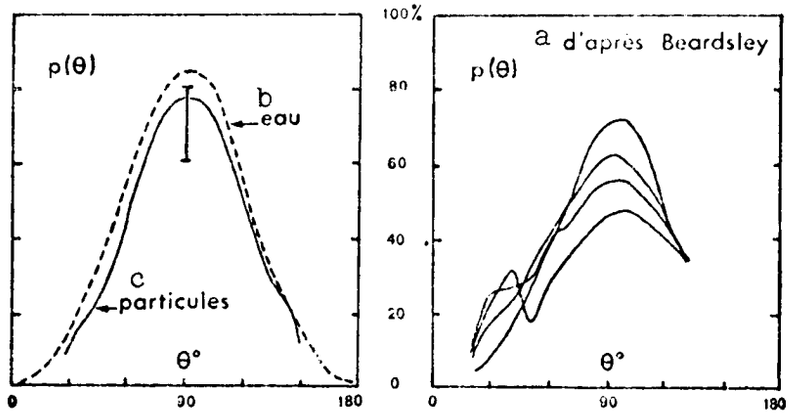

Fig. I.13. Rate of polarization p(θ) as a function of angle θ.

Key: a. After Beardsley
b. Water
c. Particles

5.2. Variability of Rate of Polarization at 90° /16

The systematic measurements performed at 90° by A. Ivanoff (1961) show, for the seawater samples studied, that the rate of polarization at this angle varies extremely widely from a value (80%) in the neighborhood of that of pure water down to low values scarcely higher than 40%. This variation occurs in a very regular manner, with the water samples with the highest scattering coefficient being roughly those showing the lowest rate of polarization. An attempt may be made to determine whether this effect is due solely to the fact that the role of molecular scattering, for which the rate of polarization is high, gradually becomes negligible, or on the other hand whether the rate of polarization of light scattering by the particles is itself variable, and what the nature of this variation may be. By definition (cf. Part 2, Section 1.1), the rate of polarization is the ratio of the intensity of polarized light i_π to the total intensity $I_n + I_\pi$ of the natural light and the polarized light. Breaking down the factors attributable to scattering by the particles and by the water itself (functions p and o respectively), the result is:

$$p = \frac{I_\pi}{I_\pi + I_n} = \frac{I_{\pi p} + I_{\pi o}}{I_{\pi p} + I_{\pi o} + I_{np} + I_{no}}$$

in the same way, one may write:

$$p_o = \frac{I_{\pi o}}{I_{\pi o} + I_{no}} \quad \text{and} \quad p_p = \frac{I_{\pi p}}{I_{\pi p} + I_{np}}$$

The denominators of these three expressions are respectively proportional to β, β_o and β_p. The result is thus:

$$p = \frac{\beta_o}{\beta} p_o + \frac{\beta_p}{\beta} p_p$$

that is, an expression corresponding to a "mixing law," where p varies with β according to a hyperbolic law:

$$p = p_p + \frac{\beta_o}{\beta} (p_o - p_p) ;$$

p tends toward the limiting value p_p when the scattering coefficient β is high, and toward p_o when the scattering is merely molecular scattering ($\beta_o/\beta = 1$).[9]

For purposes of comparison with the experimental values obtained by A. Ivanoff, the logarithm of β/β_o as a function of p was used rather than β/β_o (see Fig. I.14), two lines were plotted delimiting the range within which the experimental points were concentrated, and the median line was also plotted. The curves correspond to various values given to p_p a priori, the value for p_o being 0.84. It appears that the distribution of experimental points corresponds to a variable rate of polarization for particles from 0.7 to 0.4, and more importantly, that these variations are relatively systematic in nature. The particles in the most turbid water samples are the least polarizing, while those in clear samples show variable rates and may reach values on the order of 0.8. (This would moreover explain why the extrapolation made by A. Ivanoff resulted in a value -- 0.88 -- which was slightly high for molecular scattering.)

Finally, these values, especially those relative to 90°, are in agreement in their diversity and confirm the variability of p(90). As will be seen in Part 3, this variability is theoretically plausible, but some of the causes which may be found for this phenomenon, such as the influence of particle shape, will remain difficult to isolate.

6. Relationships Between Scattering Coefficients

The use of certain ratios for volume scattering functions has been recommended to serve as a descriptive element for the indicatrix (for example, the ratio $\beta(30)/\beta(45)$, A.F. Spilhaus, 1968). More generally, confronting the difficulty of directly measuring the total scattering coefficient b, an attempt has been made to evaluate this factor on the basis of measurements of a given

[9] There is no hypothesis in these computations with the exception of that based on the additivity of scattered waves.

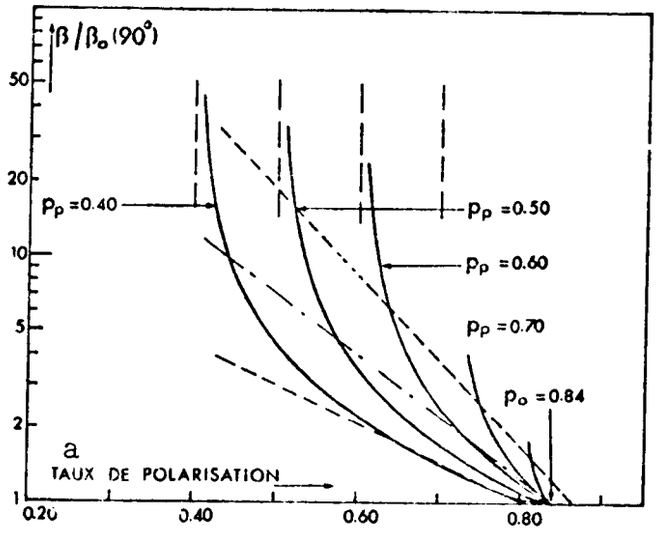

Fig. I.14. For various values p_p for the rate of polarization of particles at 90°, variations in the rate of polarization of a sample depending on the value of its scattering coefficient at 90°, unity being molecular scattering, $\beta_0(90)$, at the same angle. The ordinate scale is logarithmic.

Key: a. Rate of polarization

volume function $\beta(\theta)$. N.G. Jerlov has used this method since 1953 and derives b from $\beta(45°)$. Such methods assume that, at least on an approximate basis, the ratio $\beta(\theta)/b$ -- that is, the so-called "normalized" $\overline{\beta}(\theta)$ coefficient -- is sufficiently constant. In using these methods, the precaution of subtracting the part attributable to molecular scattering from $\beta(\theta)$ has not always been taken; this results in inaccuracies, especially if θ is greater than 45° (and even at 45°, if the water is extremely clear).

Such equations may /17 be written on the basis of the values for $\overline{\beta}(\theta)$ relative to the "typical" particle indicatrix and taking molecular scattering into account (A. Morel, 1968). The result is thus:

$$b = \frac{1}{\overline{\beta}_p(\theta)} \left(\beta(\theta) - \beta_0(\theta)\right) + b_0 ,$$

$\beta(\theta)$ being the measured value for the sample, from which the molecular part $\beta_0(\theta)$ is subtracted. With the values given in Table II, this equation is written as follows for 30, 45 and 90°:

$$b = 14 \left(\beta(30) - \beta_0(30)\right) + b_0 , \quad b = 50 \left(\beta(45) - \beta_0(45)\right) + b_0 ,$$

$$b = 445 \left(\beta(90) - \beta_0(90)\right) + b_0 .$$

Frequently $\beta_0(30)$ may be omitted, $\beta_0(45)$ may be omitted only in the case of clear water (cf. Fig. I.8), and $\beta_0(90)$ only in the case of extremely turbid water. The possibility of omitting these terms decreases, of course, as the wavelength decreases. The value b_0, which varies with the wavelength, is included in

Table I. The possibility of omitting this term is the same as that noted above.

A detailed review of the experimental values obtained by a number of investigators for these ratios, either between two angles or between the volume function and the total coefficient, will be made subsequently (Part 3, Section 2). The variability of these ratios, which actually reflects the variability of the particle indicatrix, theoretically may be interpreted as the variability term for the particles themselves.

PART 2 /18

Introduction

The search for a theoretical interpretation for the experimental results includes two aspects: first, determination of whether one's knowledge of the marine suspended matter compatible with that on scattering properties -- in other words, whether the former explain the latter; and second, whether it is possible to use observation of these scattering properties to determine information on the particles which is difficult to obtain by other methods. These preoccupations have already motivated several studies; without providing an exhaustive list, these notably include those of Y. Otchakovsky (1965), T. Sasaki (1967), and T. Sasaki et al. (1968); and recently, those of H. Pak et al. (1971), G. Kullenberg (1972) and H.R. Gordon and O.B. Brown (1972). The last three studies were made not on the basis of published and tabulated values for Mie functions, but rather with the use of data computed for this purpose. Nevertheless it does not appear that the possibilities afforded by theoretical methods have been systematically explored, nor that the comparisons made between theoretical and experimental results have been methodically carried out. It is first necessary to interpret the results of theoretical computations in order to be able to predict the influence of various parameters without having to perform additional computations. A guideline may be drawn from this condition which will aid in performing comparisons. The methods presented here are an effort in this direction. The object of this second part is thus to furnish the theoretical bases necessary to provide a solution for the problem, and to show what factors may be predicted by computation under what conditions. A comparison of the theoretical results thus obtained with experimental data is reserved for Part 3.

First of all (Chapter 1), there is a brief review of the general relationships between the state of polarization of the incident wave and that of the scattered wave. More thorough development of these relationships may be found in the frequently cited article by F. Perrin (1942), as well as the chapters dealing with this subject in the works of Van de Hulst (1957), Presendorfer (1965) and Deirmendjian (1969). The purpose here is merely to determine the framework within which the most limited case considered below may be found -- that is, that in which the incident light is assumed to be natural or rectilinearly polarized (perpendicular or parallel to the scattering plane).

Marine particles in suspension with a wide range of size variation are within the province of the Mie theory (1908). Applied to electromagnetics theory, this theory uses Maxwell equations to obtain a rigorous analytical solution to the

problem of the scattering of a flat wave by a spherical particle of any given size. From this standpoint, it coincides with the Rayleigh theory when the particles become extremely small in relation to the wavelength, and when the particles are large, on the other hand, it tends toward limiting solutions which are those furnished by geometric optics (reflection, refraction) and diffraction theory.

No attempt has been made in this work to set forth the Mie theory, which has become classical, especially since the publication of Van de Hulst's work[1]; Chapter 2 below merely reviews the formulas necessary for subsequent development. However, there did seem to be some value in using the numerical results obtained by means of this theory to describe variations in the scattering indicatrix with changes in size and index parameters, since it is not easy to form a precise idea of these variations from the publications available. In practical application, the possibility of approximately predicting results guides the choice of computations, both for indicatrices for individual particles and subsequently for indicatrices for polydispersed systems. The interpretation which must be sought for these variations actually partakes of the theories which apply at the extremities of the Mie range, that is, the theories of Rayleigh and Rayleigh-Gans on the one hand and diffraction and geometrical optics on the other. Moreover, the Rayleigh-Gans approximation furnishes elements which are highly important in predicting the scattering properties of the polydispersed systems considered.

Chapter 3 indicates how scattering properties may be computed for a population of particles of varied size, but assumed to be of the same nature ("polydispersed system"). The physical significance of these computations is discussed, taking into account the fact that the mathematical limits corresponding to minimum and maximum sizes must be posited relatively arbitrarily. This is a complex problem which will reappear on many occasions in Part 3.

The initial hypothesis for the computations was the assumption that marine particles can be assimilated by transparent spheres, which necessitates some discussion. Mie theory has been extended to the case of nonhomogeneous spheres and to the case of differently shaped particles (ellipsoids, cylinders, etc.),

[1]It is for this reason that references to the original works of Mie and also those of Rayleigh or Debye or Gans are omitted. In the work of Van de Hulst the reader will find an annotated bibliography with historical commentary at the end of each chapter.

but the computations are generally more complex. This is an initial reason to limit one's considerations to the case of spheres. A second, more convincing reason is related to the fact that marine particles are of random shape, and thus the sphere becomes the best approximation of their completely aleatory orientation. Confirmation for this hypothesis may be found in the experimental works of Hodkinson (1963) and of Holland and Gagne (1970). The latter investigators show that in practice irregular particles behave as equivalent spherical particles for scattering in natural light (except perhaps for backscattering), but that, on the other hand, polarization is appreciably affected. This possible effect will make it necessary to qualify the conclusions relative to polarization (Part 3).[2]

The other choice, that of the exclusive use of real indices should also be explained. The introduction of an imaginary component to represent particle absorption would make virtually no change in the results, since the term to be introduced, which would actually be fairly hypothetical, should in any case be very slight. Its influence would be negligible in this case, as is indicated by Fig. II.17, where, everything else in practice being equal, the computed scattering indicatrix is compared with the index 1.05 and that computed by O.B. Brown and H.R. Gordon (1972) for the index 1.05-0.10 i. The values approximately coincide, while the imaginary term corresponds to a level of absorption which is already extremely high (92% for passage through a layer 10 μm thick). /19

In conclusion, given the hypothesis used, the model thus constructed is undoubtedly idealized, but it does constitute an initial approach, or, if one prefers, a reference, in relation to which it will be possible to interpret the deviations.

1. States of Polarization and Scattering

1.1. Description of the State of Polarization by Stokes Parameters

For every beam of completely polarized monochromatic light there is a corresponding vector electrical field $\vec{E}$ whose components on two rectangular axes ($\vec{r}$, $\vec{l}$) within the wave plane are written:

$$E_r = p_r e^{i(\omega t - \phi_1)} \qquad E_l = p_l e^{i(\omega t - \phi_2)} \qquad (1.1)$$

[2] Polarization by marine particles is effectively different from that which would be due to spheres, but the difference is slight (G.F. Beardsley, 1968) (cf. Part 1, Section 5).

$\vec{r}$ and $\vec{l}$ may be of any magnitude but are chosen in such a way that the cross product $\vec{r} \wedge \vec{l}$ is oriented in the direction of propagation of the light (incident or scattered); r is perpendicular to the scattering plane, while $\vec{l}$ is within this plane (formed by the directions of propagation of the incident and scattered light considered). The four Stokes parameters are defined by:

$$I = E_r E_r^* + E_l E_l^*$$
$$Q = E_r E_r^* - E_l E_l^*$$
$$U = E_r E_l^* + E_l E_r^*$$
$$V = i\,(E_r R_l^* - E_l E_r^*) \quad .$$

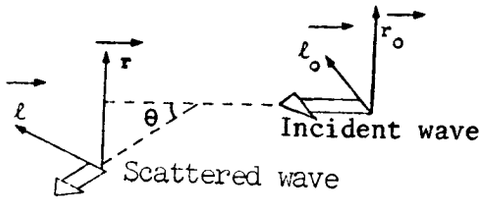

(1.2)

Given Eq. (1.1), three independent parameters are sufficient to describe the state of polarization: p_l, p_r and the phase shift $\delta = \phi_1 - \phi_2$; in actuality there is an equation linking the four Stokes parameters (see Eq. (1.6) below). Expanding Eq. (1.2) by means of Eq. (1.1), one obtains:

$$I = p_r^2 + p_l^2$$
$$Q = p_r^2 - p_l^2$$
$$U = 2\, p_r\, p_l \cos\delta$$
$$V = -2\, p_r\, p_l \sin\delta \quad .$$

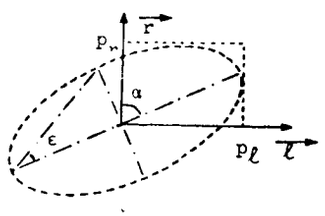

(1.3)

A simple geometric interpretation for this may be given: in a general case, the vector $\vec{E}$ describes an ellipse whose axes are different from the system $(\vec{l}, \vec{r})$. One assumes that $\tan \varepsilon = e$, where e is the ellipticity (ratio of small to large axis) and α is used to denote the angle fixing the direction of the large axis in relation to $\vec{r}$. α may be computed by reducing the ellipse to its principal axes:

$$\tan 2\alpha = 2 \cos\delta \frac{p_l p_r}{p_r^2 - p_l^2} \quad . \qquad (1.4)$$

The energy of vibration which does not depend on the phase difference is: $I = p_l^2 + p_r^2$, which is assumed equal to p^2. Geometric considerations lead to the following new expressions:

$$I = p^2 \quad , \quad Q = p^2 \cos 2\varepsilon \cos 2\alpha \quad , \quad U = p^2 \cos 2\varepsilon \sin 2\alpha \quad , \quad V = p^2 \sin 2\varepsilon, \qquad (1.5)$$

which make it possible to interpret the following specific cases:

-- If $p_l = p_r$, given Eq. (1.4), $\alpha = \pi/4$ and the vibration is:

* either linear, on the first bisecting line ($\delta = 0$) or the second ($\delta = \pi$). Q and V are nil, U is not nil, and the Stokes vector is written (1.0 ± 1.0), assuming I to be unity;

* or circular, to the right or left, depending on the sign of $\delta + \pm\pi/2$; in this case Q and U are nil, V is not nil and the result is (1, 0, 0, ±1).

-- If p_l or p_r is nil, $i = \pm Q$, the polarization is rectilinear, perpendicular or parallel to the scattering plane, respectively, and the parameters are (1, ±1, 0, 0).

Finally, in the general case, δ differs from the multiples of $\pi/2$, the vibration is elliptical and the Stokes parameters are of any magnitude. In all cases the following equation follows from Eq. (1.5):

$$I^2 = Q^2 + U^2 + V^2 \qquad (1.6)$$

which constitutes the total polarization criterion.

On the other hand, if the light is totally depolarized, E_1 and E_2 may still be assumed to exist, but they will have no phase coherence; p_l and p_r are equal and I remains defined in the same manner. However, none of the magnitudes Q, U, and V is statistically distinguishable from zero on the common time scale and the Stokes vector for natural light will be written (I, 0, 0, 0).

If partially polarized light is considered as the superimposition of natural light I_N and totally polarized light I_p, this is written as: $I = I_N + I_p$ or $I_p = (Q^2 + U^2 + V^2)^{1/2}$, resulting in the inequality: $I^2 > Q^2 + U^2 + V^2$. In its most general form, the rate of polarization (falling between 0 and 1) is the ratio:

$$\frac{(Q^2 + U^2 + V^2)^{1/2}}{I} \quad . \qquad (1.7)$$

1.2. Scattering Matrices /20

When two waves without phase correlation are superimposed, the Stokes parameters are additive. An optical device or, just

as readily, a scattering medium produces from an incident wave (I_0, Q_0, U_0, V_0) an emergent wave whose parameters (I, Q, U, V) result from linear combinations of the initial parameters; in other words, the device or the medium is characterized by a conversion matrix with 4 x 4 coefficients:

$$\begin{vmatrix} I \\ Q \\ U \\ V \end{vmatrix} = \begin{vmatrix} a_{11} & \cdots & \\ \cdots & & \\ & & a_{44} \end{vmatrix} \begin{vmatrix} I_0 \\ Q_0 \\ U_0 \\ V_0 \end{vmatrix} \qquad (1.8)$$

Changes in the vector field $\vec{E}_0$ relative to the incident wave are translated by the following linear equations linking the components:

$$E_r = A_1 E_{r,o} + A_4 E_{l,o} \qquad E_l = A_3 E_{r,o} + A_2 E_{l,o} \quad , \qquad (1.9)$$

$\begin{vmatrix} A_1 & A_4 \\ A_3 & A_2 \end{vmatrix}$ thus constitutes the amplitude transformation matrix, whose coefficients are complex. By introducing Eq. (1.9) into the definitions given by Eq. (1.2) and rearranging the factors, one computes the 16 components of matrix (1.8), which when applied to the initial parameters make it possible to compute the final parameters. These 16 coefficients are all real and consist of quadratic equations of type $A_i A_k$. For scattering, problems, "modified" Stokes parameters (I_1, I_2, U, V) are usually used; these are determined simply by: I_1 (or thus I_r) = 1/2(I + Q). I_2 (or thus I_ℓ) = 1/2(I - Q), and U and V remain unchanged. With this notation the total polarization criterion (1.6) will be written: $4 I_1 I_2 = U^2 + V^2$. The parameters characterizing natural light will be (1/2, 1/2, 0, 0) and the rate of polarization defined by Eq. (1.7) is reduced to: I_1, $I_2/I_1 + I_2$.

Scattering by Isotropic Spheres

If the particles possess certain types of symmetry, the number of independent coefficients in the matrix should be less than 16; an especially simplified case is that of scattering by isotropic spheres with a diagonal amplitude matrix ($A_3 = A_4 = 0$), the matrix of intensities which is determined from this becoming quasi-symmetrical:

$$\begin{vmatrix} I_1 \\ I_2 \\ U \\ V \end{vmatrix} = \begin{vmatrix} I_{1,0} \\ I_{2,0} \\ U_0 \\ V_0 \end{vmatrix} \cdot \begin{vmatrix} A_1A_1^* & 0 & 0 & 0 \\ 0 & A_2A_2^* & 0 & 0 \\ 0 & 0 & 1/2(A_1A_2^* + A_2A_1^*) & i/2(A_1A_2^* - A_2A_1^*) \\ 0 & 0 & -i/2(A_1A_2^* - A_2A_1^*) & 1/2(A_1A_2^* + A_2A_1^*) \end{vmatrix} . \qquad (1.11)$$

That is, noted with the intensity functions i (see definition in Appendix 1):

$$\begin{vmatrix} I_1 \\ I_2 \\ U \\ V \end{vmatrix} = \frac{1}{k^2} \begin{vmatrix} I_{1,0} \\ I_{2,0} \\ U_0 \\ V_0 \end{vmatrix} \cdot \begin{vmatrix} i_1 & 0 & 0 & 0 \\ 0 & i_2 & 0 & 0 \\ 0 & 0 & i_3 & i_4 \\ 0 & 0 & -i_4 & i_3 \end{vmatrix} . \qquad (1.12)$$

The factor $1/k^2$ (with $k = 2\pi/\lambda$) arises from the fact that the intensity functions are defined on the basis of the amplitude functions $S = kA$, by $i_1 = S_1S_1^*$, $i_2 = S_2S_2^*$ ...; the terms in the A matrix (1.11) are the effective partial cross sections p_1, p_2 ... (cf. definitions, Appendix 1). This matrix includes four terms which are not zero, of which only three are independent since they are linked by the following equation, which is easily verifiable on the basis of the expressions occurring in 1.11:

$$i_1i_2 = i_3^2 + i_4^2 \qquad (1.13)^3$$

Use of the matrix equation (1.12) makes it possible to predict the following cases:

-- if the incident light is polarized elliptically (I_1, I_2, U, V) or circularly (I_1, I_2, 0, V), or rectilinearly but not in the directions $\vec{r}$ or $\vec{l}$ (I_1, I_2, U, 0), the scattered light is generally elliptical, since $i_3 \neq i_4 \neq 0$; in addition it is completely polarized if the

---

[3] Perrin and Abragam (1951) have shown that when spheres of different size are present simultaneously, this equality no longer checks out except for the angles 0° and 180°, the direction of the inequality which replaces it being: $i_1i_2 > i_3^2 + i_4^2$. The polarization criterion can no longer be met and partial depolarization of the scattered light occurs when the incident wave is completely polarized. Perrin and Abragam, as well as Deirmendjian (1969) have suggested the use of this depolarization factor as an index of heterogeneity of size.

incident light is completely polarized, which can easily be verified by expanding the polarization criterion (1.10) for a scattered wave and incorporating the result into Eq. (1.13).

-- if the light is polarized rectilinearly in direction $\vec{r}$ or $\vec{l}$ (I_1, 0, 0, 0) or (I_2, 0, 0, 0), the scattered light integrally retains this property.

-- finally, if the light is natural (I/2, I/2, 0, 0), the scattered light is partially polarized, since in general i_1 differs from i_2; its total intensity is $I = (1/2)(I_1 + I_2)$ and the rate of polarization, as indicated above, is: $(i_1 - i_2)/(i_1 + i_2)$.

Case of 0° and 180° Angles

It will be seen later (Section 2.1.2) that $S_1(0) = S_2(0)$; given Eq. (1.11), it immediately follows that $i_1 = i_2 = i_3$ and that $i_4 = 0$: the scattering matrix is diagonal and the state of polarization, whatever it may be, is strictly maintained; a state of nonpolarization is also maintained. This may be predicted on the basis of considerations of symmetry: the previously defined "scattering plane" no longer exists, and since the particles are isotropic spheres there can be no preferred direction in this axial system. The same reasoning applies to scattering at 180°, with one difference: the scattering plane is no longer defined, but by by extension, that is, by having θ tend toward 180° (see preceding figure), it may be seen that the vector $\vec{l}$ for the scattered light is in an opposite direction to the vector $\vec{l}$ to which the incident vibration was adjusted (Eq. (1.13)). In this case (cf. Section 2.1.2), $S_1(180) = -S_2(180)$, and consequently $i_1 = i_2 = -i_3$, i_4 remaining zero. Any linear polarization remains unchanged, the reversal of direction of $\vec{l}$ compensating for the sign of U (= $-iU_0$). On the other hand, given this change in direction, V (= iV_0) retaining its sign, the direction of any circular (or elliptical) polarization is reversed. There has been research on practical applications for these last two points: the use of polarized light for illumination has been recommended in order to reduce the veil due to backscattering in submarine photography (R.O. Briggs and G.L. Hatchett, 1965, and G.D. Gilbert and J.C. Pernicka, 1966, to mention only the originators of this technique). /21

2. Scattering by a Spherical Particle

2.1. Formulation of the Mie Theory

In the case of a spherical or optically inactive isotropic particle, scattering is axially symmetrical, the axis being the direction of propagation of the incident wave; this is true on condition that the incident wave itself possesses this symmetry, which is particularly the case if the light is natural. Any plane containing this direction is a plane of symmetry; a plane which additionally contains the direction in which scattering is observed is the "scattering plane" (frequently termed "horizontal" due to the experimental arrangement frequently used). In this plane θ denotes the angle between the directions of the incident wave and the scattered wave; a single angular parameter is sufficient due to the rotational symmetry. As was previously seen (Section 1.2), the amplitudes of the components of the electrical field following the two rectangular axes considered in the plane of the scattered wave, one (index 1 or r) perpendicular and the other (index 2 or ℓ) parallel to the plane of diffusion, are $S_1(\theta)$ and $S_2(\theta)$ (S_3 and S_4 are zero). The corresponding intensity functions (without magnitude, cf. Appendix 1) are obtained by finding the square of the moduli:

$$\begin{aligned} i_1(\theta) &= S_1(\theta)\, S_1^*(\theta) \\ i_2(\theta) &= S_2(\theta)\, S_2^*(\theta) \end{aligned} \quad . \qquad (2.1)$$

Mie theory furnishes an exact solution for these amplitudes, which depend, in addition to angle θ, on:

-- the size of the particle, or more precisely, the relative size, by the intermediary of the parameter $\alpha = 2\pi r/\lambda$, where r is the radius of the spherical particle and λ the wavelength in the medium surrounding the particle;

-- the relative index of refraction m, that is, the real or complex index of the particle in relation to the index of the medium external to the particle.

This solution is expressed in the form of convergent series:

$$\begin{aligned} S_1(\alpha,m,\theta) &= \sum_{n=1}^{n=\infty} \frac{2n+1}{n(n+1)} \left(a_n \pi_n(\cos\theta) + b_n \tau_n(\cos\theta) \right) \\ S_2(\alpha,m,\theta) &= \sum_{n=1}^{n=\infty} \frac{2n+1}{n(n+1)} \left(b_n \pi_n(\cos\theta) + a_n \tau_n(\cos\theta) \right) \end{aligned} \quad , \qquad (2.2)$$

(n, positive integer, n = 1, 2, 3, ...).[4]

The parameters α, m and θ have different roles: each term in one or another of these series combines functions depending solely on the angle (by cos θ) with functions a_n and b_n which themselves depend only on the size of the index (α and m). The final amplitude appears as the sum of the amplitudes of the partial waves corresponding to each order n; the relative size of these partial waves is determined by the value of the "Mie coefficients" a_n and b_n. For a given index m, the value of these coefficients is higher if α is large, and as a result the number of partial waves to be taken into account (which may be related to those emitted by oscillating multipoles) is greater and the series slowly converge. Inversely, when α is sufficiently small the coefficients may be negligible from the second order on, and, as will be seen later, the equations are reduced to those of the Hertzian dipole; in other words, this limiting case is that of Rayleigh scattering.

2.1.1. The Functions π_n, τ_n and a_n, b_n

These are expressed by:

$$\pi_n(\cos\theta) = \frac{1}{\sin\theta} P'_n(\cos\theta)$$
$$\tau_n(\cos\theta) = \frac{d}{d\theta} P'_n(\cos\theta) \quad , \tag{2.3}$$

where P'_n is the first derivative of the Legendre polynomial of order P_n, and by:

$$a_n = \frac{\psi'_n(m\alpha)\,\psi_n(\alpha) - m\,\psi_n(m\alpha)\,\psi'(\alpha)}{\psi'_n(m\alpha)\,\zeta(\alpha) - m\,\psi_n(m\alpha)\,\zeta'(\alpha)}$$
$$b_n = \frac{m\psi'_n(m\alpha)\,\psi_n(\alpha) - \psi_n(m\alpha)\,\psi'_n(\alpha)}{m\psi'_n(m\alpha)\,\zeta_n(\alpha) - \psi_n(m\alpha)\,\zeta'_n(\alpha)} \quad , \tag{2.4}$$

where ψ_n is the Ricatti-Bessel function of order n and ψ'_n its first derivative; ζ_n is the Ricatti-Hankel function of order n and ζ'_n its first derivative. The arguments are α and the product $m\alpha$, as already defined.

These functions ψ_n and ζ_n are linked to the Bessel and Hankel functions of order n + 1/2 by:

---

[4] In these formulas and up to Section 2.2. the relative refractive index is denoted by "m" to distinguish it from the order "n.".

$$\psi_n(x) = \left(\frac{\pi x}{2}\right)^{1/2} J_{n+1/2}(x) \qquad \zeta_n(x) = \left(\frac{\pi x}{2}\right)^{1/2} H_{n+1/2}(x), \tag{2.5}$$

where

$$H_n(x) = J_n - i Y_n(x) \quad . \tag{2.6}$$

J_n and Y_n are the Bessel functions of first and second type of order n, respectively. H_n is the Hankel function of the same order.

Introducing the Ricatti-Bessel function of the second type χ_n: /22

$$\chi_n = -\left(\frac{\pi x}{2}\right)^{1/2} Y_{n+1/2}(x), \tag{2.7}$$

$\zeta_n(x)$ is thus expressed:

$$\zeta_n(x) = \psi_n(x) + i \chi_n(x). \tag{2.8}$$

It should be noted that the coefficients a_n and b_n are complex due to the presence of the function ζ_n, even when the argument (mα) is real (nonabsorbing particles). In this last case, however, real particles are immediately separable from imaginary particles, which is shown by substituting formula (2.8) in Eqs. (2.4). It is possible to compute these series in practice, since at each order, the values for functions a_n, b_n, π_n and τ_n may be derived from the relative values for preceding orders by using the recursive equations established for Legendre polynomials and for Bessel functions. This is examined in greater detail in Appendix 2, "Computation procedure and adaptation to computer." In this appendix it will be shown that in the specific case examined previously, when m is real, after separation of the real and imaginary fractions, a_n, like b_n may be given in the form:

$$\text{Re}\{a_n\} = \frac{1}{1 + p^2/q^2} \qquad \text{Im}\{a_n\} = \frac{-x/q}{1 + p^2/q^2},$$

since p and q are real numbers themselves, p/q may assume any value between $\pm\infty$ depending on the order n; this makes it possible to reveal an important characteristic of the series of complex numbers a_n and b_n, demonstrated in a slightly different manner by Van de Hulst: the locus of the pattern of the a_n (or b_n) factors is computed simply by first assuming: $X = \text{Re}\{a_n\}$ and $Y = \text{Im}\{a_n\}$ and then by eliminating p/q between X and Y; one obtains the equation $Y^2 + X^2 - X = 0$, the equation for a circle centered on the point: Im = 0, Re = 0.5, with a radius of 0.5.

Figure II.1 shows the pattern of the successive values assumed for the first term a_1 when α varies from 1 to 100, the computations being performed for an index of refraction of 1.05.

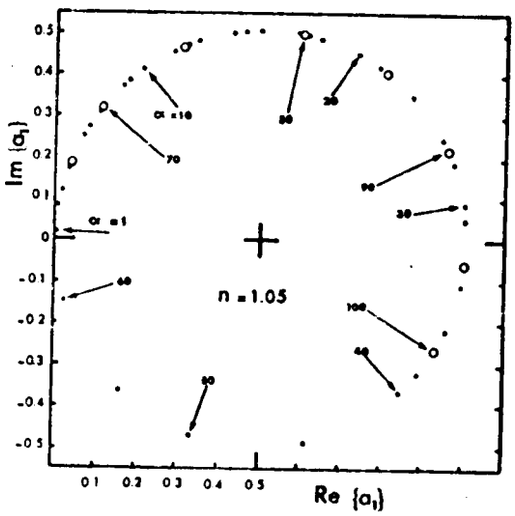

Fig. II.1. Values for the complex coefficient a_1 for a real index of refraction of 1.05. Examples corresponding to complex index values may be found particularly in the work of D. Deirmendjian (1969); the loci of the a_1 images no longer form a circle, but complex spiral curves remaining within the circle.

When θ varies from 0 to 180°, the functions π_n and τ_n operate in a manner whose complexity increases as the order n is raised; at the first orders one has:

$$\pi_1 (\cos\theta) = 1$$
$$\pi_2 (\cos\theta) = 3\cos\theta \qquad (2.9A)$$

$$\tau_1 (\cos\theta) = \cos\theta$$
$$\tau_2 (\cos\theta) = 3\cos 2\theta \qquad (2.9B)$$

At higher orders one begins to see oscillations of increasing number and amplitude; the largest amplitudes correspond to the values $\theta = 0°$ and $\theta = 180°$. Using the recursive equations (2.7) and (2.8)[5] it is easy to determine that at any order one has: for $\theta = 0°$:

$$\pi_n (1) = \tau_n (1) = (1/2)\, n\,(n+1), \qquad (2.10)$$

and for $\theta = 180°$

$$\pi_n (-1) = \tau_n (-1) = (-1)^n (1/2)\, n\,(n+1) \qquad (2.11)$$

As will be seen below, these equations will be useful when an attempt is made to interpret scattering at the specific angles considered, and also in computing the overall efficiency of extinction. (This is reduced to the overall efficiency for

[5] Established in Appendix 2.

scattering in the case of nonabsorbing particles: see Appendix: "Definitions."

2.1.2. The Intensity Functions $i_1(\theta)$ and $i_2(\theta)$

Specific case of the angles $\theta = 0°$ and $180°$

Combining Eq. (2.2) with Eq. (2.10) and then with Eq. (2.11), one immediately sees that:

$$S_1(0) = S_2(0) = 1/2 \sum_{n=1}^{n=\infty} (2n+1)(a_n + b_n) \quad . \tag{2.12}$$

and that:

$$S_1(180) = -S_2(180) = 1/2 \sum_{n=1}^{n=\infty} (-1)^n (2n+1)(b_n - a_n) \quad . \tag{2.13}$$

Taking the square of the moduli in order to obtain the intensities, it may be seen that $i_1 = i_2$ both at 0° and at 180°. The consequences in regard to polarization have been examined previously (Section 1.2).

Any given angle θ; variations in indicatrices with size (real m)

When α is sufficiently small (< approximately 0.2), the series (2.2) expressing S_1 and S_2 are reduced to the first term, π_1 and τ_1 having the values given by (2.9A). Furthermore (cf. Appendix 2), b_1, which numerically is of the same order of magnitude as a_2, is negligible, and once again Rayleigh scattering is obtained, with:

$$i_1 = |S_1|^2 = \text{Const} \qquad i_2 = |S_2|^2 = \text{Const} \cos^2\theta \quad .$$

The vertical component is constant, while the horizontal component, varying with $\cos^2\theta$, becomes zero for $\theta = 90°$; the scattered light is completely polarized. The indicatrices for the two components and for the total intensity $i_T = (1/2)(i_1 + i_2)$ are symmetrical. When α increases all the values increase, but asymmetry appears and becomes reinforced: there is less scattering at the tail end of the curve ($\theta > 90°$) than there is in its initial part ($\theta < 90°$), and the minimum i_T at 90° disappears. On the other hand, when α reaches the value 2.25, a new minimum i_T appears to the rear (180°) and "migrates" toward the center part of the indicatrix, while another minimum appears in turn at 180° when α exceeds the value 4 (cf. the figures given in Appendix 2). The same process is repeated to the extent that the size parameter increases: undulations appear at the tail end and grow more

constricted. This is the result of taking into account increasingly high orders of the functions π_n and τ_n, since when α increases the series of Mie coefficients gradually converge toward zero. Thus when $\alpha = 100$, for example, the order 117 must be reached in order for a_n and b_n to be considered zero[6], and thus the first 117 functions π_n and τ_n come into play; the corresponding indicatrix has approximately 100 undulations. Aside from these undulations, the general tendency is still reinforcement of the asymmetry. If one no longer considers the intensity i_T, but the two components i_1 and i_2, their behavior is analogous, although more complex. The rate of polarization $(i_1 - i_2)/(i_1 + i_2)$ also oscillates between +1 and -1. (The negative values correspond to cases in which the amplitude of horizontal vibration is greater than that of vertical vibration.)

This description remains qualitatively valid when the index of refraction (real) varies within relatively broad limits. However, it should be stated that if the index is extremely close to 1, the amplitude of the oscillations of i_T is maximal, and in general, the difference between the two components i_1 and i_2 is large, resulting in strong polarization. When the index differs from 1, the oscillations are "damped" (and the polarization is decreased), as shown by Fig. II.2. In addition, for a given relative α size, the number of oscillations is higher, while the overall asymmetry is less marked. These points will be discussed in greater detail below and will be interpreted with the use of the computed numerical values.

2.2. Numerical Results and Interpretation

/24

Mie theory was used to calculate scattering indicatrices in several cases, enumerated below. There is a twofold reason for this preliminary calculation. First, published Mie function tables are extremely incomplete, especially in regard to the indices and sizes used within the framework of this study, and second, the introduction of a large number of tabulated data -- when available -- into the computer remains an excessively long operation. For subsequent use, it is more efficient in the long run to provide for the generation of useful indicatrices in the program. In addition, it has been found indispensable to be able to choose the step of the calculations both in regard to the size and index of the particles and in regard to the scattering angle.

[6] This implies the choice of a criterion: a_n and b_n are considered to be zero, and consequently the calculus stops at this order, when the moduli of one or another of these coefficients reach values lower than 10^{-7} (cf. Appendix 2).

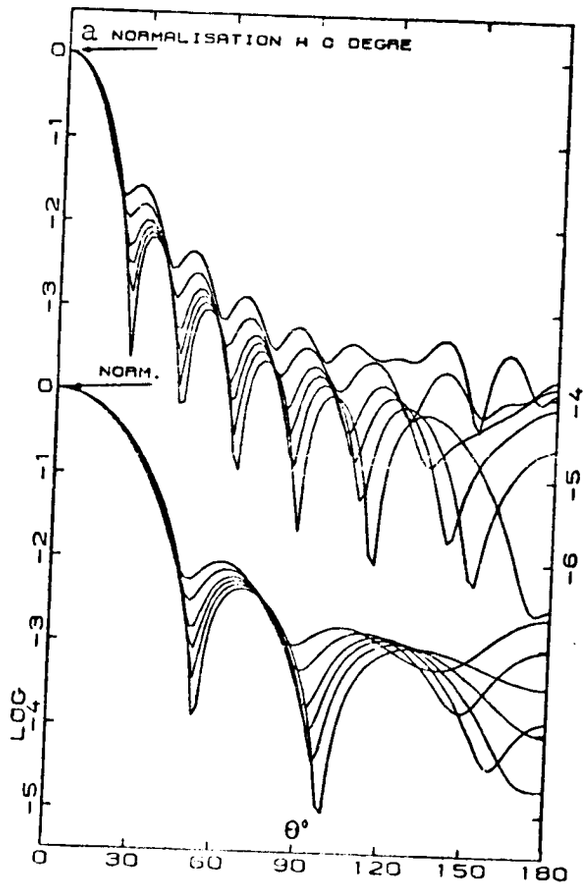

Fig. II.2. Scattering indicatrices normalized to 0°: in the upper group $\alpha = 10$, and in the lower group $\alpha = 5$. In both cases, beginning at the bottom one finds in succession indicatrices calculated for the following indices of refraction: 1.02, 1.05, 1.075, 1.10, 1.15 and 1.20. The ordinate scale is logarithmic.

Key: a. Normalization to 0°.

/25

-- the intensity functions $i_1(\theta)$ and $i_2(\theta)$, and consequently the total intensity function $i_T(\theta) = (1/2)\{i_1(\theta) + i_2(\theta)\}$ and the rate of polarization $p = \{i_1(\theta) - i_2(\theta)/i_1(\theta) + i_2(\theta)\}$ have been computed for every 2° from 0° to 180° (in rare cases a step of 1° was used).

-- for each index, the calculus was repeated for 60 values for the size parameter α, that is: 0.2, (0.2), 2, (0.5), 5, (1), 20, (2), 40 (5), 100, (10), 140,(20), and 200, the numbers between parentheses indicating the α incrementation used.

-- finally, this entire set of operations was repeated five times for the following indices of refraction: 1.02, 1.05, 1.075, 1.10 and 1.15.

-- for each case, that is, for each pair of values assigned to α and n[7], the real and imaginary fractions of S(0), the amplitude at 0°, and the scattering efficiency factor Q were also computed (cf. Appendix 1 and Section 2.2.7).

For reasons given in Appendix 2 ("Adaptation and procedure for calculation on computer"), the use of double precision (17 significant digits) is indispensable. However, it is the

[7]The notation n (rather than m) is again used to denote the index of refraction. (In the future m will designate the characteristic exponent of distribution.)

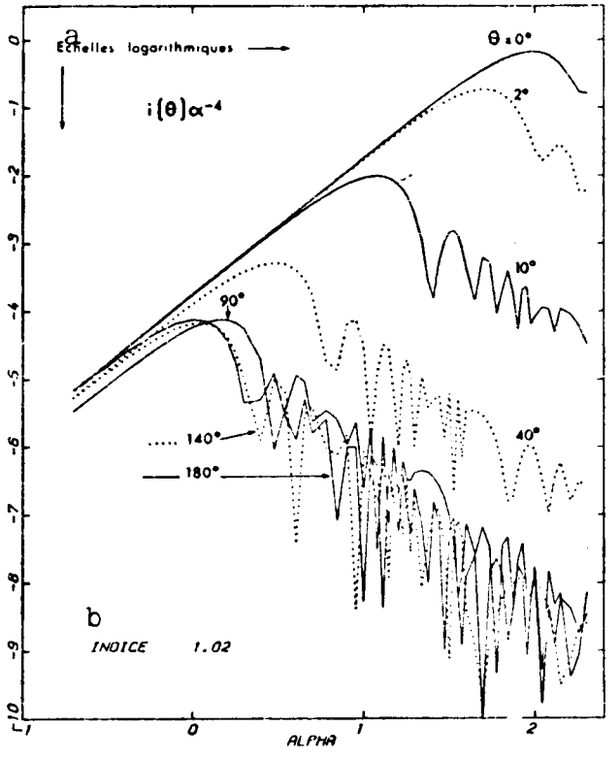

Fig. II.3

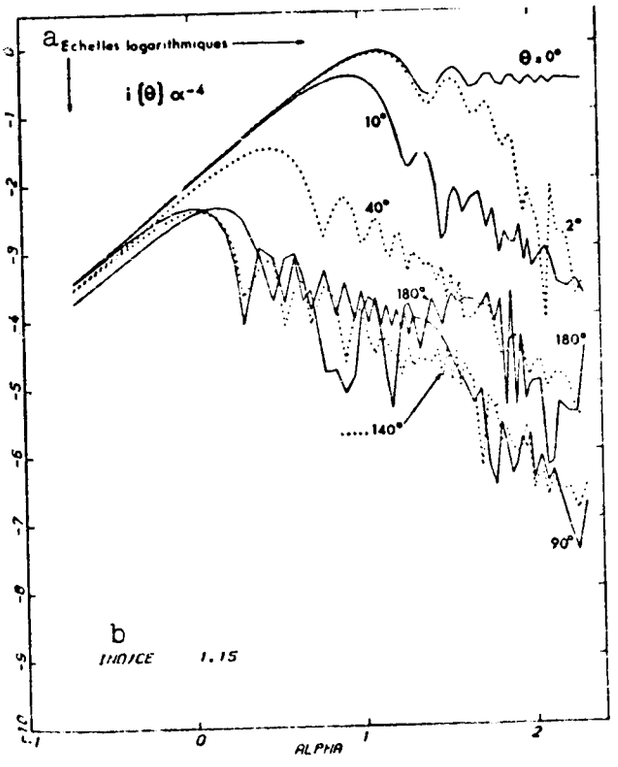

Fig. II.4

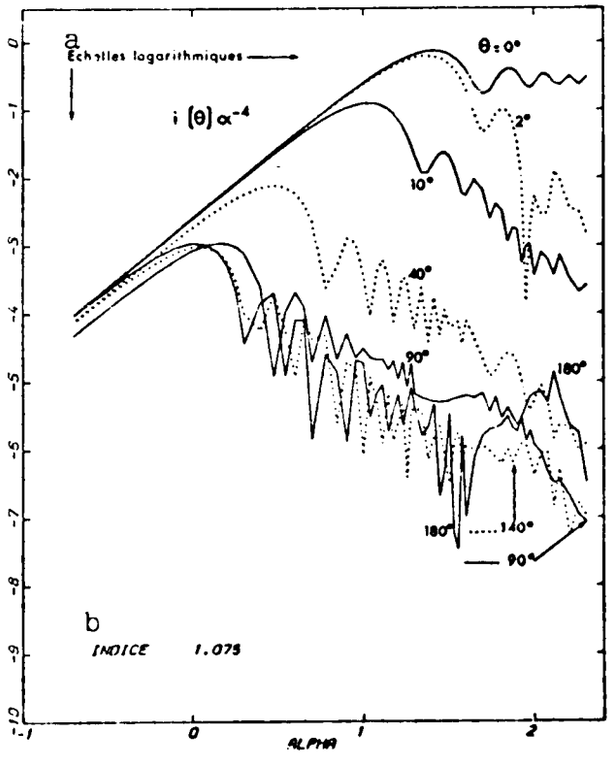

Fig. II.5

Graphs of the functions $i(\theta)\alpha^{-4}$ for the indicated values for θ. Each figure corresponds to an index of refraction. The size parameter α ranges from 0.2 to 200. The figure dealing with the index 1.05 has appeared elsewhere (A. Morel, 1972a).

Key: a. Logarithmic scales
b. Index

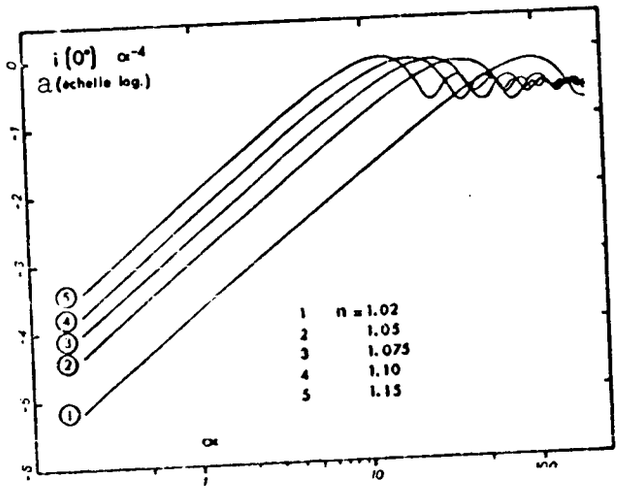

Fig. II.6. Graphs of a single function, but for $\theta = 0°$ and for various values for the index of refraction n.

Key: a. Logarithmic scale

criterion adopted for convergence of the series which, by terminating the calculus, determines its precision. In the most unfavorable cases (high values for α) the precision corresponds to six significant digits, whatever the value of the number (expressed as a floating point decimal) might otherwise be.

2.2.1. The Functions $i_T(\theta)\alpha^{-4}$

In order to present these results in summary form, variations in the functions $i_T(\theta)\alpha^{-4}$ when the size parameter α varies from 0.2 to 200 have been plotted for each value for the index of refraction (Figs. II.3 and II.5). Six curves are plotted in each of these figures, corresponding to the following six values for θ: 0°, 2°, 10°, 40°, 90° and 180°. For the sake of clarity, the number of curves has been purposely limited; however, at least schematically these diagrams show how the indicatrices vary as the size increases.

Choice of the expression, or more precisely, the exponent -4 affecting α was not arbitrary. As will be seen later (Section 2.2.8), it arises from the expression for scattering, which constitutes a limiting expression for scattering at 0° when the particles are of sufficiently large size.

The following remarks may be made in regard to these figures:

a. For the lowest values for α, the curves corresponding to symmetrical scattering angles 0° to 180° and 40° to 140°, coincide, while the curve for 90° is located below. The initial linear part of all these curves shows a gradient of +2. Finally, for a given value for α (0.2, for example), the values for $i(\theta)\alpha^{-4}$ increase regularly with the index (cf. Fig. II.6, which shows all the curves relative solely to $\theta = 0$, but corresponding to various indices).

b. In regard to the angle 0°, the linear part of this curve is extended until high values for the parameter α are reached. Figure II.6 shows that this value for α increases as

the index of refraction approaches 1. (The curves for 2° show similar development, but to a lesser degree.)

c. After the linear part has been completed and a maximum has been reached, all the curves for 0° show oscillations whose amplitude decreases as α increases. These oscillations occur around a fixed limiting value, which is 0.25.

d. The curves for angles θ other than 0° also reach a maximum, beyond which the decrease is accompanied by complex oscillations.[8] This maximum appears for values for α which are greater as θ is smaller. Comparison of these figures shows that the positions of the respective maximums are virtually not influenced by the value of the index; thus in contrast to the situation at 0°, the corresponding value for α depends only on the angle and not on the index.

e. Ignoring these oscillations, the mean gradient of these curves ($\theta \neq 0$) is established approximately around -2.3 for the indices 1.02, 1.05 and 1.075, and around -2 for the higher indices 1.10 and 1.15.

f. Finally, the curves for $\theta = 180°$ always comprise more or less of an exception: the oscillations are more erratic, and to the degree that it is still possible to speak of a mean gradient, this gradient is small or zero, especially when the index is high.

These remarks are made in view of the numerical results obtained from the Mie mathematical formulation; these findings have no interpretive value in themselves. Mie theory furnishes a rigorous solution and covers all cases from that of the extremely small particles falling within the province of Rayleigh theory to that of particles of sufficiently large size to be dealt with by the classical theories of geometrical optics and scattering. These theories, which actually are strictly applicable only to the limits and can be used only in an approximate manner in the intermediate range, are nevertheless able to furnish the elements of interpretation more easily and to give the results of computation a clearer physical significance.

---

[8] The curves are plotted by joining the calculated points in linear fashion. The intervals at which α is calculated make it possible to show the behavior of the functions only in an approximate manner, without describing this behavior in detail.

Thus Rayleigh theory acounts for the first of the above remarks, while points b and d can be elucidated by Rayleigh-Gans theory.[9] The other points -- point e only in part -- may be satisfactorily explained by reference to scattering or geometrical optics (reflection, refraction). These various interpretations will be examined in turn; their usefulness lies in the possibilities they offer for predicting the nature of the indicatrices, for a given particle as well as for a system of polydispersed particles. /26

2.2.2. Rayleigh Scattering Range

It has previously been seen (2.1.2) that in the case of low values for the parameter α (0.2, for example), the Mie formulas yielding $i_1(\theta)$ and $i_2(\theta)$ are reduced to simple equations revealing an angular dependence which is that of Rayleigh scattering. Rayleigh's radiating dipole theory gives the following expression for these components, i_1 and i_2:

$$\begin{vmatrix} i_1 \\ i_2 \end{vmatrix} = k^6 p^2 \begin{vmatrix} 1 \\ \cos^2\theta \end{vmatrix}$$

related to physical magnitudes which are the wave number $k = 2\pi/\lambda$, and the polarizability p of the particle[10], having the dimensions L^3. If the particle is an isotropic sphere with radius r, volume V and index of refraction n, the polarizability is furnished by the equation given by Lorenz-Lorentz:

$$p = \frac{3}{4\pi} \frac{n^2-1}{n^2+2} V$$

or

$$\frac{n^2-1}{n^2+2} r^3 ;$$

replacing kr with α and assuming $(n^2-1)/(n^2+2) = \Lambda$, this becomes:

---

[9] An extension of Rayleigh theory proper, made by Rayleigh himself at the time (1914) and expanded by Gans (1925) (cf. H.C. Van de Hulst, 1957).

[10] Polarizability is the induced moment $\vec{P}$ when the electric field $\vec{E}$ is at unit strength. Vectors $\vec{P}$ and $\vec{E}$ are parallel for an isotropic dielectric, and in this case p is a scalar; in the more general case it is a tensor, $\vec{P}$ and $\vec{E}$ having different directions.

(2.15)

Within the range of applicability of the Rayleigh theory ($\alpha << 1$), the quantities $i_T(\theta)\alpha^{-4}$ represented graphically are thus expressed by:

$$i_1 = \alpha^6 \Lambda^2 \quad , \qquad i_2 = \alpha^6 \Lambda^2 \cos^2 \theta \quad .$$

Given as a function of α and in logarithmic coordinates, these quantities are represented by lines with a gradient +2, no matter what values are attributed to θ. The respective positions of these lines obviously translate the symmetry of the scattering indicatrix in relation to 90° (cf. Remark a).

Finally, the index of refraction comes into play to determine the magnitude of the phenomeon through Λ^2. For a given relative size α and for a given angle (for example $\theta = 0°$, which is the case illustrated by Fig. II.6), the scattered intensity is proportional to Λ^2. If one assumes the index to be relatively close to 1, Λ is expressed approximately by:

$$\Lambda = (2/3)(n - 1) \tag{2.16}$$

i and i' being the intensities scattered by particles of the same size and the index being n and n' respectively, the result is:

$$\frac{i}{i'} = \frac{\Lambda^2}{\Lambda'^2} = \left(\frac{n-1}{n'-1}\right)^2 \tag{2.17}$$

The size of the intensity functions therefore increases as the index of refraction becomes farther from 1. As Fig. II.6 shows, for example, the intensities are multiplied by 25 when the index of refraction changes from 1.02 to 1.10.

2.2.3. Rayleigh-Gans Approximation

The applicability condition for the Rayleigh theory,

$$\alpha = (2\pi r/\lambda) << 1 \quad , \tag{2.18}$$

is based on the following physical hypothesis: the particle must be assumed to be small enough so that the electric field applied is of uniform intensity. To make a simple extension of this theory to a larger particle and to apply it to each part of this particle considered as an independent dipole, it must be

assumed that at least on a first approximation, the electric field remains the same for all the constituent parts of the particle. In other words, the amplitude and phase of the wave reaching a given part must not be changed in any appreciable manner by the presence of the other parts. This implies that the scattered energy is low and the phase retardation is negligible, which is expressed by the condition:

$$\frac{2\pi r}{\lambda} |n-1| \ll 1 \quad ,$$

λ corresponds to the wavelength within the medium outside the particle and n to the relative index of the particle in relation to this medium. (The expression corresponds to a maximum phase shift, that is, to that of the radius passing diametrically through the particle.) This condition is generally written:

$$\rho \ll 1 \qquad (2.19)$$

the parameter ρ, combining the relative index and size, being assumed equal to $2\alpha|n-1|$. This condition can obviously be met for high α values, provided that n is very close to 1.

Scattering at 0°

In general, waves scattered by the constituent parts of the particle are not merely additive, since they interfere. However, according to the initial hypothesis (stating that the material presence of the particle does not modify the condition of the wave), the scattered waves are necessarily in phase in the specific direction 0°: the prolongation of the path of the incident wave is exactly compensated by a decrease in the length of the scattered wave and vice versa, no matter what the spatial position of the various components. In this particular case, where the amplitudes are strictly additive, the expression for intensity given by Rayleigh theory retains its applicability, and although α is smaller, Eqs. (2.15) remain: $i_T(0°) = \alpha^6\Lambda^2$. This furnishes an explanation for Remark b. In reality this remark is incomplete, since the linearity on log-log graphs is extended beyond the range of applicability, while the condition $\rho < 1$ is no longer fulfilled. This prolongation provides the basis for the term given by Penndorf (1960), the "extended Rayleigh region." As will be seen later (2.2), the limit of this zone is fixed by the value 4.09 for parameter ρ; the corresponding value for ρ thus increases as the index approaches 1. /27

General Case

For angles other than 0°, geometric compensation for path differences no longer applies; consequently the amplitude of the scattered wave is obtained by multiplying the amplitude determined by means of Rayleigh theory by a factor $F(\theta)$ representing the interferences and dependent on θ (or on two angles θ and ϕ if the phenomenon considered is not one of revolution.

$$i_T(\theta) = \frac{i_1(\theta) + i_2(\theta)}{2} = (1/2)\,\alpha^6\,A^2\,(1 + \cos^2\theta)\,F(\theta)\,. \qquad (2.20)$$

$F(\theta)$ is a function whose value is 1 for $\theta = 0°$, and less than 1 for any other angle. This function is calculated by integration extended to the entire particle; the differential component consists of elemental "slices" representing constant path differences. The integral may be expressed by the usual functions in the case of particles with simple geometric shapes; with spherical particles one obtains:

$$F(\theta) = [G(U)]^2, \qquad (2.21)$$

with $U = 2\alpha \sin\theta/2$, and

$$G(U) = \left(\frac{\pi}{2}\right)^{1/2} \frac{J_{3/2}(U)}{U^{3/2}}\,, \qquad (2.22)$$

where $J_{3/2}(U)$ is a Bessel function of the first type of order 3/2. This function individually multiplies the two components i_1 and i_2; as a result, the total polarization at $\theta = 90°$ characteristic of Rayleigh scattering is retained. The scattering indicatrix becomes asymmetrical due to a decrease in the values at large angles. The effect becomes more appreciable as the size α increases. When the function $J_{3/2}$ reaches zero for the first time, that is, when the argument U reaches the value 4.49, a minimum appears which corresponds to extinction due to interference: for $\alpha = 2.25$ it appears at 180°. As α increases this minimum progresses toward the small angles, while a second minimum corresponding to a second zero appears in turn (when $\alpha = 3.86$), and so on. Successive minimums arise at the tail end and the indicatrix forms a system of increasingly constricted oscillations, while the predominance of scattering in the forward part (at 0° and neighboring angles) becomes continually more marked. The "scattering pattern" resembles the Fraunhofer diffraction pattern, but the radii of the angles of the rings are different. As the particle size increases, the one pattern gradually is transformed into the other; in British literature this transition zone is termed the zone of "anomalous diffraction." In the final

analysis, the shape of the indicatrix determined by the function G(U) is therefore independent of the value of the refractive index (given that n-1 remains low), since the argument U depends only on θ and α. If U_1, U_2 ... denote the successive values for the argument at which the function $J_{3/2}$ becomes zero, the equations:

$$\begin{aligned} 2\,\alpha \sin \theta/2 &= U_1 \ (=4.49) \\ &= U_2 \ (=7.73) \end{aligned} \qquad (2.23)$$

represent the geometric loci of successive minimums in the plane (α, θ). Curves representing the first six minimums are shown in Fig. II.7. As an example it may be seen on this figure that if $\alpha = 5$, the scattering indicatrix should have two minimums at 55° and 110° and the beginning of a third at 180°; if $\alpha = 10$, there are five minimums and the beginning of a sixth.

Figure II.2 shows that this is indeed the case for the lowest value for the index (1.02), but as the index increases, the system of minimums progresses toward small angles.

Returning to Remark d, curves corresponding to the various angles θ become detached from the curve relative to 0°, this detachment being produced by the appearance of the first minimum for the angle θ under consideration (first equation 2.23): the smaller the angle θ, the greater will be the corresponding value for α, and this will occur independent of the index, since it does not figure in the equation. The table below (first line) shows the theoretical values of α for which this minimum appears at the angles θ indicated:

θ =	180°	140°	90°	45°	20°	10°	2°
Rayleigh Gars α =	2.24	2.42	3.17	6.65	12.9	25.8	(128)
Diffraction α =			3.83	7.95	11.9	22.0	109

2.2.4. Approximation by Diffraction Theory /28

It should be noted that when the minimum occurs at 10°, that is, when $\alpha = 25.8$, the value of ρ is 1 if the index is 1.02, but ρ reaches 5 if $n = 1.10$. In other words, normally there is no longer justification for use of the Rayleigh-Gans theory at this point, and still less for an angle of 2°. For these high magnitudes, diffraction may furnish an approximation for calculation of the angular distribution of intensities, which for a circular diffraction opening is expressed by:

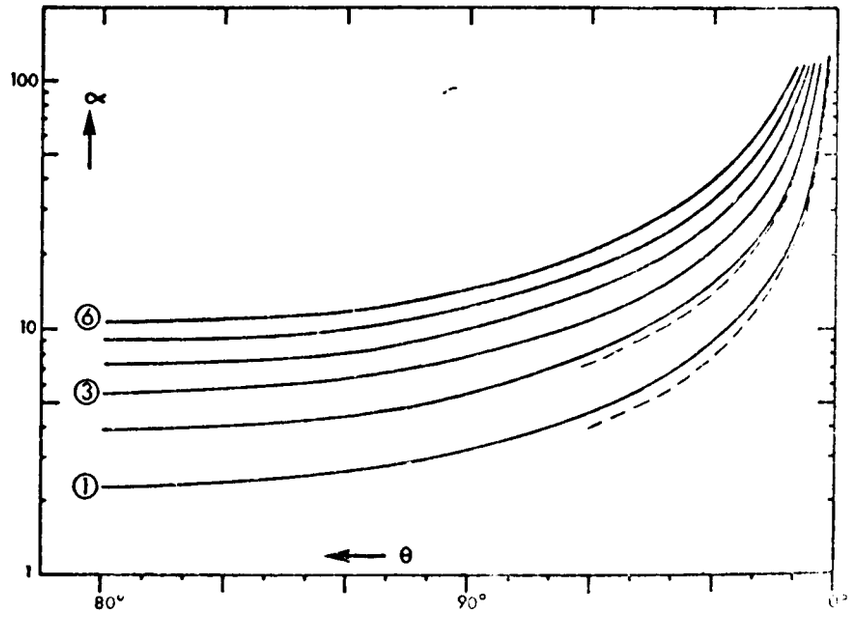

Fig. II.7. Angular position of the first six minimums according to Rayleigh-Gans theory (Eqs. (2.23)); the dotted line represents the first two diffraction minimums (see Eqs. (2.24) below).

$$F'(\theta) = \frac{2 J_1(U)}{U}, \qquad (2.24)$$

with $U = \alpha \sin \theta$. The Bessel function $J_1(U)$ first reaches zero when the argument U reaches the value 3.83. This makes it possible to compute the values which should be assumed by the size parameter α so that the radius of the angle of the first dark ring has the values 2°, 10° ...; the second line in the above table shows these values. This approximation by diffraction is more appropriate than use of Rayleigh-Gans theory to explain the shape of the indicatrix in the small angle range[11], and also for other angles if the index differs markedly from 1. This particularly explains the

[11] The diffraction minimum occurs at $\alpha = 10.9$ for all the curves corresponding to 2° given in Figs. II.3 through II.5. However, other minimums have appeared earlier (except when n = 1.02): these correspond to the minimums observed at 0° or, as will be seen later, to those of the efficiency Q. This is interpreted as the result of favorable or unfavorable interference between the wave passing through the particle ("refracted" wave) and the diffracted wave forming the central lobe.

increased number and constriction of the oscillations of the indicatrix as the index increases (Fig. II.2), as can be predicted on the basis of Fig. II.7.

In conclusion it should be noted, however, that the position of the first minimum for a given angle θ corresponds to values for α given in one or the other list, depending on the approximation which can be used; but these values are close enough to account for Remark d.

2.2.5. Role of Refraction and Reflection

Independently of diffraction, the geometrical optics approach implies taking into consideration reflection and refraction: the interaction of these three phenomena and the possible interferences among the three wave types combine to form scattering. Since the function $F'(\theta)$ can assume the value zero, the minimums would be total extinctions if the light scattered by the interplay of reflections and refractions were not added to the scattered light. The magnitude of the energy scattered in this manner is governed by the value of the Fresnel reflection coefficients and thus increases as a function of the refractiveness of the particle: the minimums are thus attenuated (cf. Fig. II.2) and the general asymmetry is not so pronounced (Figs. II.3 to II.5 and Remark e), but on the other hand backscattering (for angles in the vicinity of 180°) is accentuated (Remark f). It should be noted that the total extinction of Rayleigh-Gans theory, which brings $F(\theta)$ to zero, is no longer found in this case: in this range the minimums are also extremely marked if the index is close to 1, and are attenuated as it departs from 1. The preceding physical interpretation can be used only by extension: the size of the particle relative to the wavelength no longer permits strict use of the terms "reflection" and "refraction."

Finally, application of the laws of geometrical optics has made it possible to explain the phenomenon of the rainbow (it is generally acknowledged that Descartes himself has given a correct interpretation of this phenomenon), which is due to a concentration of energy following an internal reflection (or two internal reflections for the "second" rainbow) within the droplet. The corresponding angle of emergence, which is that of minimum deviation for the first rainbow, is 138° for water droplets. The same calculation, repeated with the use of other index values, shows that the "rainbow" moves toward lower angles θ as the index approaches 1 (Fig. II.8). The figures given in Appendix 2 show that a stable maximum is quite apparent (toward 75°, for an index of 1.075) when the size is sufficiently large.

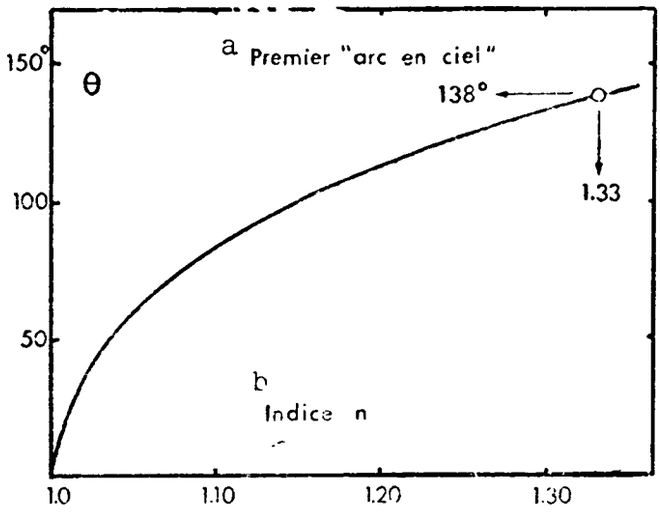

Fig. II.8. Angular position of "rainbow" depending on the index of refraction.

Key: a. First "rainbow"
b. Index n

Other indicatrices for particle systems will reveal this phenomenon very clearly, within the predicted range of angles, taking into account the value of the index (see Fig. II.17 and in Part 3, Figs. III.2, III.7 and III.12).

2.2.6. General Remarks on the Asymmetry of the Indicatrix /29

In summary, for the reasons given previously, functions $i(\theta)\alpha^{-4}$ each attain a maximum for an α value which in practice is fixed, no matter what the value of the index may be. On the other hand, the maximum reached by the curves corresponding to 0° occurs for an increasing value as the index approaches 1. As a result, the difference between the curve for 0° and the other curves, which determines the overall asymmetry, becomes greater as the index approaches 1. As an example, when $\alpha = 200$ the indicatrix covers approximately eight orders of magnitude if $n = 1.02$, and only five or six when $n = 1.15$ (cf. Figs. II.3 and II.5). This observation will take on its full importance when an attempt is made to predict the results of weighted addition of indicatrices.

2.2.7. Total Scattering Coefficient. Efficiency Factor

The scattering efficiency factor Q_{sc} is defined as the ratio of the effective scattering cross section to the geometrical cross section of the particle (πr^2 for a spherical particle of radius r), or in other words, as the ratio of the total scattered flux to the incident flux on the particle, that is, on a section of area πr^2 if the particle is spherical. These definitions are given with greater precision in Appendix 1. An efficiency factor for attenuation is also defined; this differs from the preceding only if the particle is absorbing, in which case one has:

$$Q_{attenuation} = Q_{absorption} + Q_{scattering}$$

This attenuation factor is linked to the amplitude S(0) by an equation developed primarily by Van de Hulst (1949, 1957) (and known as the "extinction formula"):

$$Q_{att.} = \frac{4}{\alpha 2} \text{ Re } \{S(0)\} \quad , \tag{2.25}$$

with $S_1(0) = S_2(0)$, which with reference to Eq. (2.12) is expressed as:

$$Q_{att.} = \frac{2}{\alpha 2} \sum_{n=1}^{n=\infty} (2n+1) \text{ Re } \{a_n + b_n\} \quad . \tag{2.26}$$

The integral, extended to 4π steradians, furnishing the scattering efficiency factor is (cf. Appendix 1):

$$Q_{sc} = \frac{1}{2 \pi a^2} \iint_{4\pi} (i_1(\theta,\psi) + i_2(\theta,\psi)) \, d\Omega \quad ,$$

or, if the phenomenon is one of revolution:

$$Q_{sc} = \frac{1}{\alpha 2} \int_0^{\pi} (i_1(\theta) + i_2(\theta)) \sin\theta \, d\theta \quad . \tag{2.27}$$

Debye (1909) has shown that, related to series, this integral is ultimately reduced to (cf. Van de Hulst, p. 128):

$$Q_{sc} = \frac{2}{\alpha 2} \sum_{n=1}^{\infty} (2n+1) \, (|a_n|^2 + |b_n|^2) \quad , \tag{2.28}$$

$|a_n|^2$, $|b_n|^2$ being the squares of the moduli of the Mie coefficients.

When the index of refraction is real, it has been noted (Fig. II.1) that images in the complex plane of numbers a_n and b_n are on a circle with radius 1/2. Geometrically it may be seen that for any value for a_n or b_n, one has:

$$\frac{|a_n|}{\text{Re } (a_n)} = \frac{1}{|a_n|} \quad , \qquad \text{or} \qquad |a_n|^2 = \text{Re } (a_n) \quad .$$

The real part of a_n is numerically equal to the square of its modulus. Eqations (2.26) and (2.28) are thus mathematically identical, which should necessarily be the case since in the

absence of absorption, the attenuation is due only to scattering. The following discussion will not be concerned with nonabsorbing particles, and the factor Q_{sc}, equal to Q_{att}, will simply be noted Q.

After Eq. (2.25), variations in this factor with the size parameter α may be studied on the basis of development of the function $S(0)\alpha^{-2}$ in the complex plane. This quantity has been computed for all the sizes and indices mentioned so far. As an example, as Fig. II.9 shows, the function $S(0)\alpha^{-2}$ is represented in the complex plane by a spiral turning around a point Im = 0, Re = 0.5, as the current parameter α increases. Contrary to the example given by Van de Hulst relative to the index 1.33 (Van de Hulst, 1957, p. 176), the spiral is more regular, which is characteristic of indices close to 1; undulations, retrogressions and ultimately retrograde loops occur for high α values when the index begins to differ sharply from 1. The "speed" at which the spiral progresses depends on the index: for example, when α increases from 0.2 to 200, a single turn is described if n = 1.02, and five turns if n = 1.10. In actuality, the angular speeds in the various cases are equal if, rather than α, the current parameter is assumed to be $\rho = 2\alpha(n-1)$. (The values for ρ for various angles of rotation are indicated in the figure.) Factor Q is equal to four times the real part of function $S(0)\alpha^{-2}$: it reaches an initial maximum when ρ is close to 4, then oscillates around the value 2, the amplitude of the oscillation decreasing as the spirals tighten. The limiting value 2[12] is that furnished by diffraction (see below),[13] whose laws are applicable if the particle is sufficiently large.

---

[12] The convergence of series (2.28) and (2.26) toward 2 does not appear to have been proven mathematically.

[13] It may be recalled that the fact that a particle scatters twice as much energy as it is able to intercept, due to its geometrical cross section, is known as the "extinction paradox" (or "Babinet paradox"). This paradox is quite apparent, and arises from the initial hypothesis stating that the distance of observation is much larger than the size of the particle. Van de Hulst playfully illustrates this phenomenon by taking the example of a flowerpot on a window ledge projecting a shadow, whose coefficient is equal to 1, while a meteorite of the same size intercepting the light emitted by a star has a coefficient of 2.

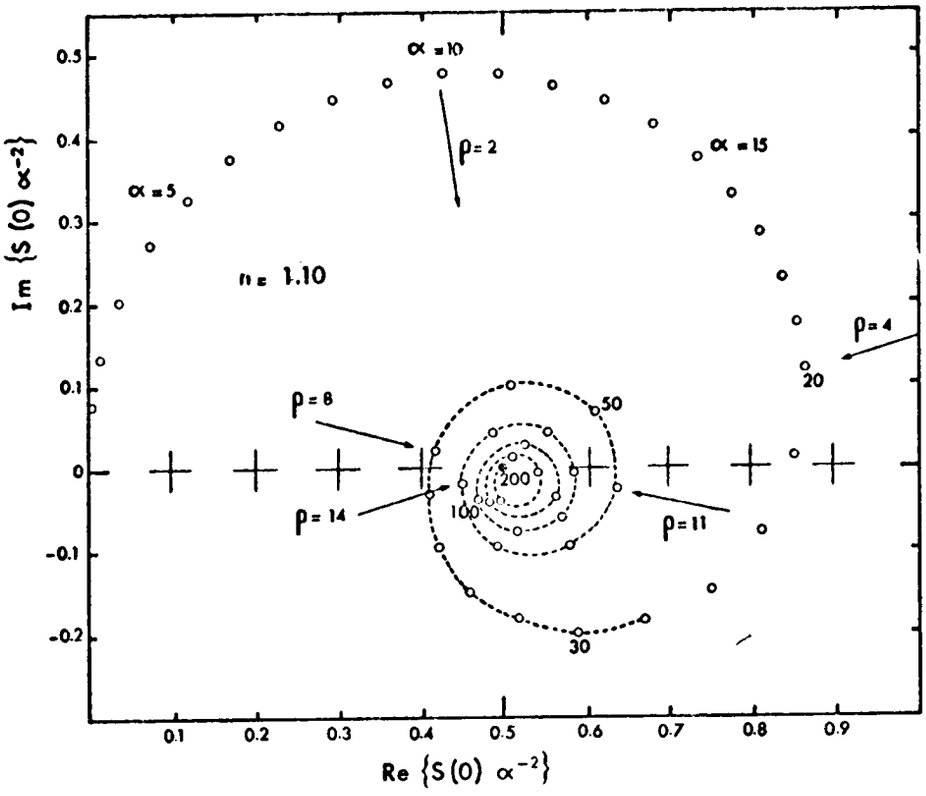

Fig. II.9. Representation of the function $S(0)\alpha^{-2}$ in the complex plane. α varies from 1 to 200.

2.2.8. Efficiency Factor and Intensity at 0°. Limiting Values (Diffraction)

The intensity function is obtained by taking the square of the modulus of the amplitude (2.1); since $S(0)\alpha^{-2}$ tends toward 0.5 as α increases, $i(0)\alpha^{-4}$ will tend toward 0.25. This was the subject of Remark c, which may be interpreted in a simple manner: the intensity diffracted in direction 0° (central spot) is proportional to the square of the surface of the diffracting opening and the amplitudes for the diffracted wave in any given direction):

$$S_1(\theta) = S_2(\theta) = \frac{\alpha^2}{2} \frac{2 J_1(\alpha \sin\theta)}{\alpha \sin\theta} .$$

When θ tends toward 0, $J_1(U)/U$ tends toward 1/2 and $i(0) = |S(0)|^2$ tends toward $\alpha^4/4$. Before converging toward their respective limits 0.25 and 2, the oscillations of functions

$i(0)\alpha^{-4} = |S(0)|^2\alpha^{-4}$ and $Q = \mathrm{Re}\{S(0)\}\alpha^{-2}$ are concomitant; the maximums and minimums of the two functions occur at the same α values, which actually correspond to fixed values for ρ, approximately marked on the spiral. More precisely (as computed with Eq. (2.29) below, which is applicable if the index is close to 1), these values are:

= 4.09 first maximum	= 7.63 first maximum
= 10.79 second maximum	= 14.00 second maximum

2.2.9. Van de Hulst Approximation

Van de Hulst has shown (1946, 1947) that the efficiency factor may be expressed simply as a function of the parameter ρ by:

$$Q = 2 - 4\rho^{-1}\sin\rho + 4\rho^{-2}(1 - \cos\rho) \quad (2.29)$$

when the index of refraction is very close to 1 ($1 \pm \varepsilon$); in fact, even when the index differs sharply from 1, this expression remains valid in most cases. Figure II.10 shows that the curve obtained from Eq. (2.29) constitutes a satisfactory approximation, even when the index is 1.15, the representative points being computed by means of the exact equation (2.26). When n is high, several systems of small oscillations corresponding to undulations or loops in the spiral are superimposed over the periodic oscillations 2π. This expression for the efficiency factor Q is a valid approximation throughout the Mie range, since ρ is any value, the sole condition being that $|n-1|$ is small. At the limit, when ρ increases Q tends sharply toward 2. Inversely, when ρ tends toward zero, that is, when the size of the particle decreases, expansion of Eq. (2.29) yields:

$$Q_{\rho\to 0} = (1/2)\rho^2 - (1/36)\rho^4 + \ldots \quad . \quad (2.30)$$

As will be seen briefly in the following discussion, this formula coincides with that resulting from the Rayleigh-Gans theory, which also assumes n to be close to 1; but it differs from the corresponding formula given by the Rayleigh theory, where the more restrictive condition $\alpha << 1$ must be met.

2.2.10. Efficiency Factor in the Rayleigh and Rayleigh-Gans Ranges /31

By combining Eq. (2.27) with formulas (2.15) giving the intensity functions for Rayleigh scattering, one obtains:

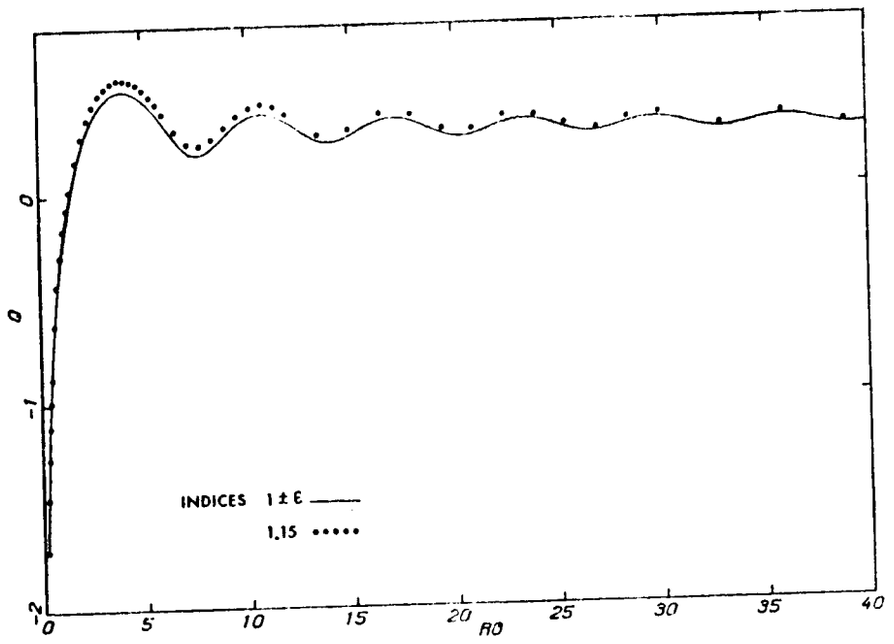

Fig. II.10. Efficiency coefficient Q adapted to a logarithmic scale as a function of the parameter $\rho = 2\alpha(n - 1)$, for two refraction values.

$$Q = \frac{1}{\alpha^2} \int_0^{\pi} \alpha^6 \Lambda^2 (1 + \cos^2\theta) \sin\theta \, d\theta \; ; \qquad (2.31)$$

the integral defined by the function θ has a value of 8/3 and thus:

$$Q = 8/3 \, \alpha^4 \, \Lambda^2 \; , \qquad (2.32)$$

in this equation the λ^{-4} law again applies, but it is in contradiction with the $e^{n\alpha^2}$ law supplied by expansion (2.30). In cases where n is assumed to be close to 1, the Lorentz term Λ is replaced by (2/3)(n - 1), in conformity with Eq. (2.16), and the result is:

$$Q = \frac{32}{27} \alpha^4 (n - 1)^2 \; . \qquad (2.33)$$

In the range of applicability of the Rayleigh-Gans approximation, the intensity functions are multiplied by the factor $F(\theta) = G^2(2\alpha\sin\theta/2)$, which thus occurs in the integral. Λ being replaced by its previous approximate expression, one may write:

$$Q = \frac{4}{9} (n-1)^2 \alpha^4 \int_0^{\pi} G^2 (2\alpha \sin\frac{\theta}{2}) (1 + \cos^2\theta) \sin\theta \, d\theta \; ; \qquad (2.34)$$

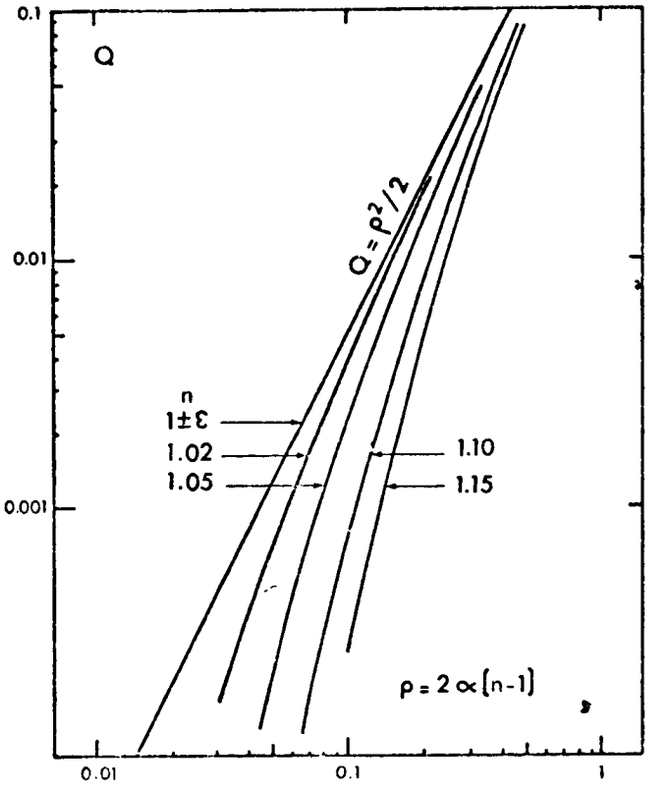

Fig. II.11. Efficiency coefficient Q in a range of low ρ values (logarithmic scales) for various indices.

This time the value of the integral defined depends on α: if α tends toward zero, the result is once again the preceding equation (2.33), valid when n is close to 1; on the other hand, if α is large, it has been shown that the value for the integral is $(9/2)\alpha^{-2}$, and the result is thus: $Q = 2(n-1)\alpha^2$, which closely corresponds to the limiting equation (2.30) of the Van de Hulst approximation.

To draw a practical conclusion, the difference between the exact values for Q calculated by means of Eq. (2.28) and the approximate values calculated by Eq. (2.29) is generally very small, as has been stated, except when ρ is small. With equal values for ρ, it is obviously all the more important that the difference between (n - 1) and 0 is greater. Figure II.11 shows that for ρ values less than 0.5 there is reason to use the exact equation (2.28).

3. Scattering by a System of Polydispersed Particles

The term "polydispersed system" is taken in its generally understood sense, denoting a system of particles of the same shape (spherical in the present case) and the same nature (and thus the same index), differing from each other only in size. Their number varies with their size, according to a law of distribution.

First (Section 3.1) there will be a discussion of the formulas permitting calculation of the scattering properties of a single system. Second, the predictions which may be made

concerning the results of the computations will be examined (Section 3.2), for cases in which the distribution is assumed to follow a power law. This leads to a consideration of the significance of the computations, taking into account the fact that these must be carried out with the assumption of mathematical limits whose physical reality is not readily apparent. Finally, by comparison with exponential laws, other types of distribution are considered.

3.1. Calculation of Scattering Properties

The particle population is characterized by a distribution function established with reference to a geometrical parameter characterizing the size: the following discussion will use the parameter α, that is, the relative size $2\pi r/\lambda$ which comes into play in scattering calculations and preserves their generality. (In applications, the radii of the presumed spherical particles being fixed, the change in wavelength is translated by an inversely proportional variation in α.) The distribution function $F(\alpha)$ corresponds to a frequency or probability of occurrence: if the entire population includes N particles with sizes ranging from zero to infinity (or from a minimum size α_m to a maximum size α_M), the quantity:

$$\frac{1}{N} \int_{\alpha_1}^{\alpha_2} F(\alpha)\, d\alpha$$

is the relative probability of occurrence of particles whose size parameter is between α_1 and α_2; the function $F(\alpha)$ is assumed to be continuous and integrable within the interval $0, \infty$ or α_m, α_M.

The additivity of the intensities scattered by randomly distributed particles simplifies computation from a formal standpoint; it is understood that in practice the integrations predicted below are replaced by summations, the size incrementation $d\alpha$ being that ruled by the preparatory computations for individual indicatrices (cf. Section 2.2, Part 2).

3.1.1. Scattering Indicatrix for a Given Number of Particles

For each angle, the intensity functions $i_1(\theta)$ and $i_2(\theta)$ for the particle system are given by the integral of the products $i_1(\theta, \alpha)F(\alpha)$ and $i_2(\theta, \alpha)F(\alpha)$. Normalizing to the integral of the function $F(\alpha)$ between the same limits renders the calculations independent of the total number of particles; otherwise, they would depend both on the distribution and on the limits adopted. From this it becomes possible to compute:

$$i_1(\theta) = \frac{\int_{\alpha_m}^{\alpha_M} F(\alpha)\, i_1(\theta,\alpha)\, d\alpha}{\int_{\alpha_m}^{\alpha_M} F(\alpha)\, d\alpha} \quad , \tag{3.1}$$

and $i_2(\theta)$ in the same way. The total intensity function $i_T(\theta) = (1/2)[i_1(\theta) + i_2(\theta)]$ and the rate of polarization $[i_1(\theta) - i_2(\theta)]/[i_1(\theta) + i_2(\theta)]$ are determined from these equations. For application, if N is the total number of particles in a unit volume, the volume scattering function is obtained simply by computing (cf. Appendix 1, "Definitions"):

$$\beta(\theta) = N \frac{\lambda^2}{4\pi^2} i_T(\theta) \quad .$$

The use of a given value for λ influences the limits α_m and α_M to be used.

3.1.2. Mean Efficiency Factor

This is defined for a system of particles as the ratio of the sum of the effective cross sections to the sum of the areas of the geometric cross sections. For the spherical particles considered, using the parameter α, one has:

/33

$$\bar{Q} = \frac{\int_{\alpha_m}^{\alpha_M} F(\alpha)\, \alpha^2\, Q(\alpha)\, d\alpha}{\int_{\alpha_m}^{\alpha_M} F(\alpha)\, \alpha^2\, d\alpha} \quad . \tag{3.2}$$

It is also possible to use the parameter $\rho = 2\alpha(n - 1)$, which simultaneously combines relative size and index. This is to advantage when the index is fairly close to 1, since in this case the Van de Hulst formula (2.29) will be applicable; this equation is simple enough that the integral in the numerator of Eq. (3.2) may be calculated numerically with a very small step ρ.

3.1.3. Normalized Indicatrix

In the final analysis, in comparing the results obtained by varying the law of distribution and its limits, it is less practical to fix the number of particles (as in Eq. (3.1)) as it is to fix the total scattering coefficient. This case corresponds to examination of sets of particles whose number

and distribution vary, but which show the same overall scattering effect; in the present case, unitary scattering. The normalized scattering coefficients (cf. Appendix 1, "Definitions") are calculated by:

$$\bar{\beta}_1(\theta) = \frac{1}{\pi} \frac{\int_{\alpha_m}^{\alpha_M} F(\alpha)\, i_1(\theta,\alpha)\, d\alpha}{\int_{\alpha_m}^{\alpha_M} F(\alpha)\, Q(\alpha)\, \alpha^2\, d\alpha} \qquad (3.3)$$

and for $\bar{\beta}_2(\theta)$ by the corresponding equation; $\bar{\beta}(\theta)$ is then calculated by means of the sum $\bar{\beta}_1(\theta) + \bar{\beta}_2(\theta)$ divided by 2. Computation of $\bar{Q}$ being performed simultaneously (3.1.2), the inverse of $\bar{Q}$ furnishes the total area of the geometric cross sections of the particles necessary to yield this total unitary scattering. For example, if $\bar{Q} = 0.5$, the total particle cross sections present within a volume of 1 m^3 must be 2 m^2 in order for the scattering coefficient b to be 1 m^{-1}.

3.2. Predictions of Results of Computation

These are possible based on the following two points:

-- variations in the shape of the Mie indicatrix for increasing sizes are replotted in general form by means of graphs of the functions $i(\theta)\alpha^{-4}$; the previous observations on the numerous gradients of the curves for various angles permit such predictions.

-- particle distribution according to size is assumed to follow a Junge law[14] expressed by a power function: $F(\alpha) = \text{constant} \cdot \alpha^{-m}$.

3.2.1. Convergence Conditions: Influence of the Upper Limit on the Indicatrix

Taking into account the form given at $F(\alpha)$, the $i_T(\theta)\alpha^{-4}$ functions already represented exactly correspond to α^{-4}

[14] It will be seen later that functions of this type satisfactorily correspond to actually observed marine particle distributions. In any case, more complex distributions can always be broken down and approximated by such forms within each range, at least theoretically.

distributions, and integration of these functions makes use of the numerator contained in Eq. (3.1) or (3.3). With the exception of normalization, it furnishes the indicatrix for the population considered (characterized by the α^{-4} law). It can immediately be seen that the integrals for the various angles will all converge, since the mean gradients for the curves are close to -2.3 (cf. Section 2.2.1, e), with the exception of the integral corresponding to the angle 0°, for which the mean gradient for the curve is zero. To put it another way, beyond a given limit, the consideration of increasingly large particles will not change the form of the resulting indicatrix except for the angle 0° and angles in the immediate vicinity, where the intensity will continue to increase. This phenomenon is shown by Fig. III.2 (Part 3), where the upper limit is increased from 50 to 200 without any appreciable change in the indicatrix, except at 0°, and also at approximately 175 to 180°. This is no longer the case if the upper limit becomes less than 50 (A. Morel, 1972a, Fig. 2).

In general, functions $i(\theta)$ increase with the size α according to $\alpha^4 + p$ laws, where p is the mean gradient read on the graphs (log-log scale) such as II.3; by way of review (cf. Section 2.2.1), these gradients have the values:

$p = +2$ for any given θ, if α is small; for $\theta = 0°$, even when α is not small, on condition that $\rho = 2\alpha(n - 1)$ is less than 4;

$p = 0$ for $\theta = 0°$ when α is large (ρ is greater than 4);

$p \simeq -2.3$ (or -2) for $\theta \neq 0°$ when α is large;

$-2 < p < 1$ for $\theta = 180°$, when α is large; the value of the gradient actually depends on the index (moreover, it is difficult to estimate an average value).

Functions $F(\alpha)i_T(\alpha, \theta)$ are α^{4+p-m} functions if -m is the exponent of distribution; the integrals to be computed are thus functions with the exponent $5 + p - m$. These integrals will converge absolutely if:

$$5 + p - m < 0 \qquad (3.4)$$

inequality to zero does not result in convergence, the integral being a logarithm.

If the progressive values for the integrals: /34

$$\int^{\alpha} F(\alpha)\, i_T(\theta,\alpha)\, d\alpha \quad , \qquad (3.5)$$

are given as a function of α for various angles (Fig. II.12), one finds that:

a. When α is small, no matter what the value for θ may be, all the curves increase by a gradient[15] whose value is 7 - m (that is, 3.5 and 2, respectively, for the two cases presented);

b. For α values whose increase is proportionate to the decrease in θ (that is, for α values corresponding to the maximum of the curves $i(\theta)\alpha^{-4}$, cf. Sections 2.2.1 d and 2.2.3), the integrals converge asymptotically and the curves show an asymptotic plateau (when condition (3.4) is met);

c. For the angle 0°, where $\gamma = 0$, there is no plateau if $m > 5$; otherwise, the integral will continue to increase with the gradient 5 - m (that is, a gradient equal to 1.5 for the higher figure and a gradient tending toward zero for the lower figure -- a branch of a logarithmic curve -- constituting a limiting case);

d. For the angle 180° the variations are more complex due precisely to the fact that the mean gradient p has a tendency to disappear as α increases (increasingly as the index becomes higher, which increases the reflection; cf. Section 2.2.5); in general, the partial integral resumes its increase after a plateau.

In conclusion, since the difference between the various plateaus characterizes the resulting indicatrix, the following predictions may be made:

-- if every curve has a plateau (when $m < 5$), the difference between the final values no longer changes and thus the indicatrix is no longer modified if the upper limit of integration continues to be raised.

-- if $2.7 < m < 5$ the conclusion remains the same, except in regard to the angle 0°; in other words, consideration of increasingly large particles does not change the shape of the indicatrix except at extremely small angles (and also toward 180°), where the increase continues.

---

[14] The slight bends which may be detected in the ascending curves (in the neighborhood of $\alpha = 2$, for example) are artifacts due to the change in step ($d\alpha$) in computing the integral, since this step is determined by the preliminary calculations for the indicatrices (cf. Section 2.2).

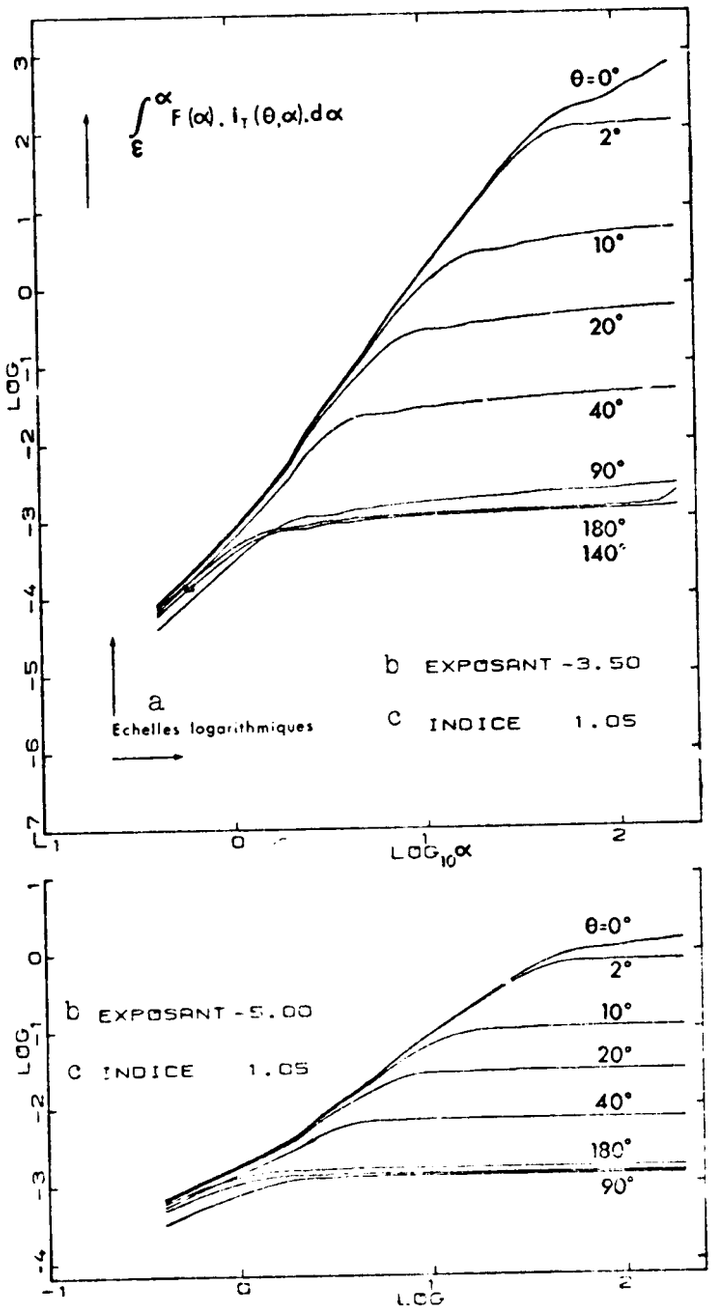

Fig. II.12. Progressive values for integrals as a function of the upper limit. The distribution exponent has the values -3.5 and -5, respectively, the index of refraction remaining 1.05 in both cases. The lower limit for the calculations is 0.2, but the curves are plotted after the first integration step, i.e., beginning at $\alpha = 0.4$. The upper limit is 200. [Key on following page.]

-- if m < 2.7 there is no mathematical limit, and the calculations are meaningful only if there is a physically real limit. /35

3.2.2. Role of Small Particles: Influence of the Lower Size Limit on the Indicatrix

It has just been seen that the calculations retain their significance within certain conditions which have been stipulated, even though the upper limit has been set arbitrarily. An analogous problem is presented with regard to the lower size limit. This quantity is physically unknown and, here again, the lower limit used in the calculations can only be arbitrary. It is necessary to predict the influence on the indicatrix of failure to take extremely small particles into consideration. Theoretically the calculations may be performed beginning at a hypothetical lower limit constituted by particles of "zero" size. In an analysis of the effect of truncation[15]

[15] Or the effect of misevaluation of the distribution laws to be used for small particles whose [continued]

Key to Fig. II.12:

a. Logarithmic scales
b. Exponent
c. Index

if integration is performed beginning with a finite limit which is not zero, two cases should be distinguished:

Case in Which the Particles Overlooked Belong to the Rayleigh Range

In this case integration is performed with a lower limit $\alpha_m = \varepsilon$, which at the most is equal to 1. An unfavorable hypothesis consists in assuming that the unknown particles continue to be distributed according to the same α^{-m} law; this hypothesis leads to continually increasing numbers of particles (and to an infinite number for size "zero"). The same scattering law is applied to all these particles (cf. Section 2.2.2), that is:

$$\begin{vmatrix} i_1(\theta) \\ i_2(\theta) \end{vmatrix} = \alpha^6 \lambda^2 \begin{vmatrix} 1 \\ \cos^2\theta \end{vmatrix}$$

For each value of angle θ, over the range considered -- for $i_T = 1/2(i_1 + i_2)$ -- the integration is written:

$$1/2 \int_0^{\varepsilon} \lambda^2 \alpha^{6-m} (1 + \cos^2\theta) \, d\alpha \, . \qquad (3.6)$$

This system of particles thus shows a Rayleigh indicatrix, expressed by:

$$i_T(\theta) = 1/2 \, \lambda^2 (1 + \cos^2\theta) \frac{1}{7 - m} \varepsilon^{7-m} \, , \qquad (3.7)$$

that is, an indicatrix of finite size, on condition that the following inequality is met[16]:

$$7 - m > 0 \qquad (3.8)$$

15(cont'd) presence is only probable by extension, since they are not observed.

16 This is obviously the reverse condition to that expressed by Eq. (3.4), with p = 2, the value for the gradient within the Rayleigh range.

otherwise, one obtains $i_T = \infty$. In other words, if there is truncation in the first case, the quantities $i_T(\theta)$ overlooked are finite and the resultant error can be computed. The error is infinite in the second case and the calculations are meaningful only if a known physical limit which is not zero exists.

In the first case, the neglected terms vary with the angle according to the Rayleigh law (that is, in a ratio of 1 to 2). If these are compared to the extremely asymmetrical indicatrix obtained when the upper limit is 200, it may be seen that the possible error is maximum for angles equal to or greater than 90°. As a relative value, this error is obtained by forming the ratio of the integrals between 0 and 0.2 and between 0.2 and 200 respectively. To refer again to the two examples illustrated by Fig. II.12, the error resulting from truncation (at 0.2) is less than 0.1% if the value of the exponent is -3.5, and on the order of 1% if this value is -5 (for angles of 90°, 140° and 180°; the error is obviously less at smaller angles). This order of size remains valid in other cases. Appendix 2 gives the values for various indices and for exponents varying from -3 to -5, computed by means of Eq. (3.7). These values are always negligible compared to those furnished by integration within the size interval 0.2 to 200.

In conclusion, the lower limit of this interval may be considered to be fixed at a sufficiently low value. The indicatrix thus obtained is significant, since particles with a size less than this value no longer have any appreciable influence (provided that their law of distribution meets condition (3.8)).

Case in Which Truncation Occurs for Greater Sizes

Here the effect may be directly predicted from graphs such as II.12. In particular, if the value of the lower limit is such that the curve relative to a given angle θ has begun to form a plateau, the effect will be considerable. For this angle the overlooked quantities may thus become greater than the quantities taken into account in integration, and the final value (when $\alpha = 200$) is consecutively decreased. Since plateaus occur for α values which become greater as θ becomes smaller (cf. Section 3.2.1, b), this decrease first affects the value at an angle of 180°, then that at 140°, etc. The asymmetry of the final indicatrix is reinforced as the lower limit α_m is raised:

if $\alpha_m = 1$, in relation to the values previously obtained with $\alpha_m = 0.2$, it appears that the values at 90°, 140° and 180° are decreased from 10 to 20%.

if $\alpha_m = 2$, the decreases at the same angles change from approximately 30 to 50%, while at 40° there appears a slight difference (-10%).

if $\alpha_m = 10$, the effect is still marked and in addition extends to a broader range of angles; a notable difference appears beginning with an angle of 20°.

Figure II.13 reveals this reinforcement of the overall asymmetry due to a decrease in the values at large angles, the values at small angles (0° and 2°) remaining unaffected. This figure repeats the upper part of Fig. II.12; in addition, it shows the curves obtained when the lower limit assumes the values 2 and 10 in turn, all things otherwise being equal. This development is more completely illustrated by the complete plotted indicatrices presented later on (Fig. III.12, Part 3). /36

3.2.3. Total Scattering; Influence of Limits on Computations

Here again the problem is to determine whether the calculation of total scattering is meaningful when only one part of the particle population is considered; the upper and lower limits are set to meet the needs of calculation, but do not represent any physical reality. This time the reasoning, analogous to that given above (3.2.1 and 3.2.2) must be applied to the integral:

$$\int_{\alpha_m}^{\alpha_M} F(\alpha)\ \alpha^2\ Q(\alpha)\ d\alpha \qquad (3.9)$$

which, with the exception of one factor, expresses the total effective cross section of particles distributed according to the law $F(\alpha)$ between the minimum and maximum sizes α_m and α_M. One need only recall that the efficiency factor Q varies as α^4 within the Rayleigh range (Eq. (2.32)) and as α^2 within the Rayleigh-Gans range (Eq. (2.35)), and that it is, on the average, independent of α within the Mie range and within that of diffraction (Section 2.2.8).

Without going into detail, it can thus be seen that in regard to the influence of the upper limit (within the Mie range), the total scattering tends toward a limit if the integral for $F(\alpha)\alpha^2$ converges, that is, if the total particle surface area itself tends toward a limit. This implies that the condition:

$$m > 3 \qquad (3.10)$$

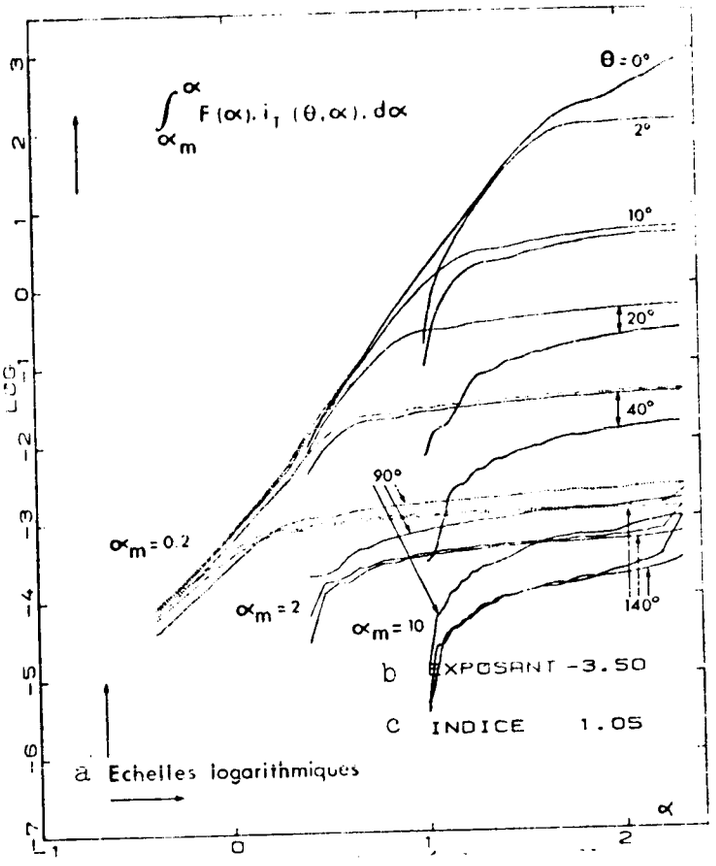

Fig. II.13. Influence of the lower limit; the dotted curves are taken from Fig. II.12 (upper part, exponent -3.5). The other two groups of curves are obtained when the lower limit of integration is at 2 and 10 in turn. The three unmarked curves correspond to an angle of 180°; they are characterized by a rapid increase for high α values.

Key: a. Logarithmic scales
b. Exponent
c. Index

is met if the distribution is as previously expressed by $F(\alpha) = C\alpha^{-m}$. The total surface area and thus the scattering increase with the logarithm of the upper limit α_M when m = 3.

In regard to the lower limit (within the Rayleigh range), the integral between 0 and α_m, corresponding to the overlooked particles, is applied to an equation using α^{6-m}, just as in calculating the indicatrix. As a result the same condition (3.8), $m < 7$, assures a finite value for this integral. For various exponents and indices, calculations show that the value of this integral between the limits 0 and 0.2 remains completely negligible in relation to the value of the integral for the particles taken into consideration (that is, between the size limits 0.2 and 200). These values are given in Appendix 2.

As has been seen (Section 3.2.2), an infinite number of particles may nevertheless yield a finite indicatrix. In a similar manner, the total diffusion, or more precisely, the total effective cross section, shown by particles whose size is between 0 and α_m may also be finite, while the total area of the geometrical cross sections of these same particles is not; the latter factor is finite only if $m < 3$. Thus when the exponent remains between the limits $3 < m < 7$, the case under consideration is actually realized.

Since this procedure has been performed for angular values, the progressive value of the integral (3.9) may also be expressed as a function of the upper limit; Fig. II.14 furnishes an example of this type for various values for the index and for an exponential value of -3.10. The value of the initial gradient of the curves is 7 - m; it then assumes the value 5 - m and finally tends to vanish; the curves then show an asymptotic plateau, since the convergence condition is met. The plateaus begin when Q becomes (on the average) independent /37
of α, that is, for α values which vary with the value of the index; in reality, these values are related since at this point the parameter $\rho = 2\alpha(n - 1)$ is equal to 4.1 (cf. Section 2.2.8 and Fig. II.10).

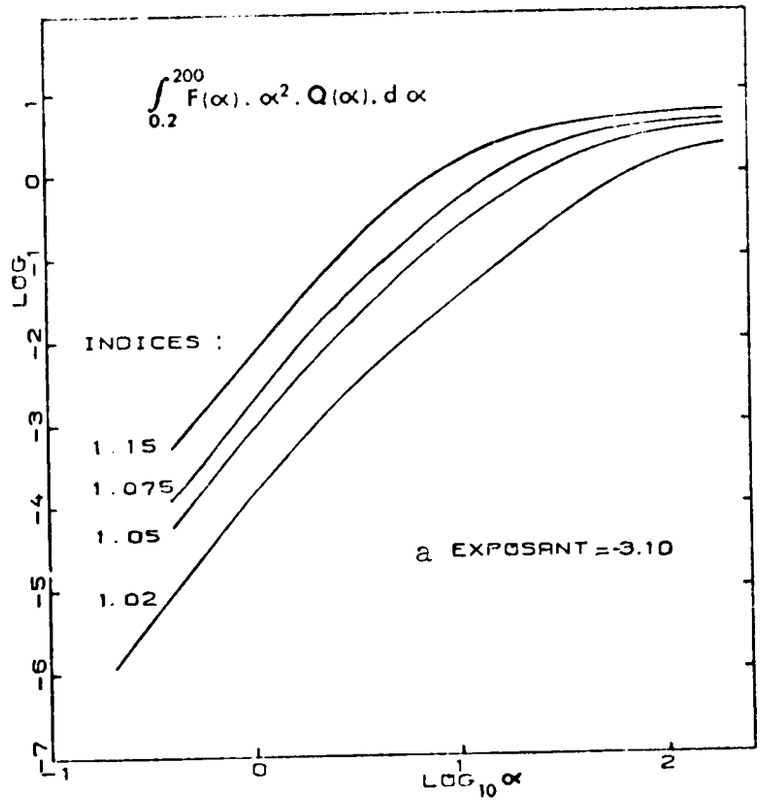

Fig. II.14. Progressive value for the integral yielding the effective cross section (3.9), as the upper limit increases to a final value of $\alpha = 200$. The curves correspond to the indices of refraction indicated and to a single value for the exponent of particle distribution.

Key: a. Exponent

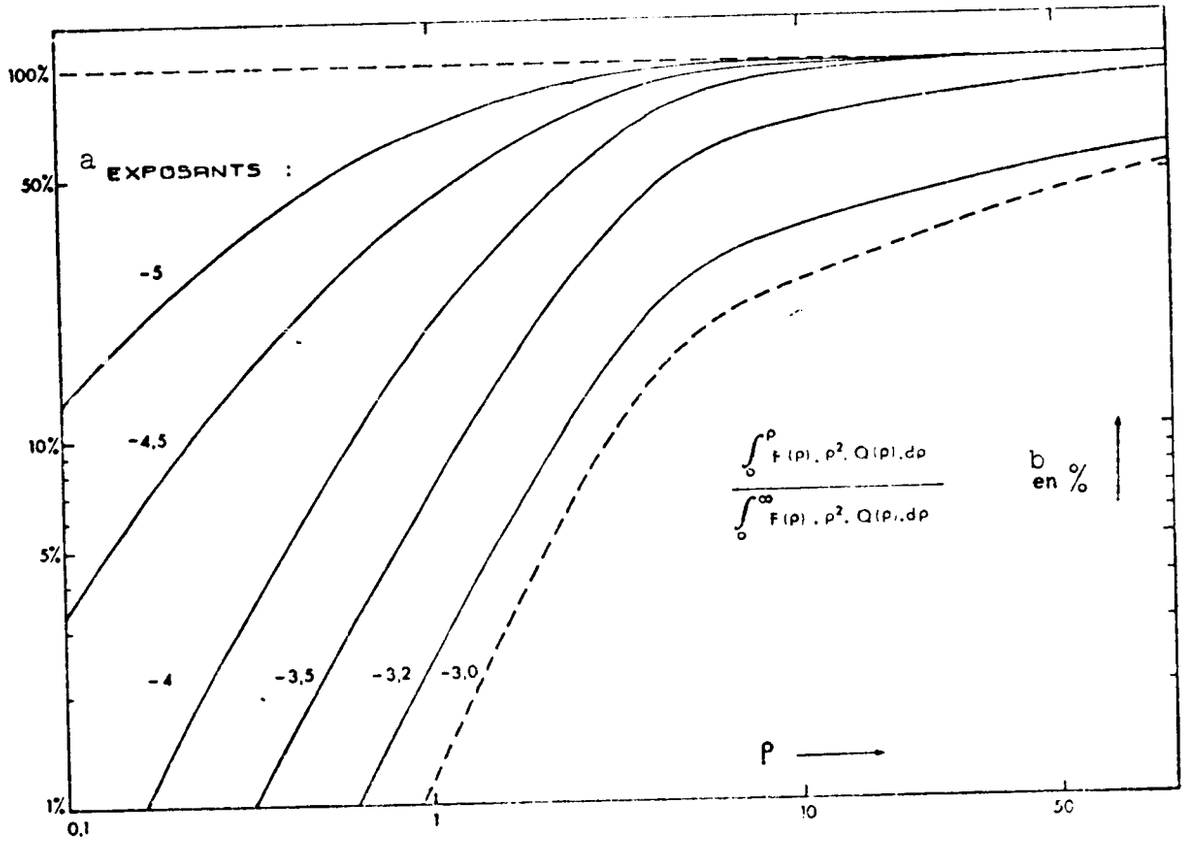

Fig. II.15. In this figure, which is analogous to the preceding, the variable α is replaced by the variable ρ. The curves correspond to the indicated exponential values; these are normalized to their asymptotic values (100%). The scales are logarithmic.

Key: a. Exponents
b. In %

In measurements where the Van de Hulst equation (2.29) is /38
a justifiable approximation (which is the case with the index values used here), a single calculation is sufficient, the variable ρ replacing α. The curves given in Fig. II.14 are actually a single curve plotted with a more or less expanded scale for the abscissa. As a result of this observation, the integrals computed in this case with the variable ρ are represented by the curves given in Fig. II.15, each of them corresponding to a different exponential value. The asymptotic values of these integrals when the upper limit increases to infinity may be computed (when condition (3.10) is satisfied); these values are used in normalizing the graph; however, the curve corresponding to the exponent -3 must be positioned

arbitrarily, since it has no asymptote. In all the curves the bend occurs when ρ exceeds 4 (see Appendix 2 for calculation of the asymptotic values).

3.2.4. Summary Dealing with Range of Validity of Calculations

The term "range of validity" is here assumed to have a precise meaning: it is the range within which the calculations retain their significance independent of the values given to the upper and lower size limits. This therefore assumes that the quantities calculated when the size limits are made to approach zero or infinity are infinite. Under these conditions, misapprehension of the physical limits does not invalidate the calculations. If by extension one assumes that a single law of distribution (exponential function) governs the population no matter what the size may be, the conditions for validity pertain to the exponent of the law. As has been seen, these conditions differ depending on the quantities to be calculated. They are collected in the following table, which indicates, with regard to the value of the exponent, whether the quantities calculated between 0 and α_m (influence of the lower limit) or between α_M and ∞ (influence of the upper limit) are finite or infinite.

It may be noted that the conditions relative to the lower and upper limits respectively are mutually exclusive in regard to the number, surface area or volume of the particles. In other words there is no range of validity as defined above; calculation is possible only if there is evidence that physical limits actually exist. The same is not true for the magnitudes relative to scattering: the two categories of conditions may simultaneously be met within some exponential intervals; this is summarized in the following diagram, where the range of validity is represented by the shaded area.

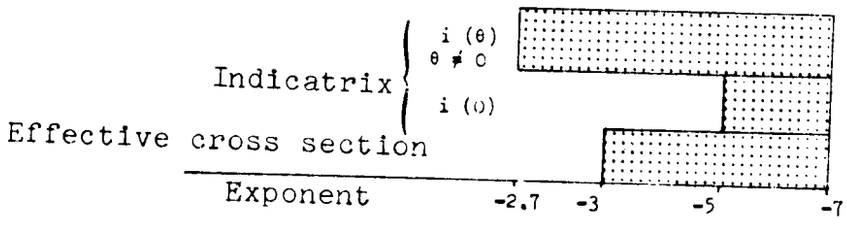

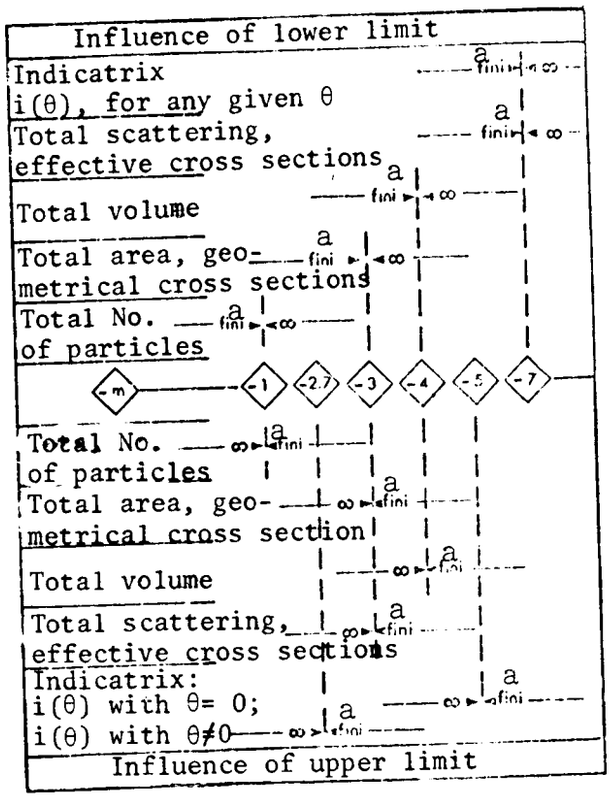

Key: a. Finite

3.2.5. Extension of Distribution Laws Differing from the Junge Law

The preceding conclusions on the validity range, at least as presented, are valid only for distributions expressed as exponential laws. However, they may be re-examined and extended to other types of distribution. The fact that the previously discussed case is easily treated mathematically makes it particularly suitable as a reference case. It is futile to consider the case of distributions according to functions of the crenellated type (rectangular, triangular, etc.), for which the problem of limits and the significance of the calculations does not occur. The case of normal gaussian distribution is of this sort, as will be seen later.

On the other hand, some discussion should be given to the case of a continuously decreasing distribution which nevertheless differs from the exponential law. The problem here is thus to choose a plausible distribution, that is, one which gives an approximation of the observed decrease within the size interval

accessible to experimentation[17]. Beyond the limits of this interval, however, the hypothesis on which the exponential laws are based no longer applies and the new distributions considered behave differently. To describe particle populations (natural or artificial), use has frequently been made of the exponential function:

$$F_1(\alpha) = A_1 \exp(-B_1 \alpha) , \tag{3.11}$$

or, more often, the gaussian-log function (or log-normal) function:

$$F_2(\alpha) = A_2 \exp\left(-B_2 (\log \alpha / \bar{\alpha})^2\right) \tag{3.12}$$

where $\bar{\alpha}$ is the value corresponding to the distribution maximum, and B_2 is the "geometrical" standard deviation. For marine particles, exponential laws (or laws of exponential type, such as the Weibull law) have been proposed by Carder et al. (1971). J.R. Zaneveld and H. Pak (1973) also used this distribution, which has been found to be suitable for all theoretical calculations due to the convergence at the limits, as will be seen below. /39

Consideration of the log-log graph of the preceding distributions is practical for the purpose of comparison with $F(\alpha) = A\alpha^{-m}$ exponential laws. The first remains exponential; two points determine it completely. The second one simply becomes a parabola; two points are not adequate to determine it and a third is necessary, or the position of maximum $\bar{\alpha}$ must be fixed arbitrarily. It is possible to verify that the normal gaussian distribution beyond the maximum is represented by an exponential curve (but with a stronger gradient than that of exponential function (3.11), since the argument is double). In Fig. II.16, the log-log graph of the α^{-4} exponential function, chosen as a basis of comparison, is represented by the line with a gradient of -4. The other distributions were made to intersect the preceding both at $\alpha = 10$ and $\alpha = 100$, and choice was made to center the gaussian-logarithmic distribution and also the normal distribution on $\alpha = 1$.

On the side corresponding to small sizes, the exponential distribution tends toward a finite value with zero gradient, and the convergence condition (3.8) is still met. The gaussian-logarithmic distribution tends toward zero and the negative gradient (between $\alpha = 1$ and $\alpha = 10$) is necessarily weaker than

[17] This observation concerning the granulometric analysis of particles, as well as the choice of numerical values for the distributions made below, anticipates the discussion at the beginning of Part 3, to which one may refer.

that of the secant representing the exponential law; condition (3.8) is met a fortiori when the exponential law observes this condition (7 - m > 0). Exponential laws with a high negative exponent are necessary so that small particles, in sufficiently high numbers, have more than a negligible role in the calculations; in practice, the distributions under consideration assign these laws a low number which corresponds mathematically to a quasi-truncation for scattering. The conclusion is identical in regard to gaussian distribution.

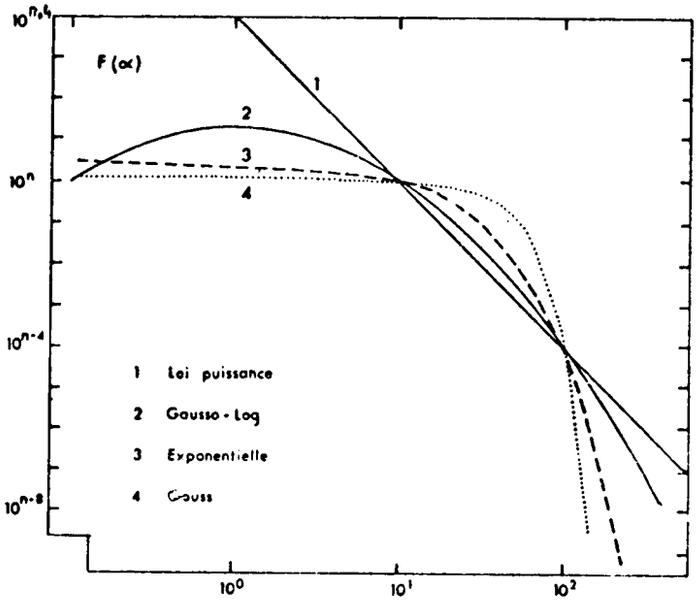

Fig. II.16. Log-log graph of various types of distribution with coinciding values for $\alpha = 10$ and $\alpha = 100$.

Key:
1. Power law: $F(\alpha) = 10^{n+4}\alpha^{-4}$
2. Gaussian-logarithmic law:

$$F(\alpha) = 10^{n} \exp(B) \exp\left(-B(\log_{10}\alpha)^2\right), \quad (3.12b)$$

with $B = (-/3) \cdot \log_e 10$

3. Exponential law:

$$F(\alpha) = 10^{n} \exp(10.B) \exp(-B\alpha) \quad (3.11b)$$

with $B = (-/90) \cdot \log_e 10$

4. Gaussian law:

$$F(\alpha) = 10^{4} \exp(A) \exp(-B\alpha^2)$$

with $A = (-/120) \cdot \log_e 10$

$B = (\log_e A)\, 9^2$

Due to the shape of the negative gradients on the side corresponding to large sizes, which are continually increasing and are greater than the righthand gradient, the convergence conditions are met for any given scattering angle θ (Section 3.2.1). The frequency of occurrence of large particles is lower with these laws than with the corresponding power laws; in practice, as in the preceding, it is equivalent to truncation. Figure II.17 illustrates this effect, making it possible to compare the indicatrices obtained with the gaussian-logarithmic law with those obtained with the power law; for the former, the distribution is extended to all sizes from 0.2 to 200 (for α), while for the latter the distribution is truncated below $\alpha_m = 10$ and above $\alpha_M = 100$. Superimposition of these two indicatrices shows that they do actually coincide (which is not entirely the case for the polarized components i_1 and i_2).

/40

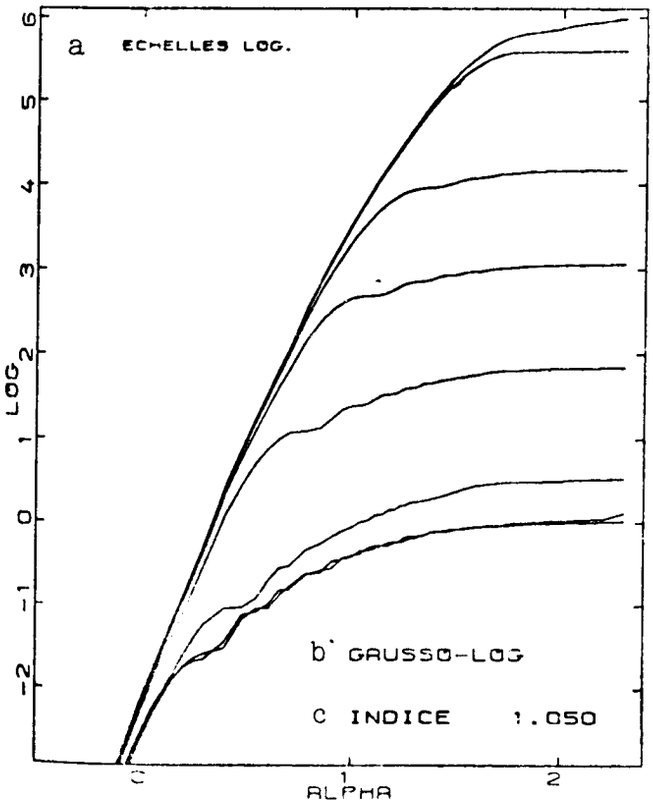

Fig. II.18. For the preceding gaussian-logarithmic distribution, this figure shows the progressive values for the integrals:

$$\int_{\varepsilon}^{\alpha} F(\alpha) \cdot i_T(\theta,\alpha)\, d\alpha ,$$

as a function of the upper limit α, and for the same values for the angle θ as previously (Fig. II.12).

Key: a. Log scales
b. Gaussian-log
c. Index

It would be futile to give further calculations and examples of this type, given the arbitrary nature of the laws used, especially in regard to the position of the distribution maximum. Suffice it to say that with exponential laws and especially log-normal laws one obtains results very close to those resulting from application of the equivalent power law (and in the case of log-normal laws, results which are as close as desired, depending on the parameters chosen). On the other hand, this is never the case with the gaussian law, even truncated beyond the maximum.

Finally, between the sizes where the distributions coincide (10 and 100 for the example given here), the curves show a convexity; as a result, these distributions tend, more than the power law, to favor particles of intermediate size (20 to 50), which play a role of comparatively greater importance in scattering. An example of this result will be given later on (Part 3, Section 3.1.2).

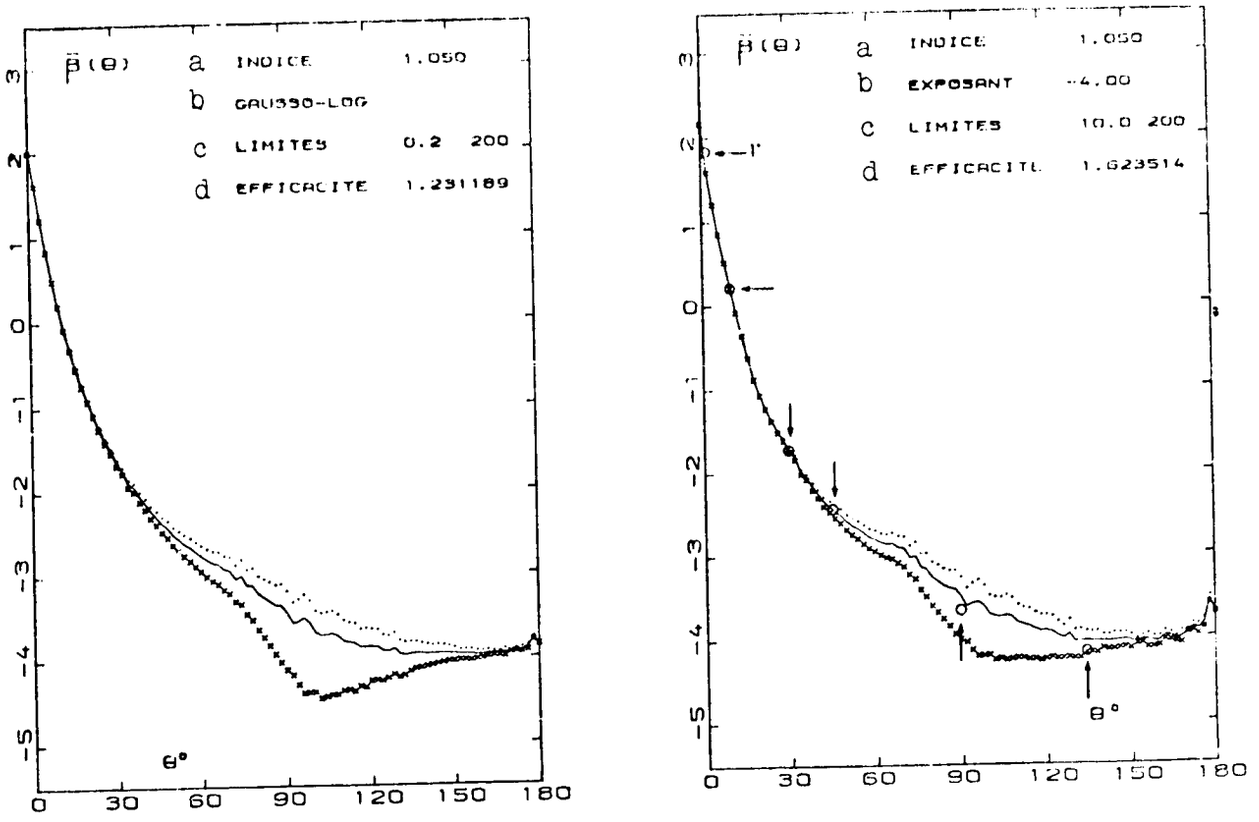

Figs. II.17. Indicatrices obtained with gaussian-logarithmic distribution (Eq. (3.12b), Fig. II.16) and with Junge distribution with an exponent of -4, truncated below $\alpha = 10$ and above $\alpha = 100$; the indicatrices are plotted with the decimal log of the normalized scattering coefficient $\bar{\beta}(\theta)$ expressed as a function of θ. The values for $\bar{\beta}_1(\theta)$ and $\bar{\beta}_2(\theta)$ corresponding to the vertical and horizontal polarized components are represented by dots and crosses, respectively.

The points indicated by arrows correspond to the calculations performed by O. B. Brown and H.R. Gordon (1971) for the same exponent, using the limits 8.6 and 86 (diameters 1 to 10 μm $\lambda = 488$ nm) and with the index 1.05-0.01 i. For comparison, the values were recomputed so as to be given in the form of a normalized coefficient $\bar{\beta}(\theta)$. The upper limit is 86 rather than 200, but taking the exponent into account, the configuration is virtually asymptotic (cf. Section 3.2.1), and the results are found to be comparable.

Key: a. Index
b. Gaussian-log
c. Limits
d. Efficiency

PART 3

Introduction

Calculation of the scattering properties of a polydispersed system involves, on the one hand, parameters related to the law and limits of distribution, and on the other hand, the relative index, which will be termed the "mean" index since it is assumed to be the same for all the particles. Various numerical applications have been presented as examples in the previous expansions, but without any discussion of the choice of values attributed to the parameters used. A few theoretical cases have been systematically treated for purposes of comparison with the experimental results, and it was necessary to make a choice of values which might be examined here.

The value assigned to the particle index of refraction could hardly be anything more than hypothetical, since no direct measurement seems to have been made. On the basis of the mineral content of particles in suspension (calcium carbonate, silica, alumino-silicates, various hydroxides, etc.), assumed to be in crystalline form, it is possible to determine an average index value. Values frequently given on the basis of these considerations are on the order of 1.15 or 1.20[1] (relative values in relation to water, that is, 1.53 to 1.60 in absolute values); calculations have been made for clays in suspension yielding the value 1.15 (and an imaginary part equal to 0.001; H. Pak. R.V. Zaneveld, G.F. Beardsley, 1971). However, first of all, it is probably not realistic to attribute the index for the crystalline form to the entire particle, even if it is basically mineral. Certain insoluble substances or precipitates may be present in strongly hydrated colloidal forms, or again, the mineral part of a detrital particle may be only a shell, for example; such mineral particles would have a "mean" index closer to that of water than that determined from the strict composition (excluding water). In addition, there is always a considerable proportion of organic substances in the suspended material, and the index for these substances is very close to that of water. Recently K.L. Carder et al. (1972) used measurements of scattering in unicellular algal cultures (Isochrysis galbana) to determine the relative index, which they found to be on the order of 1,026 to 1.036 for this organic substance). Organic materials[2], which form the heaviest proportion of total

---

[1]See for example W.V. Burt (1956), Y.E. Otchakovsky (1965), and N.G. Jerlov (1968).

[2]Particulate organic carbon was the substance actually tested, and the total weight of organic substances was determined from this quantity, generally by multiplying it by a factor of 2 (a factor of 1.80 was used by D.C. Gordon).

particle weight for surface waters in general, remain in high percentage even in deep layers; between the surface and depths of up to 4000 m, the relative abundance of particulate organic matter has been found to remain higher than 25% (D.C. Gordon, 1970) and to range from 40 to 60% (L.A. Hobson, 1967), 40 to 100%[3] (P.J. Kinney et al., 1971), 40 to 88% (C. Copin, G. Copin, 1972) and from 26 to 49% (J.E. Harris, 1972). This leads to a choice of values close to 1 for the "mean" relative particle index. In any case, preliminary individual indicatrix calculations were performed for five index values covering a sufficiently broad range, from the low values (1.02 and 1.05) considered most likely up to the characteristic value of the mineral fraction (1.15), the intermediate values chosen being 1.075 and 1.10.

There are experimental results relative to the law of distribution, as opposed to the index. In particular, the use of an electrical granulometric counter (Coulter Counter) has made it possible to obtain new data (L.A. Hobson, 1967; R.W. Sheldon and T.R. Parsons, 1967; K.L. Carder, 1970). The measurements made by H. Bader (1970), like those by J.C. Brun Cottan (1971), reveal that the Junge law (that is, a d^{-m} power law, d being the diameter) previously proposed for atmospheric particles (C.E. Junge, 1963) seems satisfactorily to describe the distribution of marine particles. This counter permits granulometric study of particles with equivalent diameters ranging from 1 µm to 15 or 20 µm[4]. In a number of cases the decrease in the number of particles as the diameter increases follows two successive laws, one with an exponent of between -3.3 and -3.9 within the interval 1 µm to 4 or 5 µm, and the second, beyond this size, with a higher exponent (in absolute value) of approximately -4 to -5.

A large number of measurements taken in very different areas of the Atlantic and the Pacific (R.W. Sheldon et al., 1972) show that in a very general manner, the distributions are such that for equal logarithmic size intervals (for example from 1 to 2 µm, then 2 to 4 µm, then 4 to 8 µm, ...), the volume of the particles belonging to these classes remains roughly constant. It may easily be verified that this property of logarithmic equipartition of volumes is that of distribution with the exponent -4. According to these investigators, this equipartition has extended to a very broad range of sizes. For surface

---

[3] 19 to 55% for particulate carbon (cf. Footnote 2).

[4] Other intervals may be studied, but corresponding to greater sizes; 1 µm is approximately the lowest detection threshold for the Coulter system. The diameters determined from the measurements are those of equivalent spheres, that is, spheres with the same volume as the actual particles, independent of their shape.

water and in productive regions, the preceding distribution frequently is limited by maximums (toward 16 to 20 μm, for example) indicating the presence of phytoplanktonic particles. The exponents for the calculations (from -3 to -5 with an increment of 0.1) have been chosen within an interval widely covering the experimental values. Systematic results for eight exponential values within this interval and for the five index values have been presented elsewhere (A. Morel, 1973); the same source presents results obtained with log-normal and exponential distributions. Even if the power laws are found to be slightly oversimplified in relation to reality, more complex distributions may be broken down into several successive laws of this type. In any case, they are convenient for computation and, as has been seen, they may also serve as a basis for prediction of results in cases where other distributions must be considered (cf. Section 3.2.5, Part 2).

There are apparently no results concerning the laws ruling /42
the distribution of particles with dimensions less than 1 μm; for those with dimensions greater than 20 μm, -m exponential laws continue to be applicable (m may become slightly greater than 4, since the volumes for classes of increasing order have a tendency to decrease; R.W. Sheldon et al., 1972). However arbitrary they may be from a physical standpoint, limits must be set to facilitate computation. Their influence has also been studied, to the degree in which it is predictable. Preliminary individual indicatrix computations have been performed for α values ranging from 0.2 to 200, and the integrals to be computed for polydispersed systems have been computed between these limits.[5]

From a practical standpoint this brings us back to the correspondence between relative parameters α and ρ and diameters d. By way of review: $\alpha = \pi d n_e / \lambda_o$ and $\rho = 2\alpha(n_r - 1)$, where d is the diameter of the sphere, λ_o the wavelength in a vacuum, n_e the refractive index of water (1.33), and n_r the relative index of the particle in relation to water. The calculations performed between $\alpha = 0.2$ and $\alpha = 200$ correspond to particles with diameters ranging from 0.02 μm to 20 μm, when $\lambda = 419$ nm (in this case $\alpha = 10$ d), or on the other hand from 0.04 μm to 40 μm if $\lambda = 838$ nm. In addition $\rho = d$ if n_r is given the value 1.05 when $\lambda = 419$ nm; this case is frequently taken as an example. Thus in order to compare the various distributions, these were made to coincide for $\alpha = 10$ and $\alpha = 100$ (Part 2, Section 3.2.5), or for d = 1 and 10 μm if $\lambda = 419$ nm, that is, for diameters within the range covered by the measurements.

[5] Computations have also been performed between the theoretical limit $\alpha = 0$ (zero size) and $\alpha = 0.2$ (cf. Appendix 2 and Section 3.2.2, Part 2).

In this respect, the gaussian-logarithmic law used could have been approximated by two power laws, one with the exponent -3.4 up to $\alpha = 40$ ($d = 4$ μm), and the other with the exponent -4.5 between $\alpha = 40$ and $\alpha = 200$ (d being 4 to 20 μm), which constitutes a rational example (see above).

In order to orient comparisons of the experimental and theoretical indicatrices, it is first necessary to examine how the theoretical indicatrices vary with the index and the exponent of distribution (Chapter 1). Various comparisons are made and probable exponent and index values are determined on the basis of the agreement observed (Chapter 2). Various applications for the theory are studied, in particular its use to explain the spectral selectivity of scattering and polarization. Conclusions are also drawn on the different roles of various particles and the relationships between the concentration of the suspended material and scattering (Chapter 3).

1. Theoretical Variations in the Indicatrix

1.1. Influence of the Exponent of the Law of Distribution on the Indicatrix

Figure II.12, presented in Part 2, has already shown the direction in which this influence is exerted. The difference between the various plateaus characterizing the final indicatrix was found to vary with the exponent, and it is possible to determine the manner in which it varies. The various plateaus begin at fixed values for α which depend on the angle θ involved.[6] As a result the differences are determined directly by means of the initial gradient, which is the same for all the curves (no matter what the angle may be) and whose value is 7-m. This makes it possible to calculate[7] a phenomenon which is already predictable from a qualitative standpoint: when large-size particles are proportionately more abundant, that is, when m

[6] These are the α values for which the curves $i_T(\theta)\alpha^{-4}$ begin to diminish and which, it will be remembered, are independent of the index, except if the angle θ is small (2°, for example). This property is demonstrated by the Rayleigh-Gans theory (cf. Part 2, Sections 2.2.3 and 3.2.1b).

[7] For example, if α_1 and α_2 are the α values for which, according to the Rayleigh-Gans theory, the first dark ring attains the angles θ_1 and θ_2, the ratio of scattering intensities at these angles $i(\theta_1)/i(\theta_2)$ will vary with the exponent proportional to: $(\alpha_1/\alpha_2)^{7-m}$. The corresponding values for α and θ are given in a table in Part 2, Section 2.2.3.

decreases in absolute value, the initial gradient of the curves is stronger, the plateaus thus occur at a later stage and the overall indicatrix is more asymmetrical. This development of the indicatrix is shown in Fig. III.1. It has been plotted with the values of the integrals expressed as a function of m (varying from 3 to 5):

$$\int_{\alpha_m}^{\alpha_M} i_T(\theta,\alpha)\ \alpha^{-m}\, d\alpha\ ,$$

for various angles θ; the upper and lower limits remain constant (0.2 and 200 respectively). The intensity at 0° serves as a normalization value. It can be seen in this figure that the widest variation is that of the ratio $i_T(2°)/i_T(0°)$, but this has no significance since the integral for 0° does not converge, as has been seen. The significant shapes are those of curves for angles other than 0°. Thus the indicatrix (from 2° to 180°) covers five orders of magnitude for the exponential value -3 and three orders for the value -5. Another point which will be seen to have some importance may be noted: between the exponential values -3 and -4, the various curves remain approximately parallel. This indicates that within this range the indicatrix is not very sensitive to variations in the law of distribution, at least for "mean" angles (since the 180° angle is an exception to some degree, and no statement can be made for the 0° angle).

Some consideration should also be given to cases in which the distribution, rather than following a single law, follows a law in which the exponent successively assumes two values m_1 and m_2. As has been observed, the second value is greater (in absolute value) than the first; it corresponds to the law applying to particles with a diameter greater than 5 μm (that is, $\alpha > 50$). In reality, the integrals for the various angles, except for 0°, have virtually reached their asymptotic value at $\alpha = 50$ (see Fig. III.2). As a result, the fact of whether the particles are distributed according to a $-m_1$ or $-m_2$ law beyond a value of 50 for the α parameter has no influence on the final form of the indicatrix, except for the value at 0°. Figure III.2 manifestly shows this fact: indicatrices corresponding to populations extending from $\alpha_m = 0.2$ to $\alpha_M = 200$ or from $\alpha_m = 0.2$ to $\alpha_M = 50$ are plotted for two index values; within the latter α range it is obvious that beginning with $\alpha = 50$, the second exponent m_2 becomes infinite. The indicatrices virtually coincide, except at 0°. In conclusion, with the laws of distribution considered, large particles play a small role and the more or less heavy depletion of these particles (more or less high m_2) has little effect on the shape of the indicatrix.

1.2. Influence of the Index of Refraction on the Indicatrix /43

The value of the exponent influences the shape of the resulting indicatrix, but the shape of the individual indicatrices involved in integration, on the other hand, is governed by the value of the index of refraction. Figure III.3 furnishes an example of this influence: the exponent being fixed (m = 3.5), the ratios $i_T(\theta)/i_T(0°)$ are given this time as a function of the index, and the upper and lower limits of the integrals retain the same values as previously (0.2 and 200). It was pointed out in Part 2 (Sections 2.2.5 and 2.2.6) that the influence of the index for individual indicatrices is virtually restricted to extreme ranges of small angles (0° to 10°) or large angles (in the vicinity of 180°). The summations performed do not change this property, permitting the following observations:

-- the overall asymmetry of the indicatrix decreases as the value of the index increases. Thus the ratio of scattering intensities at 2° and 140° corresponds to six orders of magnitude when n = 1.02 and only four orders if n = 1.15.

-- however, it may be found that this variation in asymmetry is virtually solely attributable to variations in the ratio $i_T(10°)/i_T(2°)$. On the other hand, the curves for angles ranging from 10° to 140° (and even the curve for 160°, which is not shown) remain appreciably parallel, and as a result the "mean" region (10° to 160°) of the indicatrix depends very little on the index of refraction.[8]

-- finally, the curve corresponding to an angle of 180° shows that in relative value, backscattering becomes more marked as the index increases (as a result of the increase in the reflection factor).

It now may be noted that on the basis of the preceding findings, criteria exist which at least theoretically would make it possible to derive a rational value for the index from the measurements. The ratio of scattered intensities at 2° and 10° is a criterion of some importance, especially if the index varies between 1.02 and 1.075; for the higher values, 1.075 and 1.15, backscattering would constitute another criterion (unfortunately poorly suited for experimental use). Another detail revealed

---

[8] It is not possible to generalize this finding; this property is linked to the index values considered, which are close enough to 1 to make the Rayleigh-Gans approximation valid and applicable (cf. Part 2, Section 2.2.3).

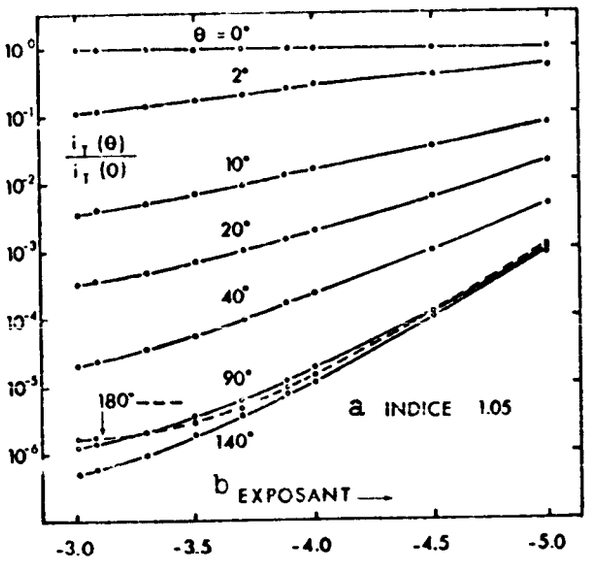

Fig. III.1. Influence of the exponent of the law of particle distribution on the indicatrix; the index of refraction is 1.05. The size parameters corresponding to the limits of distribution are 0.2 and 200.

Key: a. Index
b. Exponent

by the complete indicatrix curve may also serve as a criterion: this is the fact that a slight relative maximum may be noted whose angular position is directly linked to the value of the index (about 60° for n = 1.05 and about 85° for n = 1.10; Fig. III.2).[9] The maximum becomes more pronounced as the calculations take larger particles into account, since only these particles are capable of producing this effect.

From a practical standpoint, measurements of indicatrices have seldom been performed with a sufficiently small angular interval for this phenomenon to be definitely shown. It may be noted, however, that the mean indicatrix obtained by Jerlov (1961) and that given by Otchakovski (1965) possess a sharp convexity toward 60 to 70° (which would correspond to an index of approximately 1.05). A device continuously recording the scattering coefficient as a function of the angle would make it possible to determine whether this effect is more or less permanent and thus whether it is possible to use it to determine a mean refractive index. In this respect, the indicatrix determinations made by J. W. Reese and S. P. Tucker (1970) show that a slight maximum occurs very frequently between 55° and 75°.

The problem remains, whether it is possible to determine criteria for the exponent similar to those which have just been indicated for the index. Referring again to Fig. III.1, one finds that the total amplitude of the indicatrix is a priori the quantity which truly varies with the exponent. However, for the reasons of non-convergence already given, the value at 0° cannot

---

[9] See also the indicatrices given in Appendix II. The equation linking the index with the angle at which this energy concentration occurs has been shown in a graph (part 2, Fig. II.8).

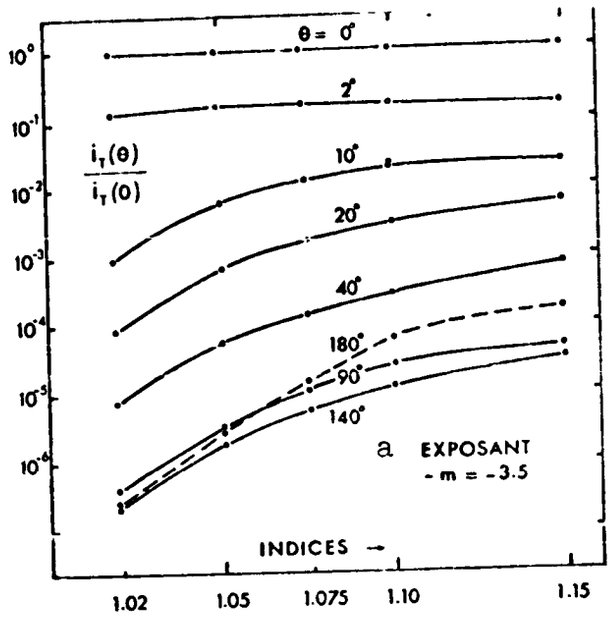

Fig. III.3. Influence of the index of refraction on the indicatrix; the exponent of the law of distribution is -3.5. The size limits are unchanged.

Key: a. Exponent

be taken into consideration. In addition, as has just been seen, the angular range 2 to 10° is particularly sensitive to the value of the index. Use of the ratio of intensities at 2° and 140° to define the amplitude would result in a magnitude for which the influence of the exponent could not be distinguished from that of the index. On the other hand, as shown by Fig. III.3, the ratio i(10°)/i(140°) is virtually independent of the index. The amplitude of the indicatrix, which is no longer total but restricted to the range 10° to 140°, might well constitute the criterion desired. /44

1.3. Conclusions To Be Drawn from Theoretical Variations in the Indicatrix

An initial conclusion may be drawn from the preceding. This is the fact that when the index of refraction varies within relatively broad limits, the scattering indicatrix undergoes little change, at least with reference to the "mean" angles (10° to 140°, to set these values); the same is true when the exponent of distribution varies, although this occurs within slightly narrower limits (from approximately -3 to -4). This may consti an initial explanation for a finding which has been made experimentally: the low value of the indicatrix for marine particles. (It may be noted that this fact has been established primarily on the basis of measurements at mean angles. This explanation will be expanded and discussed in more detail in the following chapter. The case of small angles where the variability is greater will also be examined.

2. Interpretation of Observations and Applications

It should first be shown that the relatively non-variable theoretical indicatrices which have just been mentioned do

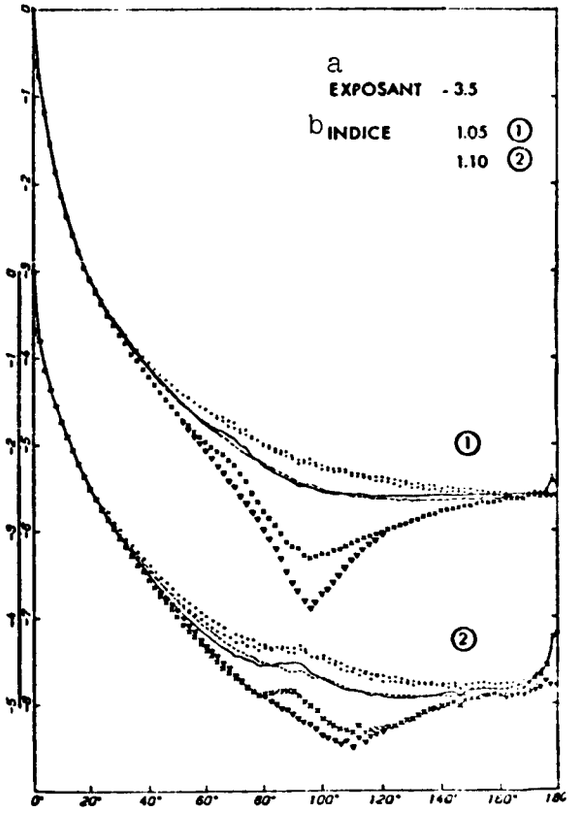

Fig. III.2. The curves shown as unbroken lines correspond to indicatrices calculated for size limits of $\alpha_m = 0.2$ and $\alpha_M = 200$; for the indicatrices shown as dotted lines, the upper limit α_M has been lowered to 50. Positioning of the curves marked 1, relative to the index 1.05, and 2, relative to the index 1.10, is arbitrary. On the other hand, in each of these two cases, the dotted line curve and the unbroken line curve are correctly placed in relation to each other, in such a way that the total scattering coefficient is the same (that is, they are correctly placed if the angular coefficients are considered to be normalized). The crosses and triangles correspond to the horizontal polarized component i_2, when $\alpha_M = 200$ or when $\alpha_M = 50$, respectively; the dots correspond to the vertical component i_1, without any distinction between the values obtained in the two cases.

Key: a. Exponent
b. Index

coincide with the experimental indicatrix; subsequently an attempt will be made to determine whether some variations within the range of possible variations more accurately represent the experiment. This procedure may make it possible to derive probable values for the index of refraction and the exponent of distribution.

To make comparisons, use will be made (Section 2.1) of those properties -- such as the ratios $\beta(10°)/\beta(2°)$ and $\beta(140°)/\beta(10°)$ -- which have been found to vary sufficiently, either with the index or with the exponent, to be able to serve as criteria. Ratios of angular coefficients to the total coefficient will also be used (Section 2.2), that is, normalized coefficients $\overline{\beta}(\theta)$, whose values depend conjointly on the index and the exponent. If the experimental variability of these ratios is found to be smaller than the theoretical variability, this will indicate that actual indices and exponents vary within a

a more limited range than that considered for the computations. Each property will result in the delimitation of a range of this type; if all these ranges are compatible or at least have one part in common, one may expect to deduce rational values for the index and the exponent from the experiment. Indicatrices calculated with these values are compared to the experimental indicatrix (Section 2.4). /45

Methods for evaluating the total scattering coefficient on the basis of angular measurements have been proposed by various investigators. Examination of the theoretical variability of a few normalized coefficients (normalized to 90°, 45°, 6° and 4°; Sections 2.2 and 2.3) so as to determine the index and the exponent at the same time provides a means of reconsidering the basic validity of such methods.

2.1. Application of Criteria to the Index and the Exponent of the Law of Distribution. Ratio of Angular Coefficients

As has been seen (Section 1.2), the ratio of scattering coefficients at 10° and 2° is much more sensitive to variations in index than variations in exponent; inversely, the ratio of coefficients at 140° and 10° is dependent almost exclusively on the exponent; the index and exponent variables are separated to some degree. The theoretical variations in these ratios with the two variables considered are given in Fig. 3.4. Experimental values for the same ratios are listed in Table 1. Relatively few measurements were performed conjointly at 2° and 10° or at 10° and 140°. In addition, for their use here, the measurements taken at 140° had to be expressed in absolute values so that the proportion due to molecular scattering, which is frequently substantial, could be subtracted; only on this condition is the ratio $\beta(140°)/\beta(10°)$ physically significant. Use of the values $2 \cdot 10^{-2}$ and $5.5 \cdot 10^{-2}$ to set experimental limits for variations in the ratio $\beta(10°)/\beta(2°)$ and transfer of these values to the graph (III.4) of theoretical variations results in a range being defined by intersection. This corresponds to the combined values for both the index and the exponent, for which the calculations represent the experiment. Due to the very nature of this criterion, this range leaves the exponential values undetermined, but restricts the possible values for the index; it thus appears necessary to set aside any values outside the interval 1.02 to 1.06. In the same manner, choosing the experimental values $0.6 \cdot 10^{-3}$ and $2.3 \cdot 10^{-3}$ as limits for the second ratio, another range may be determined which gives little information on the index (less than 1.10, however), but stipulates the values for the exponent; for example, if the index is assumed to be equal to 1.05, the exponential values compatible with the experimental results are approximately -3.8 to -4.3.

For the sake of clarity, the two ranges defined in this way are given on an m-m diagram (that is, one whose coordinates are

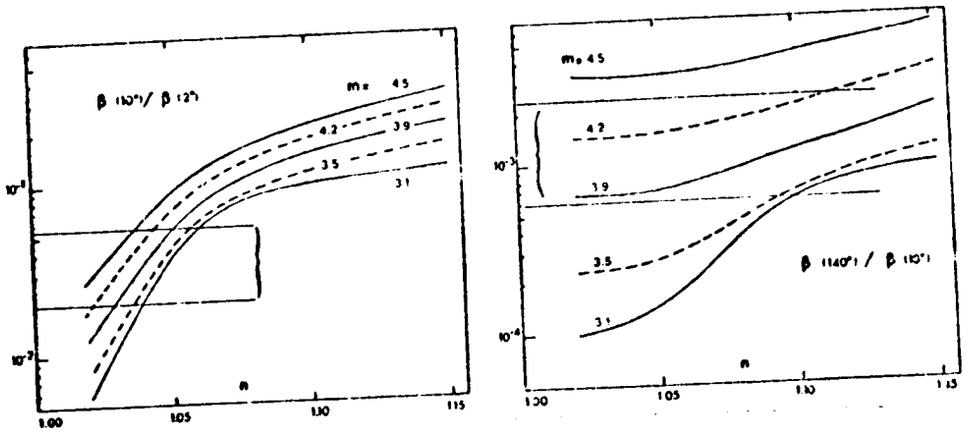

Fig. III.4. Theoretical variations in the ratios $\beta(10°)/\beta(2°)$ and $\beta(140°)/\beta(10°)$ as a function of the index of refraction, for the exponential values indicated. The experimental values are located within the bands designated by braces.

the exponent and the index; see Fig. III.6). The common part thus corresponds to rational values for the index and the exponent, taking the experimental results available into account.

Spilhaus (1968) has considered the possibility of using the ratio $\beta(30°)/\beta(45°)$ to characterize the shape of the indicatrix. Figs. III.1 and III.3 show that the curves plotted for 20° and 40° remain appreciably parallel when the index or the exponent varies. It thus appears that in a final analysis, this ratio, which theoretically shows little variation, is a relatively poor choice for the discounted index. All the same, the theoretical values agree perfectly with the experimental values (on condition that, here again, molecular scattering is subtracted; moreover, this is a problem in interpreting this ratio which Spilhaus apparently did not take into consideration). Table 2 shows both the theoretical values and a few experimental values for this ratio. Even though from a statistical standpoint the values are significantly distinct (A. F. Spilhaus, 1968), it may be seen that it is difficult to draw conclusions on the slight variations observed, except perhaps in regard to the exponent: these experimental values would show that this value may vary basically from -3.5 to -4.2, the most frequent value being -3.9, which is not at all contradictory to the conclusions drawn from application of the preceding criteria.

2.2. Relationships between $\beta(45°)$ or $\beta(90°)$ and b

As early as 1953, Jerlov (N. G. Jerlov, 1953) recommended deriving the total scattering coefficient b from measurements made at 45°. Subsequently a number of investigators have advanced

the opinion that theoretical proof of the constancy of the ratio between $\beta(45°)$ and b has been supplied by D. Deirmendjian (1963). In actuality, this theoretical work dealt with scattering by fog and clouds, the computations being performed with the index of refraction of water and specific laws of distribution. The conclusion drawn by Deirmendjian, stating that $\bar{\beta}(40°)$ is virtually constant (and is moreover equal to 10^{-1}) has not been extended to all cases, since it does not comprise a proof properly speaking, but rather the verification of a numerical property characteristic of the distributions used. Thus Fig. III.5 shows the manner of variation of $\bar{\beta}(44°)$ with the index for four values for the exponents of the law of distribution.[10] Contrary to the distributions considered by Deirmendjian, the power laws result in a considerable variability for the normalized coefficient $\bar{\beta}(44°)$, at a constant index value. /47

Table III gives a number of values obtained for the ratio $\beta(45°)/b$ -- that is, $\bar{\beta}(45°)$ -- values which are relatively certain to be obtained in measurements where computation of b by integration is based on experimental values at small angles, and not on extrapolated values, to the extent that it is possible to subtract the fraction attributable to molecular scattering from $\beta(45°)$. These observations are also valid for the experimental values for $\bar{\beta}(90°)$ shown in the same table. An examination of this table reveals that the experimental values for $\bar{\beta}(40°)$ are located within a narrower interval than the theoretical values, implying that the effective variations in index and exponent are smaller than those considered in the computations. As previously, the corresponding ranges are obtained by comparing the computed values with the experimental values chosen as limits, that is, $1.5 \cdot 10^{-2}$ and $3.6 \cdot 10^{-2}$ for $\bar{\beta}(45°)$, and $1.5 \cdot 10^{-3}$ and $4 \cdot 10^{-3}$ for $\bar{\beta}(90°)$. The ranges, which virtually coincide, are shown in the m-n diagram (Fig. III.6).

In sum, although in practice the relationship between b and $\beta(45°)$ is relatively invariable, as was expected, this has not been borne out theoretically. Inversely, this relationship tends to show the relative stability of the properties of marine particles, both in regard to their distribution and to their average composition, on which the index depends.

---

[10] The curve for the exponent -3.10 is not represented, since for this exponential value, the asymptotic value of the total scattering coefficient is far from being reached with the upper limit α_M used (that is, $\alpha_M = 200$, which corresponds to a variation in ρ from 8 to 60, depending on variations in the index from 1.02 to 1.15); as a result $\bar{\beta}(44°)$ is overestimated in this case. With the exception of a few percentage points, this effect no longer exists with other values for the exponent (cf. Part 2, Section 3.2.3 and Fig. II.15). This problem does not occur for Fig. III.4, since the angular coefficients making up the ratio have reached their asymptotic value, even for the exponent -3.10.

TABLE I. EXPERIMENTAL VALUES FOR THE RATIOS $\beta(10°)/\beta(2°)$ AND $\beta(140°)/\beta(10°)$

$\beta(10°) / \beta(2°) \times 10^2$								$\beta(140°) / \beta(10°) \times 10^3$		
5	2.6 (2.2 - 3.0)	2.7	3.0	3.2	4.7	4.8 (4.5 - 5.4)	3.8	1.39 (1.00 - 1.70)	1.05	1.97
Medit.	English Channel & Medit.	Argus Island	Long Island Sound	Mediterranean		Atlant.	Pacif.	English Channel-Medit.	0.60 - 1.90	1.66 - 2.28
(1)	(2)	(3)		(4a)	(4b)	(5)		(2)	Atlant.	Pacif.
									(5)	

(1) Ratio computed on the basis of values read on the curve given by Y. E. Otchakovsky (1965).

(2) Average values for ratios corresponding to the mean particle indicatrix. The latter is obtained by combining values at angles ranging from 30° to 150° (A. Morel, 1965) with values for small angles, from 1.5° to 14° (D. Bauer, A. Morel, 1967).

(3) R. E. Morrison (1970), ratios measured on curves plotted by a method termed "Duntley" extrapolation by this investigator (Fig. 4, in Ref.)

(4) Ratio corresponding to the average of measurements made in situ at three wavelengths; (4b) to the average of measurements made in vitro at two wavelengths (laser) (F. Nyffeler, 1970). For the in situ measurements it was necessary to extrapolate from 3° to 2° to construct the ratio.

(5) Three measurements taken in the Atlantic (the Bahamas) and two in the Pacific (in the San Diego area) (T. J. Petzold, 1972). For 140°, molecular scattering was subtracted from the absolute values given by the investigator prior to calculating the ratio.

2.3. Characteristic Properties of Coefficients $\beta(4°)$ and $\beta(6°)$ /48

The numerical property revealed by Deirmendjian for a scattering angle of 40° has an equivalent in the case of the indices and Junge laws of distribution considered here. If the indicatrices obtained for the various indices and exponents are examined (A. Morel, 1973) when they have been plotted as normalized $\bar{\beta}(\theta)$ values, one finds that they assume approximately the same values at approximately 4° and 6° (on the order of 12 and 6, respectively). The values for $\bar{\beta}(4°)$ and $\bar{\beta}(6°)$ are given as a function of the index for various exponential values in the same figure, III.4. It may be observed that for a given index value, the variations in these coefficients with the exponent are slight compared to those of the coefficient $\bar{\beta}(44°)$. Even if variations in

TABLE II. THEORETICAL AND EXPERIMENTAL VALUES FOR THE RATIO $\beta(30°)/\beta(45°)$

Theoretical values

Exponent	Index of refraction 1.02	1.05	1.075	1.10
-3.5	3.748	3.875	4.005	4.006
-3.9	3.382	3.407	3.441	3.435
-4.2	3.053	3.057	3.066	3.055
-4.5	2.725	2.724	2.725	2.714

Experimental values (standard deviations)

3.70 ± 0.40 Eng. Chan.-Medit.	3.33 ± 0.22 coastal	3.69 ± 0.67 Bermudas
3.85 ± 0.25	3.32 ± 0.14 N.W.Atlant.	3.53 ± 0.67 (Argus Island)
3.63 ± 0.40	3.53 ± 0.28 Gulf stream	3.28 ± 0.19
3.77 ± 0.75 Indian Ocean	3.61 ± 0.26 Sargasso Sea	3.52 ± 0.33 Long Island Sound
	2.91 ± 0.06 Bermudas	3.32 ± 0.24
	(2)	(3)
3.43±0.39 Baltic	3.00 3.28	3.17 3.38
3.38±0.61 Medit.	2.83 (a) 3.48	3.18 (b) 3.64
	2.97	3.33
(4)	Atlant. Pac.	Atlant. Pac. (5)

(1a) Average value for 20 measurements taken in the English Channel and 40 in the Mediterranean (A. Morel, 1965).

(1b) Average values, at wavelengths of 546, 436 and 366 nm respectively, for 17 samples from the Indian Ocean (Madagascar, unpublished, A. Morel, 1967).

(2) Average values for five types of water sampled between Woods Hole and the Sargasso Sea (A. F. Spilhaus, 1968).

(3) R. E. Morrison, 1970.

(4) Twelve measurements made in the Baltic Sea (excluding 1.25 m station) at four wavelengths (655, 632, 525 and 450 nm), G. Kullenberg (1969).
Sixteen measurements made in the Mediterranean (633 nm), G. Kullenberg and N. B. Olsen (1972). These are the scattering coefficient ratios only for the particles considered here.

(5a) Ratios obtained from the values observed by T. J. Petzold (1972).

(5b) Ratios obtained from the preceding values but with the fraction attributable to molecular scattering subtracted ($1.67 \cdot 10^{-4}$ m^{-1} at 90° for λ = 510 nm, A. Morel, 1968).

the index -- at least between 1.02 and 1.10 -- are taken into account, the conclusion remains the same; thus, for example, $\beta(4°)$ varies from approximately 9.6 to 14. This supports a recent observation made by V. I. Mankovski (1971) with reference to indicatrices plotted in normalized $\bar{\beta}(\theta)$ coefficients (Fig. III.6B). All these indicatrices merge toward θ = 4.5°, on the average, and statistical analysis shows that the correlation coefficient is highest when the regression between b and $\beta(\theta)$, θ has a value of 4.5°. This regression yields $\beta(4.5°) = 9.0b$. Assuming (on the

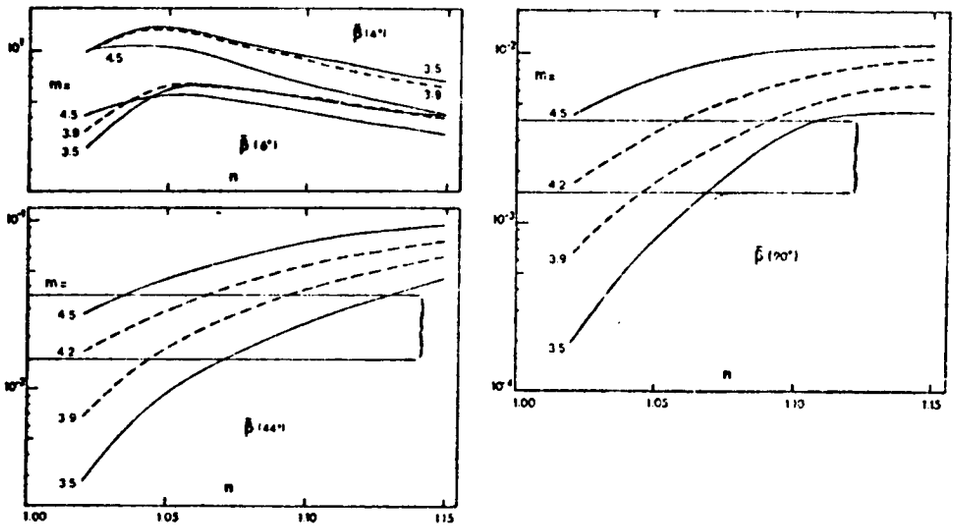

Fig. III.5. Theoretical variations of normalized angular coefficients with the index and the exponent, for 4°, 6°, 44° and 90°. As in Fig. III.4, the brackets correspond to variations observed for single coefficients. These theoretical values, like those in Fig. III.4, are computed for particles whose relative sizes α range from 0.2 to 200.

basis of the gradient of the indicatrix) that $\beta(\theta)$ varies by $\theta^{-1.5}$ within this range of angles, for 4° the preceding value is transformed into $\bar{\beta}(4°) = 10.7$. This value is identical to that given here: 4750/444 = 10.7 (±17%) (D. Bauer, A. Morel, 1967, and Table II, Part 2).

One obvious result of the fact that the normalized coefficient $\bar{\beta}(4°)$ depends very little on the index and the exponent is that comparison of experimental and theoretical values will furnish little information on rational indices and exponents. However, if the value 10.5 ± 2 is used, for example, this value eliminates the possibility of indices higher than 1.10; from another standpoint, if one assumes the index to have a value of 1.05, all exponents (between -3.2 and -5) are possible. One might add that $\bar{\beta}(10°)$, which theoretically is already more variable than $\bar{\beta}(6°)$ or $\bar{\beta}(4°)$, nevertheless remains close to one; it varies from 0.8 to 1.8 when the index is between 1.02 and 1.05 and the exponent between -3.5 and -4.2. It may be noted, without going into further detail, that this fact is confirmed by measurements[11] (on the

[11] See p. 12: $\bar{\beta}(10°) = 1.126$, and also the values obtained by Mankovski: approximately 0.7 and 1.3, and by Petzold: 0.85, 1.13 and 1.04 for the three measurements made in the Atlantic, and 0.88 and 0.99 for the two measurements made in the San Diego area.

TABLE III. EXPERIMENTAL VALUES FOR $\bar{\beta}(45°)$ AND $\bar{\beta}(90°)$ AND STANDARD DEVIATIONS

$\bar{\beta}(45°) \times 10^2$				$\bar{\beta}(90°) \times 10^3$			
2.0 ± 0.5 English Channel and Medit. (1)	2.4 ± 0.9 Baltic (2a)	2.5 ± 0.7 Medit. (2b)	1.6 ± 0.4 Atlant. (3)	2.25 ± 0.4 (1)	3.0 ± 1.3 (2b)	2.9 ± 0.6 (3)	3.16 2.00 2.13 1.63 1.85 (5)
2.3 ± 0.7 Medit.	1.9 ± 0.3 Atlant. (4)	3.4 ± 0.2 Black Sea	2.58 1.82 3.05 1.78 2.80 Atlant.Pacif. (5)				

(1) Mean particle indicatrix (A. Morel, 1965) normalized by the value 444 for the integral yielding b, computations performed assuming $\beta(90°) = 1$ (A. Morel, 1968, and corrected computations, 1970). Normalized by the value 337 given by F. Nyffeler (1969) for the same integral, the values $2.0 \cdot 10^{-2}$ and $2.25 \cdot 10^{-3}$ respectively become $2.6 \cdot 10^{-2}$ and $3.0 \cdot 10^{-3}$. Twenty-seven measurements taken in the English Channel and 40 in the Mediterranean.

(2a) Sixteen measurements made in the Baltic Sea (G. Kullenberg, 1969).

(2b) Fourteen measurements made in the Mediterranean Sea (G. Kullenberg, N. Olsen, 1972); the measurement made at 150 m, station A2, was left out of the averages.

(3) Inverse of the ratios $b/\beta(\theta)$ given by R. E. Morrison (1970), b being the value obtained with the inclusion of measurements at small angles (termed "Sp" by Morrison).

(4) Twenty-three measurements made in the Mediterranean, 90 in the Atlantic, 104 in the Black Sea; measurements performed by V. I. Mankovski (1971).

(5) Measurements made by T. J. Petzold (1972); before the ratios were formed, molecular scattering was subtracted from the values given by the investigator.

other hand, $\bar{\beta}(10°)$ becomes greater than 2 for any exponent if the index is equal to or greater than 1.075). For this angle of 10°, the angular coefficient and the total coefficient have close numerical values.

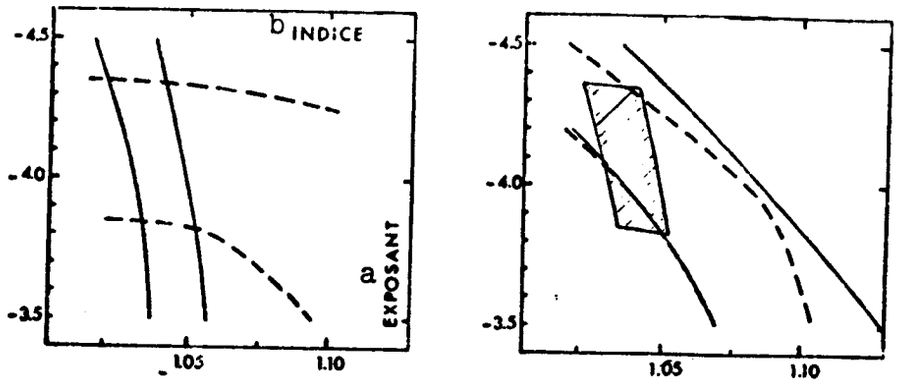

Fig. III.6. Diagrams plotted in the m-n plane (n being the index of refraction forming the abscissas and m being the negative exponent of the law of distribution forming the ordinates) to reveal the ranges in which the theoretical and experimental values are compatible. In the lefthand figure, the band between the two unbroken curves corresponds to application of the criterion constituted by the ratio $\beta(10°)/\beta(2°)$, and the band between the two dotted curves, to application of the criterion $\beta(140°)/\beta(10°)$. The area common to these two ranges has been transferred to the figure on the right. This figure also shows the ranges obtained by comparison of the theoretical and experimental values for normalized coefficients $\beta(44°)$ (range defined by the unbroken curves) and $\beta(90°)$ (range defined by the dotted curves).

Key: a. Exponent
b. Index

2.4. Rational Values for Index of Refraction and Exponent of Law of Distribution

Each of the comparisons which have just been made result in definition of an index and exponent range yielding compatible experimental data and theoretical values. As shown by Fig. III.6, these ranges possess a part in common in which all the criteria used are simultaneously met. Thus the combined values for the index and the exponent which may be considered rational are defined. One may note that the exponential values (from -3.8 to -4.2) are in agreement with the values furnished by a direct particle count (cf. introduction to Part 2) and also that the index values derived in this way, ranging[12] from 1.02 to 1.05,

[12] It may be noted that the central value of 1.04 is the value permitting the widest variations in the exponent within the compatibility range. The examples given below, however, correspond only to cases in which the index is [continued on following page]

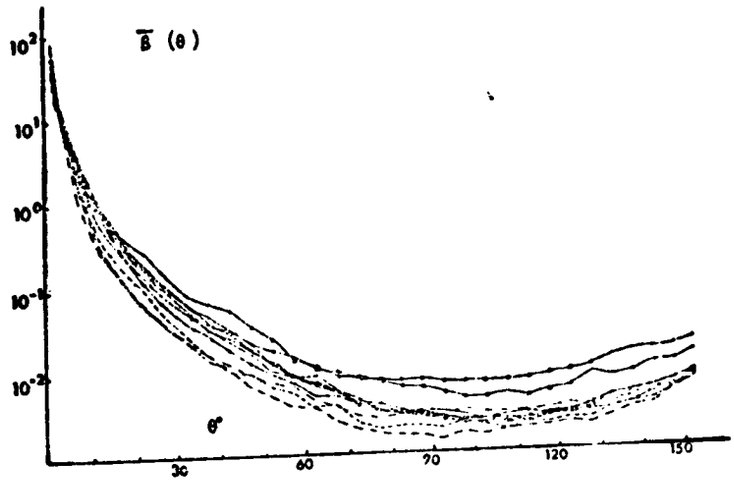

Fig. III.6B. Reproduced from V. I. Mankovski (1971). Scattering indicatrices plotted in normalized values $\bar{\beta}(\theta)$. The measurements were made in the North Atlantic.

appear to be rational. In reference to this last point, H. R. Gordon and O. B. Brown (1972) recently concluded that the indicatrices determined by G. Kullenberg (1968) in the Sargasso Sea may be correctly interpreted if the index is given a value of 1.05 to 0.01 i. By a very different method based on the selectivity of scattering, J. R. Zaneveld and H. Pak (1973) have computed relative index values approximately ranging from 1.02 and 1.04 for particles from both surface and deep layers (3000 m). It should be added that there is no single solution; various index and exponent combinations result in proximate and acceptable indicatrices, taking into account the variability of the experimental indicatrix. A few examples are given below. Lack of information on the physical limits of the population to be used in computation makes it necessary to examine the influence of these limits on the preceding conclusions.

/49

2.4.1. Comparison of Indicatrices

Comparisons may be made at all angles by plotting the indicatrices computed within the previously defined conditions. A few examples are furnished below (Fig. III.7); the mean experimental indicatrix is also given, plotted on the same scale, with tabulated values for the normalized coefficients (cf. Part 1). Other examples of theoretical curves, including cases falling outside the range of rational values, are given elsewhere in more complete form (A. Morel, 1973).

/50

Optimum agreement is obtained when the exponent is assumed equal to -4, the index being 1.05; under these conditions it is virtually impossible to distinguish the experimental curve from the theoretical curve. This agreement, which remains satisfactory

---

12 (cont.) assumed equal to 1.02 or 1.05, taking the preliminary individual indicatrix computations into account (Section 2.2, Part 3).

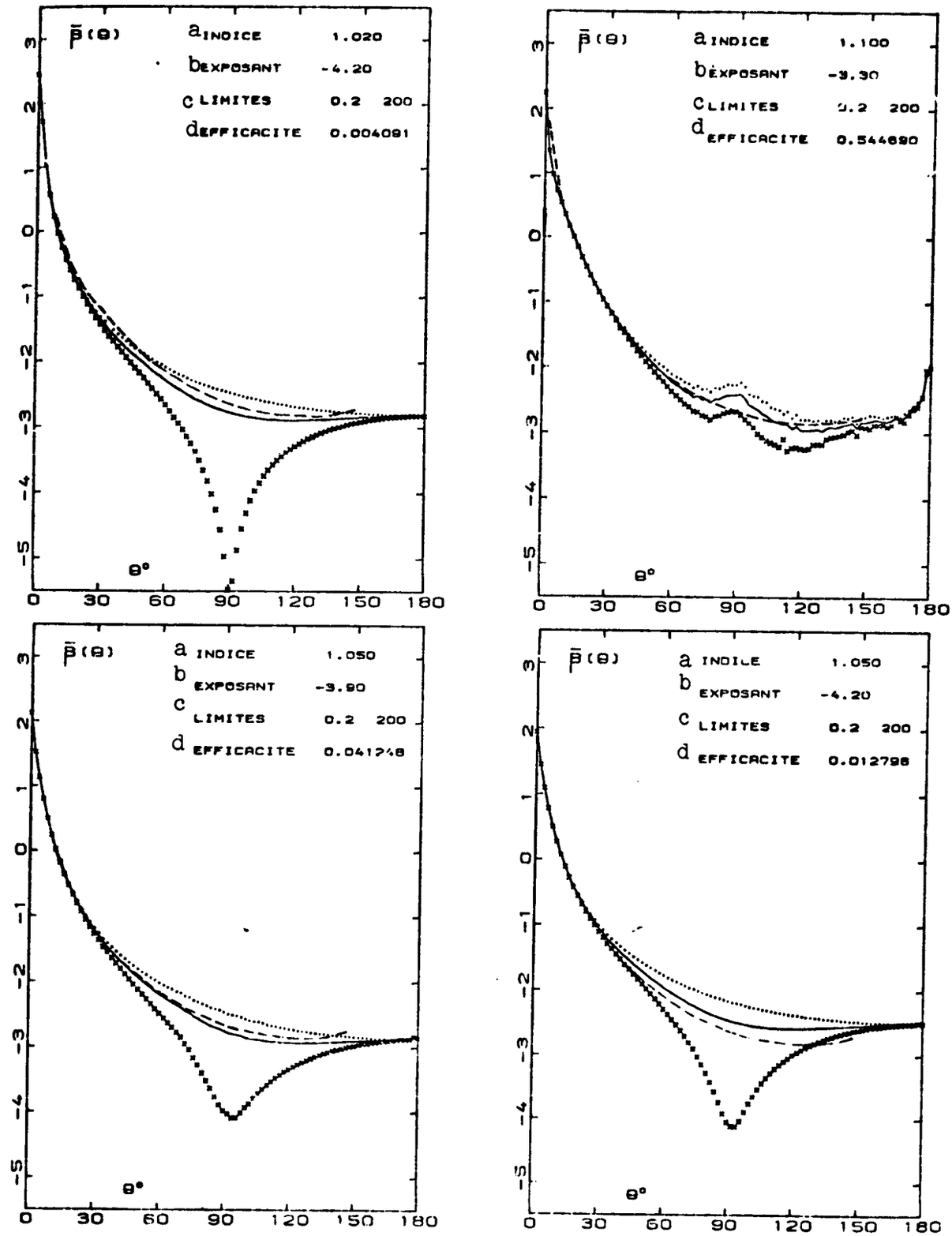

Fig. III.7 (caption on following page)

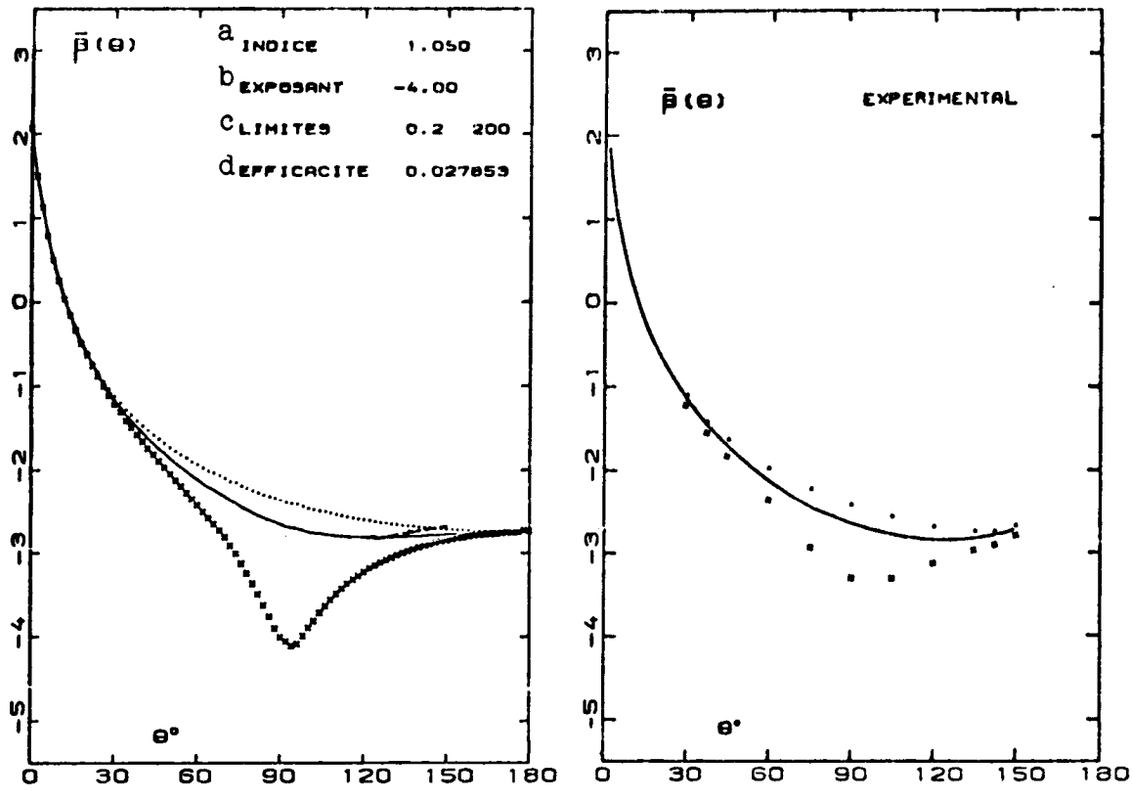

Fig. III.7. Theoretical indicatrices computed for the indices, exponents and limits indicated, are plotted in unbroken lines, with the decimal log of the normalized coefficients $\bar{\beta}(\theta)$ given as a function of θ. The dots and crosses correspond to vertically and horizontally polarized components, $\bar{\beta}_1(\theta)$ and $\bar{\beta}_2(\theta)$, respectively. The experimental indicatrix is shown in an identical manner. It is also shown as a dotted line in the preceding figures. "Efficiency" is an abbreviated notation denoting the mean efficiency factor $\bar{Q}$, whose computed value (equation 3.2, Part 2) is indicated for each case.

Key: a. Index
b. Exponent
c. Limits
d. Efficiency

for neighboring index and exponent values, pertains to an indicatrix in natural light. Two observations should be made on this subject:

a) agreement between experimental and theoretical values for the total intensity $\beta(\theta)$ does not necessarily entrain agreement between values for the two polarized components. For example, if $n = 1.05$ and $m = -3.90$, and if $n = 1.02$ and $m = -4.20$, the computed values for $\bar{\beta}(\theta)$ are virtually identical, but the polarization is much more pronounced in the second case (it becomes total at 90° with the exception of 10^{-3}). This problem will be examined in greater detail later on (Section 4).

b) referring to Fig. III.6, it may be noted that three criteria out of four may be met when the index has higher values and the exponent has lower values (in absolute values). Taking an index of 1.10 and an index of -3.3 as an example, one obtains a curve[13] which compares satisfactorily with the experimental indicatrix, with the obvious exception of the small angle range. The theoretical ratio $\beta(10°)/\beta(2°)$ (0.101) is 2 to 5 times as large as the experimental ratio, and the gradient within this range of angles is too slight.

This second observation once again points up the usefulness of the criterion given by the ratio $\beta(10°)/\beta(2°)$ for indirect determination of a mean particle index.

2.4.2. Initial Observation on the Rational Limits of Distribution

Theoretically there will be coherence between experimental results relative to particle distribution and to scattering, on condition that the index of refraction is assigned certain values and that these values appear reasonable. However, in order to arrive at this coherence, it was necessary to construct another category of hypotheses pertaining to the values for the two limits; consideration should be given to whether or not these limits make the conclusions doubtful. The possible effects are examined in turn:

Upper limit: Since the value assigned to this limit has very little influence on the shape of the final indicatrix, except at an angle of 0°, results on the validity range obtained without use of the value at 0° remain in force. The specific case of a 0° angle will be examined later on (Section 3.1.3), as will the problem of polarization (Section 3.3), whose assigned value at this limit is a determining factor, as will be seen.

---

[13] By abstracting the maximum around $\theta = 85°$, whose position is dependent on the value of the index (Part 2, Section 2.2.5) and whose amplitude increases as the exponent decreases in absolute value.

Lower limit: When truncation[14] progresses toward increasingly high sizes, the asymmetry of the indicatrix becomes more marked (due to a decrease in scattering first at large angles, and then at increasingly small angles; cf. Part 2, Section 3.2.2). Of the ratios chosen to serve as criteria, the first to be affected is $\beta(140°)/\beta(10°)$, and then $\bar{\beta}(90°)$; $\bar{\beta}(44°)$ is affected only if the lower limit α_M exceeds 5; finally, $\beta(10°)/\beta(2°)$ or $\bar{\beta}(4°)$ are not affected as long as α_m remains less than 10 (cf. Fig. II.12). Under these conditions, the ratio $\beta(140°)/\beta(10°)$ being decreased, no matter what the index and the exponent may be, the curves showing the variations in these factors (Fig. III.4) all approximately undergo a translation of more than one order of magnitude, if $\alpha_m = 10$. In the same manner, the curves determined for $\bar{\beta}(90°)$ are also shifted by nearly one order of magnitude. Compared to the theoretical values thus decreased, the experimental values could be explained only by the presence both of high indices, greater than 1.15, and high exponents (in absolute value), greater than 5 or 6. As a result, the various ranges shown in Fig. III.6 will be separated with the use of these new hypotheses, and they will no longer have a part in common. It thus follows that it is impossible to calculate an indicatrix capable of taking into account experimental values for all ranges of angles simultaneously. /51

In conclusion, the coherence noted previously has also disappeared. In order to preserve this coherence, the lower limit α_m of the computations must be set at a value not greater than 1. Although this argument could not constitute an irrefutable proof, there is every reason to believe that this is the case in reality; one need only assume that the law of distribution established experimentally for particles as low as 1 μm in diameter can in fact be extended to particles 0.1 μm in diameter.

3. Other Conclusions and Applications of Theoretical Computations

The first contribution of theory was to show that the general shape of the indicatrix is satisfactorily explained by granulometric data, by means of certain hypotheses whose likelihood has been demonstrated. Theoretical analysis also gives an indication of other consequences in regard to the different roles which the various classes of particles would play in scattering, some classes having a predominant role (Section 3.1). This idea of "effective" classes is essential in approaching the problem of spectral selectivity and in facilitating its interpretation

[14] Or an effect equivalent to truncation, if the distributions are to be extended to small sizes by means of log normal or exponental laws rather than Junge laws (cf. Section 3.2.5, Part 2).

(Section 3.2). There will be a special examination of the problems regarding polarization which have just appeared in comparing the theoretical and experimental indicatrices. Finally, the relationships between particle content and scattering are examined from a practical standpoint in the form in which they may be determined theoretically (Section 3.4).

3.1. Different Roles of Various Classes of Particles

3.1.1. Case of Total Scattering

In the case of a population of particles following a continuously decreasing size distribution, that is, in a case in which it is impossible to determine an average size, nevertheless there may be a class of particles playing a predominant role in the scattering phenomenon. This arises from the factors examined in Part 2 (Section 3.2.3) leading to determination of the range of validity of computations. It was seen that "small" particles, although numerous (and even in infinite numbers) may show finite and low total scattering because the efficiency factor Q is low; inversely, "large" particles, for which Q is constant and equal to 2, are too few in number according to the laws of distribution to be able to have any notable effect on total scattering. Between these two extremes there thus exists a favorable case, that is, a category of particles which are basically responsible for scattering due to the fact that both their number and efficiency are sufficiently high. To determine the size of these particles one need only consult Fig. II.15, which gives, for various exponential values, the value for the parameter ρ corresponding to a given fraction of the total scattering (this latter factor being computed for particles with sizes ranging from 0 to infinity. These values may be presented in another manner which more explicitly reveals the dominant role of certain classes of particles. Thus Fig. III.8 gives the values for ρ corresponding to given fractions of the total scattering (1%, 5%, 10%, 50%, 90%, 95%, 99%) as a function of the exponent.

All these curves tend toward infinity for an exponential value of -3, since with this value and with a theoretically unlimited population, scattering itself is infinite. On the other hand, for other values it may be seen that most scattering (90%, for example, which corresponds to the band delimited by the curves for 5% and 95%) is instigated by particles belonging to the intermediate range: as an example, if the exponent of distribution is -4, particles with a diameter of between 0.4 and 20 μm are responsible for 90% of scattering, and those with a diameter of between 0.6 and 10 μm, for 80% (diameters computed assuming an index of refraction of 1.05 and a wavelength of 419 nm). Table 3.4 gives these values in a more complete manner, also

including the values for ρ corresponding to 50%. These latter values to some extent define a median class with regard to scattering: the sum total of particles of larger size than those in this class and the sum total of particles of smaller size also contribute to scattering. As may be predicted (Part 2, Section 3.2.5), the law of normal and exponential laws of distribution result in a narrower size interval for an identical fraction (80%) of scattering.

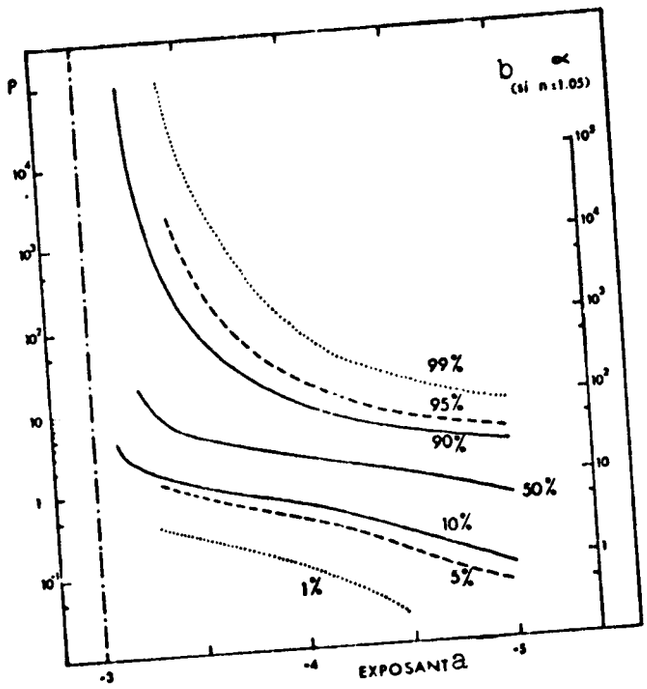

Fig. III.8. As a function of the exponent, values for the parameter ρ corresponding to a given percentage of the total scattering. The latter is computed for an unlimited population and is thus at its maximum possible value. The scale for the α parameter corresponds to a value of 1.05 for the index of refraction.

Key: a. Exponent
b. (If n = 1.05)

Other conclusions may /52 be drawn from Fig. III.8. Thus, for example, the fact that small particles are not accessible to experimentation and particularly to counting does not make it impossible to calculate scattering, since an upper limit for error may be assigned. Along the same lines, although it is acknowledged that the power law is not extended to extremely small sizes and that naturally particles do not decrease in size and increase in number ad infinitum, abandonment of this hypothesis has very little effect on the results; the position of the curve for 1% sets the order of magnitude of this effect. Results obtained with other laws of distribution confirm this point.

Furthermore, the total scattering coefficient which comes into play in the phenomenon of light penetration into the sea, that is, into an infinite medium, is probably greater than can be measured with a device for which the scattering volume is limited. In this case, large particles which produce an intense and erratic signal are not included in the measurements. However, it is reasonable to assume that the change in scale corresponds to an increase in the coefficient of only a few percentage points.

TABLE IV. VALUES FOR ρ* CORRESPONDING TO 10%, 50% 90% OF TOTAL SCATTERING

Exponents	-3,4	-3,6	-3,8	-4,0	-4,2	-4,5	GL**	EX.
10 %	1,42	1,04	0,78	0,60	0,42	0,22	1,20	1,79
50 %	5,60	3,80	3,01	2,46	2,10	1,22	2,70	3,20
90 %	317	48	19	10,2	6,6	4,3	5,50	8,1

* If n = 1.05 and λ = 419 nm, the diameter (in m) is numerically equal to ρ.

** The last two columns correspond to values for ρ in the case of gaussian-logarithmic distribution and exponential distribution, respectively, equations for which were given in Part 2 (caption for Fig. II.16). These distributions are to be compared to the power law distribution with an exponential value of -4.

3.1.2. Case of Angular Scattering Coefficients

The preceding conclusions may be generalized in order to consider the case of angular scattering rather than total scattering. The concept of a dominant class of particles remains, but the limits or the median value for this class will vary with the angle considered. The progressive values for the integrals giving the angular coefficients (Part 2, Fig. II.12) make it possible to determine the value of the parameter α for which the scattering coefficient reaches a given fraction of its final value (considered to be asymptotic). It may immediately be seen that at large angles (θ = 90° to 180°), the greater part of scattering is due to small particles, since the asymptotic plateau is reached at a very early stage; inversely, larger size particles will become more effective in scattering at small angles. It may thus be stated that each part of the indicatrix preferentially represents a given class of particles, the smaller angles corresponding to larger particles. Fig. II.12 also makes it possible to predict that these classes will cover a size interval which will be all the greater as the initial gradient of the curves becomes more slight, that is, as the exponent increases (in absolute value). The class is enlarged in this way by lowering the lower limit and shifting the effectiveness towards smaller size particles.

In order to situate this class in the size scale, it is convenient, as previously, to make use of a median size (this is the value α at which the angular coefficient considered reaches 50% of its final value). Fig. III.9, based on an index of refraction

of 1.05, shows the variations of this median size with the exponent for various values for the scattering angle θ. The median size varies approximately in a ratio of 30 when the scattering angle θ changes from 140° to 2°; the value of this ratio is affected relatively little by the value of the exponent, at least if it is less than 3.70. The median size corresponds to a diameter of 0.1 μm (if λ = 419 nm) for scattering at large angles, 90° or 140°, while the class of particles centered at 3 or 4 μm constitutes the dominant class when scattering occurs at 2°. /53

By now fixing the value of the exponent, it is possible to determine the "effective" class for each angle more accurately than by its median point. For this purpose, it will be necessary, for example, to limit this class by α values for which the angular coefficient considered reaches 10% and 90% of its final value respectively. This is schematically illustrated by Fig. III.10 (the diameter scale is derived from the α scale, letting λ = 419 nm).

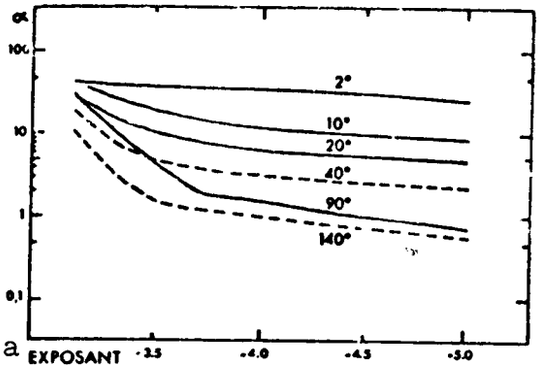

Fig. III.9. As a function of the exponent and for the scattering angles indicated, α values corresponding to median size (size for which the angular coefficient considered reaches 50% of its final value, when α = 200). The index of refraction has a value of 1.05.

Key: a. Exponent

In regard to distribution according to a power law (exponent -3.90 for this example), the effective class gradually broadens and shifts towards smaller particle sizes as the angle θ increases. It may be noted that particles with a diameter of less than 1 μm are responsible for almost all scattering at 140° or 90°; it may be noted that these particles are relatively inaccessible to experimentation. On the other hand, the dominant role is played by particles of 2 to 5 μm in the case of scattering at 2°. If another wavelength is considered, these values must be modified proportionately, since the classes are defined in relation to α; thus the preceding diameters must be doubled if the wavelength itself is doubled (838 nm). This problem, which is directly linked to the problem of selectivity of scattering, will be taken up in more detail later on (Section 3.2). The results are fairly different with the gaussian-logarithmic distribution considered. The preferential effect is less marked than it is in the case of Junge distribution. This may be seen since in relation to the

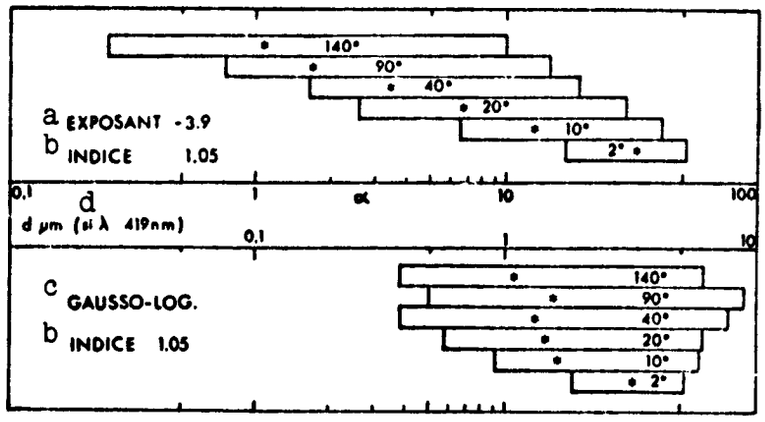

Fig. III.10. The ends of the rectangles correspond to α values for which the volume scattering function considered has reached 10% or 90% of its final value (that is, 100% when α = 200). The median size is marked with an asterisk. The upper part corresponds to computations with a -3.9 power law, and the lower part to computation with the gaussian-logarithmic law for which the equation has been given (Part 2, Fig. II.1¢).

Key: a. Exponent
b. Index
c. Gaussian-logarithmic
d. (if ...)

latter, the initial distribution truncates the population for small and large sizes to some extent, and consequently brings intermediate particles into a more dominant role in scattering; this is a consequence of the phenomena noted earlier (Part 2, Section 3.2.5).

3.1.3. Specific Case of the Angle 0°

The preceding discussion has not been concerned with scattering at 0°, and more generally, with scattering at extremely small angles. When the computations are performed for a population whose exponent is less than 5 in absolute value, the integral giving the value for the scattering coefficient at 0° does not converge (cf. Part 2, Section 3.2.1). This absence of any asymptotic value makes the definition of an effective class for this angle arbitrary; more exactly, by extension this class will always consist of the largest particles, that is, to the last particles taken into account by the integral. However, a few useful concepts may nevertheless be drawn from theory. In figures such as III.12, which give the progressive values for the integrals:

$$\int i_T(\theta,\alpha)\, F(\alpha)\, d\alpha \ ,$$

the curve for 0° continues to increase with a gradient of 5 - m, while the curve for 2°, on the other hand, begins to form a plateau for a value α_2 for the parameter α, a value which varies with the index[15], and is on the order of 40 if, for example, the index is assumed to be equal to 1.05. Thus it is immediately possible to determine what the size of the largest particles present must be, for which the ratio $i(0°)/i(2°)$ has a given value k; this value is:

$$(\alpha_o / \alpha_2)^{5-m} = i(0°) / i(2°) = k$$

An attempt may be made, at least in an approximate manner, to apply this equation to the measurements made by T. J. Petzold (1971). The results obtained by this investigator deal with an angle of 0.1° rather than 0°. The ratio between $i(0.1°)$ and $i(2°)$ is on the order of 10^2; assuming the ratio k to be on the same order (and giving the index of refraction a value of 1.05), one thus will have: $(\alpha_o/40)^{5-m} = 10^2$, which results in: $\alpha_o = 4000$ if $m = 4$, or $\alpha_o = 862$ if $m = 3.5$. Although it is only approximate, this estimate nevertheless shows that the upper limit of the integral must be increased to well beyond $\alpha = 200$ in order to deal with experimental results obtained at extremely small angles[16].

This also points up the relative but poorly defined nature /54
of the indicatrix within this specific range of angles, since its shape probably depends on the spatial scale considered. Thus the indicatrix to be used in computations for long-distance transmission, or the indicatrix which may be derived from the transfer function of spatial modulation (W. H. Wells, 1970) might show a more "pointed" lobe than would an indicatrix determined with the use of an experimental device using a shorter optical trajectory. Simple geometrical considerations show that this conclusion is not contradictory to the fact that the total scattering coefficient increases very little as the scattering volume under consideration increases (cf. Section 3.1.1): when large particles are brought into consideration due to a change in scale, this front lobe, becoming increasingly pointed, also becomes increasingly narrow. It may be seen by extension that in this case particle scattering is complemented by scattering due to

[15] As was seen earlier, this value for α should be such that the parameter $\rho = 2\alpha(n - 1)$ is equal to 4.1 (Part 2, Sections 2.2.4 and 2.2.7).

[16] Except perhaps for problems related to transmission of images, this capacity for prediction of results makes it relatively futile to extend the computations to $\alpha > 200$, a procedure which is very time-consuming, even with a fast computer.

heterogeneities in the index which this time are on a macroscopic scale, as are the fluctuations which produce them.

3.2. Dependence of Scattering on the Spectrum

For a particle population whose distribution follows a law of crenelated type, which at least in practice amounts to distribution following normal or log normal laws (cf. Part 2, Section 3.2.5), there is no theoretical difficulty in computing the spectral selectivity of scattering, since there is no problem of limits. For a distribution determined in relation to the true size (diameter), modification of the wavelength results in an inversely proportional modification of the relative size α, and also of the parameter $\rho = 2\alpha(n - 1)$. This change simultaneously affects the quantity to be integrated and the limit of integration in the equations giving the mean efficiency coefficient $\overline{Q}$ or the volume scattering function (equations 3.2 and 3.3, respectively, Part 2). Whether $\overline{Q}$ is computed with the parameter α or with the parameter ρ in order make use of the approximate Van de Hulst equation (2.29), it is always necessary to assign a value to the index of refraction.

It is simple to predict the scattering selectivity (total) for a population whose polydispersion is relatively slight. This selectivity depends on the size on which the distribution is centered and, at the same time, on the value given to the index; that is, the computations must be performed taking into account the parameter ρ and the value assumed by this parameter at the average size. Referring to Figs. II.10 and II.11 in Part 2, one may see that if the average size is such that at λ, the change in wavelength always has values less than 4, scattering will be selective with a negative exponent, that is, with λ^{-x}. If as ρ varies with λ it remains extremely small, x will be equal or close to 4; if ρ remains between 0.1 and 2, x will be on the order of 2, and then will become less than 2 and will tend towards zero as ρ approaches 4. Finally, if ρ varies between 4 and 7 due to the change in wavelength, an inverse of this selectivity will be the result, that is, one expressed by a λ^{+x} law. All this can immediately be deduced on the basis of the undulations in curve $Q(\rho)$. To conclude, if ρ always remains high, the selectivity will be virtually zero. If the polydispersion of the population is no longer slight (if, for example, with distribution according to a log normal law, the geometrical standard deviation is relatively large), the preceding selectivity factors may still occur, but due to the effect of the mean deviation, they will become increasingly attenuated as the distribution becomes more polydispersed.

Applications for these principles have been sought in oceanographic optics, particularly by W. V. Burt (1955, 1956).

The governing idea of the interpretation sought consists first in assuming that the distribution is gaussian-logarithmic, and then in centering the maximum of this distribution precisely within the range where ρ is less than 4, in order to obtain selectivity in conformity with that found experimentally; for this purpose, it was necessary to use a fixed index. The main drawback of this approach is that it yields a result which, first, presupposes the existence of a distribution maximum, and second, makes the value assigned to the index depend on the position of this maximum. Thus Burt obtains maximum numbers of particles for diameters ranging from 0.6 to 1.2 μm which, for example, would be 1/10 the size obtained if the index had been assumed equal to 1.015 rather than 1.15. If one refrains from making any hypothesis on the limits of the distribution and the existence of a maximum, one is confronted with the problem of determining whether the theory remains practicable and whether or not a given selectivity is rational. In addition, the influence of the choice of index should be examined given these new conditions.

3.2.1. General Case: Selectivity in the Case of an Unlimited Junge Distribution

This α^{-m} distribution is assumed to extend to all particles, ranging in size from zero to infinity[17]; although the index of refraction is not stipulated, it should remain constant within the wavelength considered, so that for a given class of particles, variations in the ρ parameters are not due to variations in λ. The following reasoning may be used: with a population which remains unchanged, if the wavelength is modified, λ becoming λ', with $\lambda' = k\lambda$ (k is greater than 1, for example), those particles with dimensions which are k times greater than previously will play the same role in scattering. More precisely, given a class of particles of diameter d, within an interval Δd in which the Q factors have a given value, when the wavelength is modified, this same value for Q may be assigned to be class of particles of diameter kd within an interval $k\Delta d$. According to the law of distribution, the number of particles of size kd is smaller than that of particles of size d in the ratio k^{-m}, but the class itself is broadened in the ratio k; finally, the number of particles of class "kd" is k^{1-m} times that of the corresponding class "d." The geometrical cross section of these particles is k^2 times greater, and thus the total surface area for class "kd" of size $k\,d$ is k^{3-m} times that of the class initially serving the same function. Now, Q is unchanged; thus the scattering, the product of the surface area and the efficiency factor, is itself multiplied by k^{3-m}. Since this reasoning may be applied to

[17] The number of particles is obviously infinite, which does not preclude the possibility that scattering may be finite, under certain conditions which have been discussed previously (Part 2, Section 3.2).

all classes, and since all the classes exist, the selectivity of scattering for the entire population consequently follows a law of λ^{3-m}.[18]

This very simple result may appear to correspond to an ideal case and thus be inapplicable in practice. The previously discussed concept of a "dominant" class in scattering (Section 3.1.1) makes it possible to determine the possibilities for application by showing the influence of hypotheses dealing with the index and the limits. It is now possible to affirm that selectivity is not solely a property of suspensions whose polydispersion is slight. /55

3.2.2. Modification in the Case of Non-Unlimited Distribution

The λ^{3-m} law applies to the integral $\int_0^\infty F(\rho)\, Q(\rho)\, \rho^2\, d\rho$. If the limits are no longer 0 and ∞, but rather ρ_m and ρ_M, the same law continues to apply, but another effect is added. This consists in the fact that the value of the integral itself is modified, since the change in wavelength results in a change in the limits related to the diameters d_m and d_M rather than to ρ; if λ becomes $k\lambda$, ρ_m and ρ_M become ρ_m/k and ρ_M/k. The results may be predicted by referring to Fig. II.8, which reveals the "effective" classes.

To take an initial example, let us assume a population of particles extending between sizes giving ρ the values 0 and ρ_M, and let us assume that for a given wavelength λ, ρ_M is such that the scattering reaches 95% of its maximum possible value (computed when ρ_M tends toward infinity). If the wavelength is doubled, since ρ_M is divided in half, the integral will assume a lower value, corresponding to 90%, for example. As a result, the selective effect in λ^{3-m} will be modified slightly (if the exponent $3 - m$ is negative, the modification is in the direction of reinforcement of the selectivity). The opposite example of a population for which ρ varies from ρ_m to infinity shows that the same change in wavelength increases the value of the integral; the selectivity will be decreased in a more or less appreciable manner, depending on the initial value of ρ_m (it will always be decreased in cases where $3 - m$ is assumed to be negative).

---

[18] This result may easily be found by computation using the equation giving the mean efficiency $\bar{Q}$ (Part 2, equation 3.2) and taking 0 and ∞ as limits. This time, the computations need only be performed as a function of d, n and λ, rather than ρ, and by substituting $k\lambda$ for λ. The denominator (total area) remains unchanged and the mean factor $\bar{Q}$ is multiplied by k^{3-m} when the distribution is expressed by $F(d) = \text{Const.} d^{-m}$).

In general, it may be seen that if the particle population broadly covers the effective classes, the law of selectivity remains unchanged; otherwise it may be more or less affected. It will be affected, for example, in the two following cases, even if there is a broad range of particle size: if the relative index is assumed to be very close to 1 (resulting in low values for ρ), or if the exponent of distribution, as shown in Fig. II.8, approaches the value -3 (since in this case the concept of effective classes tends to disappear). In practice, in conformity with the conclusions found on the rational values for the index and exponent (Section 2.4), that is, for example, 1.05 and -4 respectively, the dominant classes responsible for 98% of scattering (from 1% to 99%) will possess diameters ranging from 0.1 to 100 μm (for λ = 419 nm). Under these conditions, which are probably close to reality, a change in wavelength, with the exception of a few percentage points, will preserve the value of the integral and thus the law of selectivity, which will be expressed approximately by λ^{-1}. Numerical examples will be given below (Section 3.4).

3.2.3. Shape of Indicatrix and Wavelength

In practice, this discussion is related to that given in Part 2 (Sections 3.21 and 3.2.2) concerning the influence of limits on the result of computation of the indicatrix. When the convergence conditions are met, and provided that the range of sizes is sufficiently broad, the shape of the resultant indicatrix is not heavily influenced by the values assigned to the limits, as has been seen. A change in wavelength resulting in a change of limits will thus have no appreciable effect, except once again for scattering in the immediately vicinity of 0° (if $m < 5$). In this respect, Fig. III.2 may be considered to represent variations in the indicatrix for a variation in wavelength in a ratio of 4. (Strictly speaking, when α_M changes from 200 to 50, α_m should become 0.05 rather than retaining its value of 0.2, but this would have no influence on the results; cf. 3.2.2, Part 2.) If in practice the Junge distribution is not to be extended to small sizes and must be truncated, one predictable effect will be an accentuation of the asymmetry of the indicatrix as the wavelength decreases; this asymmetry may be figured on the basis of the numerical values indicated previously[19].

[19] Cf. Part 2, Section 3.2.2, "Case in Which Truncation Occurs for Sizes Outside the Rayleigh Range."

3.3. Polarization[20]

Until now, the problem of polarization has been set aside; it has been mentioned only when the experimental indicatrix was compared to theoretical indicatrices. As an initial commentary on the results yielded by theoretical computation, the following remarks deal simultaneously with the properties of individual indicatrices and those of indicatrices for polydispersed systems:

a) computations performed for individual cases have revealed oscillations for the two polarized component $i_1(\theta)$ and $i_2(\theta)$ which are still greater than for the total intensity $i_T(\theta)$, where, due to the the mean effect, they have become slightly attenuated (cf. the examples given in Appendix 2). In addition, the polarization may be reversed, when i_2 ("horizontal" or "parallel" component) is greater than i_1 ("vertical" or "perpendicular" component); the rate of polarization, which is written (cf. Part 2, Section 1.2):

$$p(\theta) = \frac{i_1(\theta) - i_2(\theta)}{i_1(\theta) + i_2(\theta)}$$

thus becomes negative.

b) the integration procedure making it possible to deal with the case of a polydispersed system of particles results in smoothing. The normalized values relative to polarization $\bar{\beta}_1(\theta)$ and $\bar{\beta}_2(\theta)$ (cf. Equation 3.3, Part 2) are not much more irregular than the quantity $\bar{\beta}(\theta)$ itself; the normalized values which persist are probably due to the fact that the number of terms in the weighted addition which replaced integration in practice is no longer sufficient.

c) for individual indicatrices, polarization generally tends /56 to decrease for small and for large angles, theoretically disappearing at 0° and 180°. It reaches a maximum at 90° in the case of small particles, that is, for those belonging to the Rayleigh and Rayleigh-Gans ranges. Extension of integration to the entire population does not result in a disappearance of the general characteristics. It may be noted that, other things begin equal (exponent, limits), polarization increases as the index draws

---

[20] As was stated in Part 2, this problem will not be considered in its more general aspects, since only components i_1 and i_2, and not i_3 and i_4, were computed in the preliminary Mie theory computations. As a result, the polarization of scattered light may be studied for cases in which the incident light is natural, but not for cases in which the incident light itself is polarized (rectilinearly, circularly, etc.).

dloser to 1[21]; this is the significance of the deviation between $\bar{\beta}_1(\theta)$ and $\bar{\beta}_2(\theta)$, especially in the vicinity of $\theta = 90°$. As shown by Figs. III.2 and III.7, the very marked minimum for $\bar{\beta}_2(\theta)$ is centered on 90° for an index of 1.02, but for higher indices, this minimum is flatter and is located at angles slightly greater than 90°. Fig. III.11 reveals this fact.

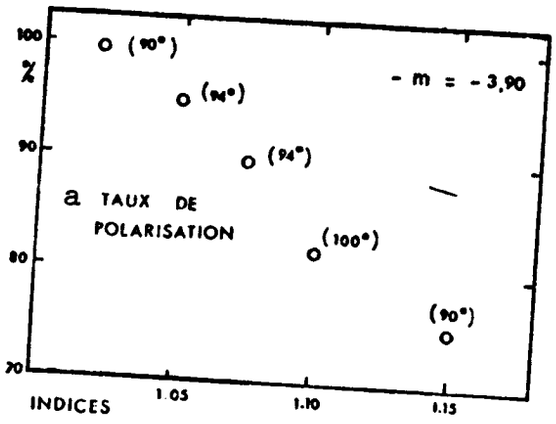

Fig. III.11. Theoretical values of maximum rates of polarization as a function of index of refraction, with both population distribution and limits remaining unchanged (exponent -3.9, limits $\alpha_m = 0.2$ and $\alpha_M = 200$). The figures in parentheses indicate the angle θ at which the polarization maximum occurs.

Key: a. Rate of polarization

3.3.1. Influence of Limits and Interpretation

Fig. III.2 illustrates the effect of the upper limit: when the upper limit α_M is raised from 50 to 200, the indicatrix for natural light $\bar{\beta}(\theta)$ undergoes little change, and the same is true of the vertical component $\beta_1(\theta)$. On the other hand, the maximum polarization (and even the polarization at other angles) decreases, since the minimum for the horizontal component $\beta_2(\theta)$ is less marked.

Fig. III.12 shows the opposite example of the influence of the lower limit α_m. When this limit is raised from 1.2 to 10, in this case, as has been seen, $\bar{\beta}(\theta)$ decreases except at small angles, and the same is true of the component $\bar{\beta}_1(\theta)$. On the other hand, the minimum for the indicatrix for component $\beta_2(\theta)$ remains unchanged.

To summarize, taking the typical case of $\theta = 90°$, the rate of polarization in the first case is decreased by an increase in $\beta_2(90°)$, while in the second case this decrease is the result of a decrease in $\beta_1(90°)$.

[21] This may be explained by the fact that in this case the Rayleigh-Gans range extends to relative sizes α which may be proportionately greater without violating the condition $\alpha < 1$ (Part 2, Section 2.2.3).

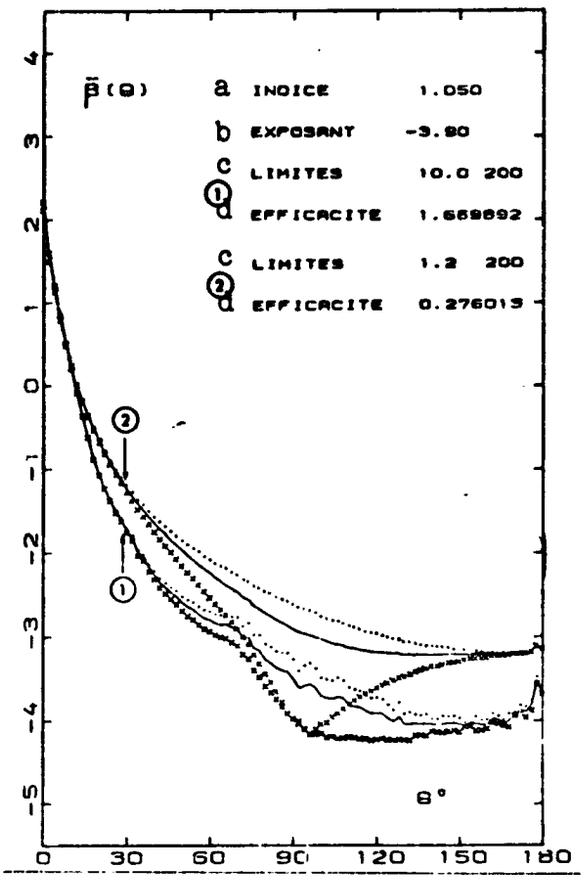

Fig. III.12. Theoretical indicatrices computed on the basis of the indicated values and plotted using the same scales and symbols as previously: points for $\bar{\beta}_1(\theta)$ and crosses for $\bar{\beta}_2(\theta)$. The two cases shown here may be compared with that given earlier (Fig. III.7), where the lower limit was $\alpha_m = 0.2$, the index and exponent otherwise being the same.

Key: a. Index
b. Exponent
c. Limits
d. Efficiency

Interpretation of these effects is based on reasoning analogous to that used for the total intensity i_T. (The discussion will be limited to an examination of polarization at 90°.) A graph of the functions $i_1(90°)\alpha^{-4}$ and $i_2(90°)\alpha^{-4}$ reveals differences in the behavior of these two quantities (Fig. III.13). The decrease in $i_1(90)\alpha^{-4}$ to which that of $i_T(90)°\alpha^{-4}$ may roughly be transferred thus occurs along a gradient of close to -2.3 for this same refractive index of 1.05. For the horizontal component the corresponding quantity decreases more slowly, with a gradient on the order of -1 which even tends to disappear for high α values, on the order of and greater than 100. When computation is performed for the entire population, the two integrals will not converge simultaneously (equation 3.3 and Section 3.2.1, Part 2). The convergence will be slower for the horizontal component (index 2) than for the vertical component (index 1); in fact, it may even be lacking, since the condition $5 + p - m < 0$ (condition 3.4, Part 2) may not be met in the first case (where $p \sim -1$ or 0) while it is met in the second ($p \sim -2.3$). This is approximately the case illustrated by Fig. III.14 (where $m = 3.9$); the curve representing the progressive value of the integral continues to increase for the horizontal component; on the other hand, the curve for the vertical component has an asymptotic plateau.

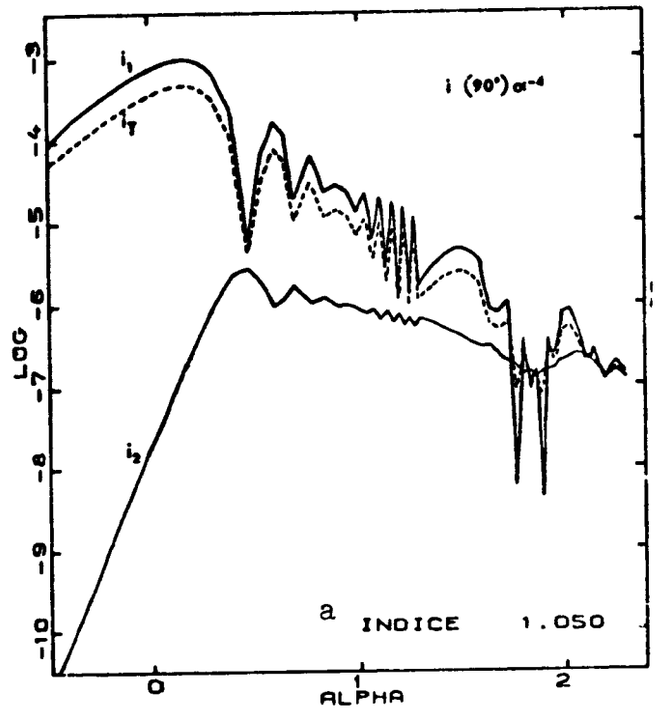

Fig. III.13. As a function of the relative size α, variations in the functions $i_1(90°)\alpha^{-4}$, $i_2(90°)\alpha^{-4}$ and $i_T(90°)\alpha^{-4}$ with $i_T = (1/2)(i_1 + i_2)$. The scales are logarithmic. This figure may be compared with those given in Part 2 (Figs. II.3 and II.5) or the analogous figure relative to the index 1.05 (A. Morel, 1972).

Key: a. Index

3.3.2. Conclusions; Second Observation on the Value of the Limits

Applying the preceding, in practice $\bar{\beta}_1(90°)$, like $\bar{\beta}(90°)$, can be influenced only by a change in the lower limit α_m, while $\bar{\beta}_2(90°)$, whose value is determined by the upper limit α_M[22], is not affected by this change. This is the case shown in Fig. III.12. On the other hand (case shown in Fig. III.2), a change in the upper limit α_M affects only the component $\beta_2(90°)$ to the exclusion of $\bar{\beta}_1(90°)$, and consequently $\bar{\beta}(90°)$; as α_M increases, $\beta_2(90°)$ continues to increase and the polarization decreases. In short, each of these two limits exerts an influence selectively on one or the other of the two polarized components.

For the same reasons, an analogy may be drawn between the case of forward scattering and right-angle polarization, more precisely, an analogy between the behavior of $\bar{\beta}(0°)$ and $\bar{\beta}_2(90°)$ (cf. 3.1.3): these quantities continue to increase with the upper limit (except when m is greater than 5).

When the experimental indicatrix was compared with various theoretical indicatrices, it was noted that there could simultaneously be satisfactory agreement for values obtained for natural light -- $\bar{\beta}(\theta)$ -- and unsatisfactory agreement for polarization. In no way can this lack of agreement constitute an argument, and it was not taken into consideration in conclusions on the values for the

---

[22] As previously, the upper limit α_M must be assumed to have an adequate value, that is, the polydispersion of the population must be assumed to be slight.

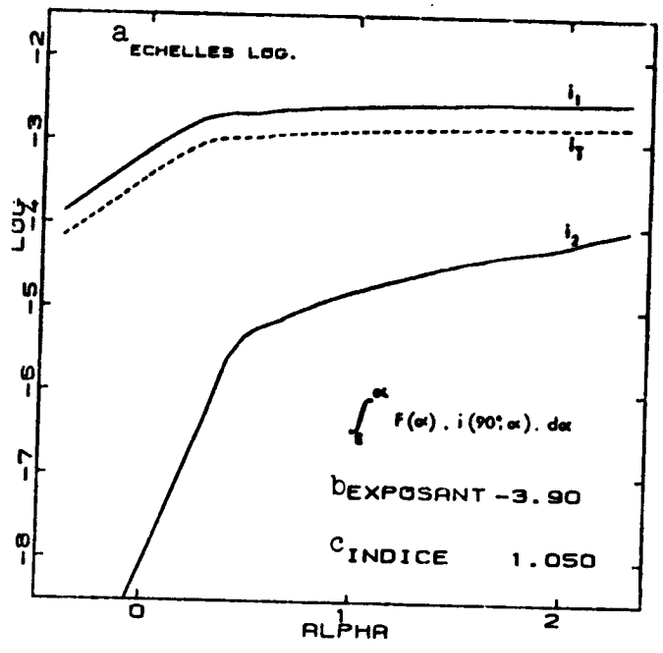

Fig. III.14. Analogous figure to Fig. II.12 in Part 2, but in this case based on the angle $\theta = 90°$ alone. In addition to the curve showing the progressive value of the integral for the total intensity (dotted line), curves for the two polarized components are also plotted.

Key: a. Log scales
b. Exponent
c. Index

exponent and the index (Section 2.4). For example, the case in which the index and the exponent are 1.02 and -4.2, respectively, results in an extremely high theoretical rate of polarization, which will quite likely be reduced by raising the upper limit, nevertheless without any effect on the values for $\bar{\beta}(\theta)$. Thus the values indicated remain rational in spite of the lack of agreement with reference to polarization. These considerations also have a negative aspect, since they demonstrate the limiting possibilities for interpretation of experimental results. Caution must be exercised /58 in assuming and even computing a high upper limit with regard to polarization, as was done in order to take into account the scattering observed at small angles. The extension of the curve $i_2(90°)\alpha^{-4}$ is not predictable in a simple manner as is that of the curve for 0°; thus any conclusions on the upper limit must necessarily remain questionable. It should also be recalled that although the assumption that marine particles are spherical is justifiable for the total intensity, it is less so with regard to polarization (cf. Preliminary Remarks, Part 2, and Holland and Gagne, 1970).

3.4. Relationships Between Scattering and Particle Content

One of the most frequently cited reasons for systematic measurement of light scattering is, justifiably, an attempt to estimate the concentration of suspended matter in seawater. However, there are a number of uncertainties involved in determining quantitative relationships, both from an experimental and a theoretical standpoint. These arise from the hypotheses which

must be made on the mean efficiency factor $\overline{Q}$, the index, the extreme sizes to be considered, possibly on the weight per unit volume of the particles, and so forth. These problems have already been recognized by Y. E. Otchakovsky (1965 b) and by G. F. Beardsley et al. (1970), to name only two examples. It is useful to examine the influence of these hypotheses before indicating how the results of theoretical computations may be applied, and what precautions should be taken in applying them.

3.4.1. General Observation on Possible Variations in the Mean Efficiency Factor $\overline{Q}$

The first problem consists in computing the total scattering coefficient when the number of particles, counted between two size limits, is known, as well as the law governing their distribution. The reverse problem consists in determining data on the quantity of particles (volume, surface area, number) on the basis of observed scattering coefficients. In the first case, the amount of scattering due to the counted particles may be computed with absolute accuracy when the index is known (or is chosen); nevertheless, the solution to the problem remains incomplete, since the scattering which would be observed experimentally for the same sample is a priori greater than that which is computed, since it involves uncounted particles. The fact that "effective" classes exist (cf. Section 3.1.1) shows that in some cases the influence of the limits is slight; it is possible to estimate an order of magnitude for the difference between calculable scattering and real scattering. Solution of the reverse problem requires a still greater number of hypotheses: those relative to the index and the limits must be added to those dealing with the law of distribution.

The relationships which may be determined are dependent on these hypotheses. The method for revealing this dependency consists in analyzing variations in the mean efficiency factor $\overline{Q}$ with the index n, the exponent m and the maximum and minimum diameters in the distribution d_m and d_M (or the corresponding parameters, α_m and α_M or ρ_m and ρ_M). For the index values considered, use of the limiting Van de Hulst equation is justified to compute Q (Part 2, Equation 2.29), and in this case the mean factor, more conveniently defined in relation to ρ rather than α, is written:

$$\overline{Q} = \frac{\int_{\rho_m}^{\rho_M} F(\rho)\, Q(\rho)\, \rho^2\, d\rho}{\int_{\rho_m}^{\rho_M} F(\rho)\, \rho^2\, d\rho}$$

Thus various applications may be drawn from a single computation procedure, depending on the value assigned to the index. (By way of review -- cf. Part 2, Section 2.2.10 -- Q must be determined by means of the exact formulas when ρ is small; in practice, less than 0.2.) Fig. III.15 (A. Morel, 1972 b) shows variations in $\overline{Q}$ with the exponent of distribution, the various curves corresponding to different pairs of values given to the limits ρ_m and ρ_M.

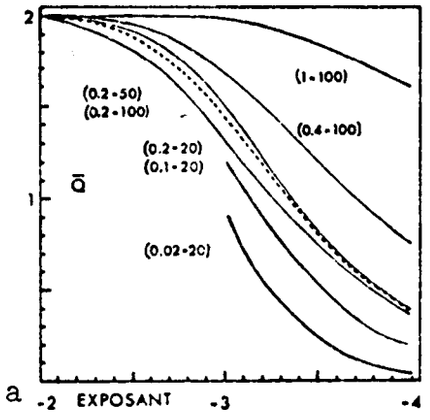

Fig. III.15. Variations in mean efficiency factor $\overline{Q}$ with the exponent of distribution. The values in parentheses correspond to the parameters ρ_m and ρ_M computed for the limits of distribution.

Key: a. Exponent

When the exponent is equal to -2, the surface areas of all the classes of particles are equal, and the mean value $\overline{Q}$ is actually the mean value of the function $Q(\rho)$ (cf. Fig. II.10, Part 2), and thus $\overline{Q}$ is close to 2 no matter what the lower limit may be, and provided that the upper limit is fairly high (ρ_M = 10 or 20, for example). $\overline{Q}$ may be slightly greater than 2 if the chosen interval ρ_m - ρ_M is small and favors a maximum in the curve $Q(\rho)$. As the exponent increases (in absolute value), the increasing relative significance of the small particles results in a decrease in $\overline{Q}$. When m reaches and exceeds 4, there is little influence exerted by particles of small size, and thus by the upper limit α_M, and in practice, $\overline{Q}$ depends only on the value of the lower limit.

Finally, the factor $\overline{Q}$ may vary considerably with the exponent, with the limits, and consequently with the index and the wavelength, since these parameters influence the values of the limits. This reveals the difficulties which emerge in practical application due to the assumptions which must be made, while at the same time a perfect mathematical solution is obtained. /59

3.4.2. Examples of Application

The concrete value of these various influences may be determined by taking the example of a population of particles distributed according to a power law within a size interval limited by the diameters d_m = 1 µm and d_M = 20 µm. Taking into account the values assigned to the index and the wavelength, the values α_m and α_M or ρ_m and ρ_M in the following table correspond to these diameters:

TABLE V. CORRESPONDENCE BETWEEN d, α AND ρ FOR TWO WAVELENGTHS AND THREE INDICES

d (m)	α	ρ			
	if λ = 419 nm	if n =	1.03	1.05	1.10
d_m = 1	α_m = 10	ρ_m =	0.6	1.0	2.0
d_M = 20	α_M = 200	ρ_M =	12	20	40
	if λ = 546 nm	if n =	1.03	1.05	1.10
d_m = 1	α_m = 7.7	ρ_m =	0.46	0.77	1.54
M = 20	α_M = 154	ρ_M =	9.24	15.4	30.8

Using the equation reviewed above, it is possible to compute the mean factor $\bar{Q}$ between the limits constituted by the various pairs of values ρ_m - ρ_M for different exponents for the law of distribution. The results are given in Table 6. The percentages indicated[23] correspond to the ratio of scattering due to particles within the interval 1 - 20 μm to the hypothetical scattering of an unlimited population. This reveals that in some cases, especially if a high value is assigned to the index, the "explained" fraction of scattering is slight. In a favorable case (λ = 546 nm, n = 1.05, m = 3.9), theoretically (and at a maximum), 14% of scattering would be attributable to particles with a diameter of less than 1 μm (ρ < 0.77), 9% to those with a diameter greater than 20 μm (ρ > 15.4), the scattering due to particles between 1 and 20 μm forming 77% of the theoretical total. This comes down to the fact that in this case the particles considered basically make up the effective classes (cf. Fig. III.8).

Fig. III.16 shows variations in the mean factor $\bar{Q}$ as a function of the index, for the two wavelengths and for various exponents. Fig. III.17 reveals the fact that the selectivity of scattering depends on the exponent. The curve plotted is that corresponding to the theoretical law applicable to an unlimited population, that is, the λ^{3-m} law (cf. Section 3.2.1), and the dots represent the characteristic selectivity ratios $\bar{Q}_{419}/\bar{Q}_{546}$ for the limited population[23] (1 to 20 μm) considered.

---

[23] The percentages indicated in Table III.6 theoretically make it possible to determine the values corresponding to an unlimited population. Thus the values represented by crosses, which normally should be found on the curve given in Fig. III.17, are computed. A slight degree of inaccuracy which may be expected in this type of computation results in an overestimate of the percentages and explains the slight disagreement.

TABLE VI. FOR VARIOUS INDICES AND WAVELENGTHS, THE MEAN EFFICIENCY FACTOR $\bar{Q}$ VALID FOR A POPULATION OF PARTICLES RANGING FROM 1 TO 20 μm AND DISTRIBUTED ACCORDING TO POWER LAWS WITH EXPONENTS AS INDICATED

λ = 419 nm	Exponents							
	-3,6		-3,9		-4,2		-4,5	
n = 1.03	72.3	1.282	79.2	1.089	76.9	0.920	66.8	0,780
n = 1.05	73.0	1.756	74.7	1.626	67.4	1.496	54.5	1.374
n = 1.10	63.3	2.307	57.5	2.338	46.0	2.355	31.3	2.365
	%	$\bar{Q}$	%	$\bar{Q}$	%	$\bar{Q}$	%	$\bar{Q}$
λ= 546 nm								
n = 1.03	69.7	1.028	78.3	0.828	79.3	0,663	72.6	0,533
n = 1.05	72.7	1.539	77.1	1.375	71.9	1,222	60.4	1,086
n = 1.10	67.8	2.171	64.4	2.148	54.0	2.111	40.6	2.064

Direct Problem: Computation of Scattering

The following example may be used in providing a practical application for the preceding: let us assume a known total number of particles per unit volume between two size limits corresponding to the diameters d_m and d_M, that is, the number:

$$N = \int_{d_m}^{d_M} F(d)\, d(d) ,$$

and assume the distribution to be expressed by $F(d) = Ad^{-m}$. Both the total surface area S of the geometrical cross sections and the total volume V of these particles may be computed. To facilitate application, it is convenient to give the ratio of these magnitudes S and V to the number N. One thus obtains: /60

$$\frac{S}{N} = \frac{\pi}{4} \frac{m-1}{m-3} \frac{d_M^{m-3} - d_m^{m-3}}{d_M^{m-1} - d_m^{m-1}} \frac{(d_m\, d_M)^{m-1}}{(d_m\, d_M)^{m-3}}$$

and

$$\frac{V}{N} = \frac{\pi}{6} \frac{m-1}{m-4} \frac{d_M^{m-4} - d_m^{m-4}}{d_M^{m-1} - d_m^{m-1}} \frac{(d_m\, d_M)^{m-1}}{(d_m\, d_M)^{m-4}}$$

(The first equation assumes m > 3, and the second, m > 4; if these conditions are not met, the modified equations can easily be found.) Replacing d_m and d_M with 1 and 20 μm, and assuming m = 4.2, the result is that: $S = N \times 2.04\ \mu m^2$ and

$V = N \times 5.77\ \mu m^3$. Choosing a concentration typical of clear water beneath the surface layer, $N = 10^{10}\ m^{-3}$ (that is, 10,000 particles per cubic centimeter; cf. J. C. Grun-Cottan, 1971, H. R. Gordon, O. B. Brown, 1972), the result is: $S = 2.04 \cdot 10^{-2}\ m^2/m^3$ and $V = 5.77 \cdot 10^{-8}\ m^3/m^3$. (It should be noted that if a density of 1 is assigned to the particles, this concentration by volume corresponds to 57.7 µg/liter.) Assuming an index equal to 1.05, using the values for $\bar{Q}$ given in the preceding table one may compute the total scattering coefficient $b = S \times \bar{Q}$, that is: $b_{419} = 3.05 \times 10^{-2}\ m^{-1}$ and $b_{546} = 2.49 \times 10^{-2}\ m^{-1}$.

Referring to Fig. III.8, it may be seen that these coefficients computed for particles from 1 to 20 µm in size could be 15 to 20% smaller than the experimental coefficients, which theoretically correspond to a broader population. In this manner[24], assuming the index to be equal to 1.05, scattering coefficients at 546 nm have been computed for samples from the Mediterranean whose granulometry was established by J. C. Brun-Cottan (1971); the complexity of the computations are slightly increased due to the fact that, in general, two efficiency factors must be computed for each population, one between 1 and 4 µm and the other between 4 and 20 µm. Measurements of the angular coefficient at 30°, $\beta(30°)$, had been performed for the same samples, and from these it was possible to determine (cf. Part 1, Section 6). Moreover, these values for b are in excellent agreement with those obtained in situ by means of the integrator (D. Bauer, A. Ivanoff, 1971). The computed coefficients are compared with the coefficient determined on the basis of the measurements (Fig. III.18). The agreement is fairly satisfactory for the measurements made in November 1969, but it is less so for those made in June 1969, especially for the samples taken at a depth of 100 to 400 m (an index of 1.03 would be better suited to check these measurements).

Reverse Problem: Utilization of Scattering Measurements

Three hypotheses are necessary to solve this problem. Thus, as an example, by choosing an index of 1.05, assuming the distribution to be governed by a law with an exponent -4 and the size limits to correspond to diameters of 0.5 µm and 50 µm (this lower limit corresponds to a truncation like that approximately resulting from filtration through an HA millipore), the following equations may be set up, although obviously their validity is contingent on all the reservations imposed by the preceding choices. The mean efficiency factor for $\lambda = 546$ nm is: $\bar{Q}(0.5 \rightarrow 50, 546) = 0.70$ (for $\lambda = 419$, its value would be 0.92). The value for the total area of geometrical cross sections is: $S(m^2/m^3) = b(m^{-1}) \times (1/0.70)$. From the equation giving S/V, the following

[24] But without correcting for the 15 or 20% which remains doubtful.

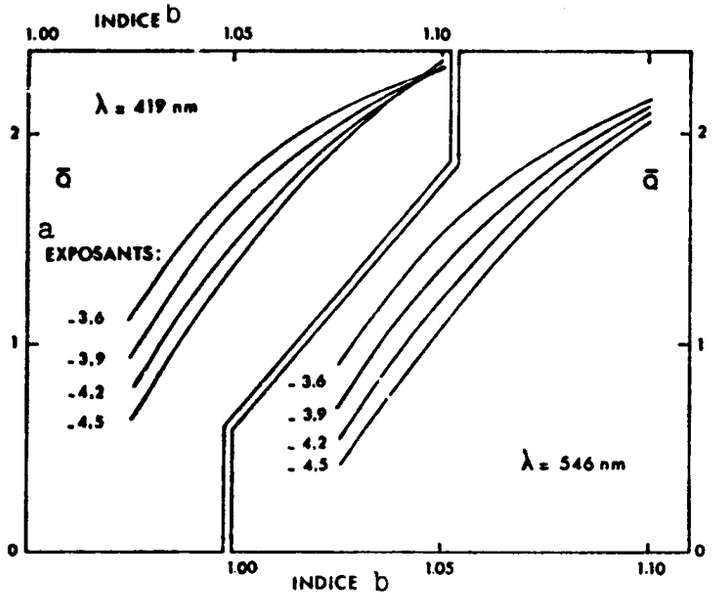

Fig. III.16. Variations in the efficiency factor $\bar{Q}$ as a function of the index of refraction for the two wavelengths indicated. $\bar{Q}$ is computed for a population of particles whose extreme size limits are 1 μm and 20 μm and whose distribution is governed by power laws with the exponents indicated.

Key: a. Exponents
b. Index

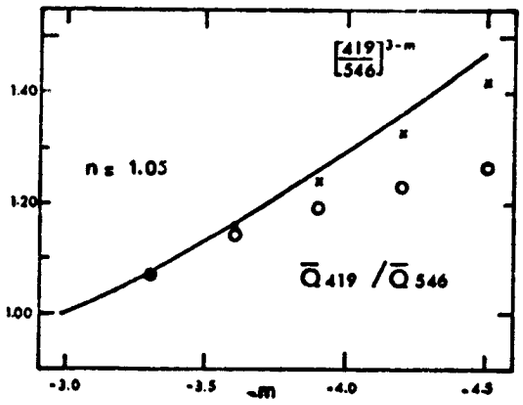

Fig. III.17. Ratios of scattering at 419 nm to scattering at 546 nm, revealing selectivity which varies with the exponent of the law of distribution (see text and observation in Section 3.4.2 above).

may be drawn: $N(m^{-3}) = 10^{12} \times 1.715\ S$; from the equation giving V/S (which becomes V/S = 1/3 log 100, since in this specific case of an exponent of -4, the integral yielding V is a logarithm), one obtains $V(m^2/m^3) = 10^{-6} \times 1.535\ S$.

If, for example, one wishes to compare the results of a scattering measurement which with those of a particle count performed between 1 and 20 μm, and also the results from a filtration assumed to be effective between the sizes 0.5 and 50 μm, it is advantageous to know the distribution of the number, surface area and volume magnitudes among the three classes, from 0.5 to 1 μm, 1 to 20 μm and 20 to 50 μm, respectively. Let us assume that measurement of b at 546 nm yields the value 0.07 m^{-1}, for example; the total geometrical cross sections are thus 0.10 m^2/m^3, and for N, S and V, one will have the following distribution expressed as a percentage of the total:

	class 0,5 → 1µm	class 1 — 20 µm	class 20 — 50 µm	total 0,5 — 50µm
N (m^{-3})	87.5%	12.5%	≈ 0	$17.15.10^{10}$
S (m^2/m^3)	51%	48%	1%	0.10
V (m^3/m^3)	15,0%	65,0%	20%	154.10^{-9}

The relationship between b and V (b in m^{-1} = $0.455 \cdot 10^{-6}$ V, which is in m^3/m^3) is shown in Fig. III.19, which also shows the diffusion coefficients determined for the same samples (see also Fig. 6, A. Morel, 1970) as a function of the dry weight particle concentrations (10^{-9} g/g, that is, in µg/liter). It appears that the ratio between dry weight and theoretical volume is much lower than 1, which in any case would be explained by marked hydration of the particles. A more precise determination would be futile, first because the relationship has been determined on the basis of mean parameters (index and exponent), and second, because the filtration does not produce a sharp truncation (at d = 0.5 µm), but rather a progressive truncation which may also be variable. Thus the retention efficiency of G. F. Whatman filters would decrease from 100% to 40% between the diameters 4 µm and 0.7 µm respectively (R. W. Sheldon, W. H. Sutcliffe, Jr., 1969). This fact should not be forgotten in comparing dry weight measurements either with each other or with scattering measurements, especially if one assumes that a large fraction of the particles by weight and volume is located in the small size range. According to Lisitsin and Bogdanov (1968), 40 to 60% of the particulate

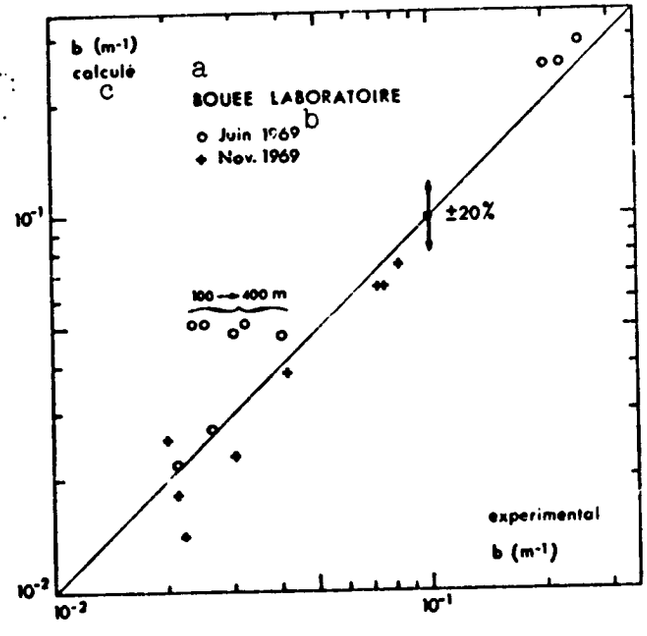

Fig. III.18. Scattering coefficients computed from granulometric data, compared to measured coefficients (see text). Bouée Laboratory. Latitude = 42°14 N, longitude = = 05°35 E.

Key: a. Bouée Laboratory; b. June 1969; c. Computed

mass consists of particles smaller than 1 μm in size, which with an exponent of -4 could be extended to diameters of 0.02 μm; with this exponent, there is logarithmic equipartition of volumes, and thus, for example, the two classes 0.02 to 1 μm and 1 to 50 μm have the same total volume.

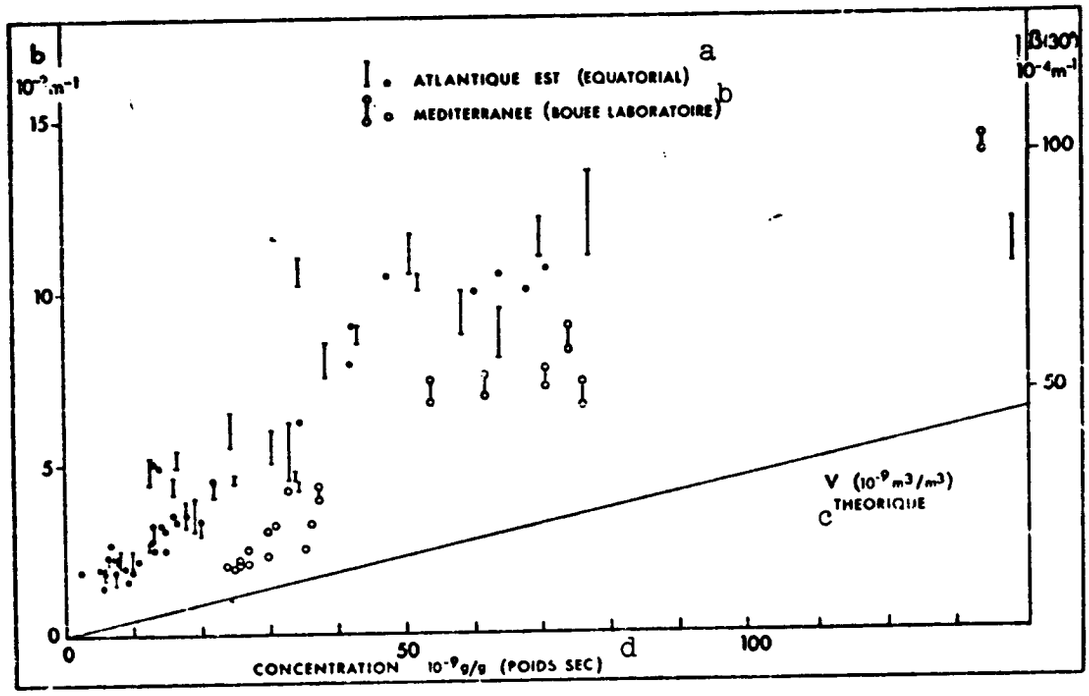

Fig. III.19. Dry weight of particles retained by G. F. Whatman filters (measurements performed by G. Copin) compared to scattering coefficients measured -- using $\beta(30)$ -- for the same samples. The Atlantic measurements were made as part of the Harmattan series (1971).

Key: a. East Atlantic (equatorial)
b. Mediterranean (Bouée Laboratory)
c. Theoretical
d. Dry weight)

Conclusion

/62

In dealing with findings which are virtually based on the natural sciences, it would be futile to try to find complete agreement between experimentation and theory, which is necessarily simplified. On the other hand, it is useful to construct a fairly simple theoretical model which can still constitute a valid

approximation of a complex set of real conditions. Experimental deviations may thus be interpreted by comparison with this model. For this purpose, the influence of various factors must be brought out with some degree of clarity; this explains the importance assigned to the chapter of this work dealing with these factors, and the earlier chapter dealing with the properties of individual indicatrices.

This aspect of research, which facilitates prediction to some extent, nevertheless is not always indispensable. For example, in atmospheric optics, Deirmendjian (1969) found little necessity of dealing with this subject due to the fact that experimental data on aerosols are more complete. This is not the case in oceanographic optics, where virtually the reverse problem is presented: that of obtaining information on suspended particles which is lacking, or at least to permit an investigation of these particles by optical methods, which are fast and reliable, but which furnish results whose significance must be demonstrated.

Despite its limitations, the model provides information on a large number of properties. The shape of the calculated indicatrices is compatible with information on the particles which has already been obtained; simultaneous study of scattering and granulometry would permit a more precise determination of the effective index, that is, something of the nature of the particles and especially the state in which they occur. The intensity of the phenomenon of scattering and its spectral variations are given a satisfactory interpretation leading toward possible applications. For some of these applications, simultaneous measurements of all the parameters -- granulometric, chemical and optical -- remains highly desirable, since theory is the least problematic area, especially since it can easily be perfected.

Dedicated to the memory of George F. Beardsley.

APPENDIX 1: DEFINITIONS /63

The Committee on Radiant Energy in the Sea of the International Association of Physical Oceanography has defined the magnitudes and fixed the terminology for oceanographic optics (Proceedings of the UGGI [Union Géodésique et Géophysique Internationale], No. 57, 1964). A proposal for translation into French has been made subsequently (A. Ivanoff, A. Morel, 1970). A number of magnitudes for description of scattering properties have been defined.

In scattering theory, other magnitudes are used. These are not defined on the basis of an elementary scattering volume as previously, but by considering scattering due to a single particle and its interaction with the electromagnetic wave. These magnitudes should be related to the preceding magnitudes, which were purely phenomenological. The definitions given correspond to the most frequent experimental case, in which the incident light is natural, the scattered light generally being polarized. However, the immediate generalization of these definitions is indicated at the end of the Appendix. These definitions correspond to cases in which the state of polarization of the incident wave is random (cf. Sections 1.1 and 1.2, Part 2). Finally, it should be noted that the French and English terminology for these magnitudes used in theory has not been systematized; the terms given here are those which appear to be the most frequently used.

Magnitudes Defined by the Committee on Radiant Energy in the Sea (AIPO)

These magnitudes are defined by considering the case of a fine beam of monochromatic light consisting of parallel rays. The relative loss in flux dF/F for this beam is proportional to the path lengths dx considered to be elementary, the coefficient of proportionality being the attenuation coefficient c:

$$c = -\frac{dF}{F}\frac{1}{dx}.$$

The loss in flux occurs due to the combined effect of absorption and scattering: $c = a + b$, where a is the absorption coefficient and b the total scattering coefficient. As a result:

$$a = -\frac{d\,F\,(abs)}{F}\,\frac{1}{dx}\,, \quad \text{and} \quad b = -\frac{d\,F\,(diff)}{F}\,\frac{1}{dx}\,,$$

where dF (abs) is the flux subtracted due to absorption, and dF (diff) is the flux subtracted from the flux normally transmitted along the direction of propagation of the beam, which is actually dispersed in space.

Consequently a section of the beam of length dx and volume dv = S dx, seen from a relatively long distance, behaves as a point light source with its direction making an angle θ with the initial direction of the beam, and with an intensity of dI(θ), proportional to the volume scattering function β(θ):

$$\beta(\theta) = d\,i(\theta)\,\frac{1}{F}\,\frac{1}{dx} \qquad \text{or} \qquad \beta(\theta) = d\,i(\theta)\,\frac{1}{E}\,\frac{1}{dv}\ ,$$

E being the illumination on the entry face of surface area S of the scattering volume dv (E dv = F dx).

In most cases in oceanography, coefficients a, b and c, homogeneous in the reciprocal of one length, are expressed in m^{-1}. The volume function is expressed in $m^{-1}str^{-1}$. By integrating the scattered flux throughout space in all directions θ, one obtains the equation:

$$b = \iint_{4\pi} \beta(\theta)\, d\Omega \qquad \text{becoming} \qquad b = 2\pi \int_{0}^{\pi} \beta(\theta) \sin\theta \, d\theta\ ,$$

if the scattering phenomenon is one of revolution around the axis of the beam. Integr tion performed on non-elementary paths in a homogeneous medium (a and b being constant) results in an exponential decrease in the flux due to absorption, scattering or both at once.

The representation of the volume scattering function β(θ) as a function of θ is termed (in French especially) the scattering indicatrix.

Other Magnitudes Used in Theory

Intensity Functions i_1 and i_2

I_0 being the intensity of the natural (and monochromatic) incident light being propagated in a flat wave (parallel light beam), and I being that of the light scattered in a random direction (θ, φ) at a distance D (assumed to be large) from the particle, one may state

$$i = i_0\,\frac{1}{k^2D^2}\,F(\theta,\phi)$$

$F(\theta,\phi)$ is a dimensionless function in the direction indicated by two angles θ and ϕ. k is the wave number $k = 2\pi/\lambda$; k^2 should be homogeneous at L^{-2}. If the phenomenon is one of revolution, as in the case of the spherical particles considered here, a single angle θ comes into play, measured between the direction of propagation of the incident wave and that of the scattered wave under consideration; these two directions define the "scattering plane." The incident light being natural, the scattered light is generally polarized, and the following may be written:

$$i = i_0 \frac{1}{k^2 D^2} \cdot \frac{i_1(\theta) + i_2(\theta)}{2}$$

where $i_1(\theta)$ and $i_2(\theta)$ are the intensity functions.

These are dimensionless quantities, obtained by finding the square of the moduli of complex amplitudes $S_1(\theta)$ and $S_2(\theta)$; index 1 (or in some cases r, or again, $\perp$) is related to vibration perpendicular to the scattering plane, and index 2 (or ℓ or =) to vibration within the scattering plane. The ratio $(i_1 - i_2)/(i_1 + i_2)$ expresses the rate of polarization which produces scattering when the incident light is natural (see Part 2, Sections 1.1 and 1.2).

Angular Mie Scattering Coefficient; Scattering Efficiency Factor /64

This is a dimensionless number expressed in sterad^{-1}, defined in the following manner:

$$q(\theta) = \frac{i_1(\theta) + i_2(\theta)}{2} \cdot \frac{1}{k^2} \cdot \frac{1}{S}$$

where S is the area of the geometric cross section of the particle, that is, the projection of the particle onto the plane of the incident wave. If one considers the case of the spherical particle $S = \pi r^2$, introducing the size parameter $\alpha = 2\pi r/\lambda$:

$$q(\theta) = \frac{1}{2\pi\alpha^2} \left(i_1(\theta) + i_2(\theta)\right)$$

which may be interpreted as the flux scattered by a particle per unit of solid angle in a direction θ related to the incident flux on the geometrical cross section (here, πr^2). Integration extended over the entire space:

$$\iint^{4\pi} q(\theta) d\Omega = \frac{1}{\alpha^2} \int_0^{\pi} \left(i_1(\theta) + i_2(\theta)\right) \sin\theta \, d\theta = Q$$

yields the number Q, the scattering efficiency factor: this is the ratio of the total scattered flux to the incident flux on the particle.

Effective Cross Section and Differential Cross Sections

The differential (or angular) cross section for direction θ is defined by:

$$s(\theta) = S\,q(\theta) = \frac{\lambda^2}{8\pi^2}\left(i_1(\theta) + i_2(\theta)\right)$$

the dimensions are L^2, the unit $m^2 sterad^{-1}$. Integrating over 4π furnishes the effective cross section S:

$$s = \frac{\lambda^2}{4\pi}\int_0^{\pi}\left(i_1(\theta) + i_2(\theta)\right)\sin\theta\, d\theta = \frac{\lambda^2}{4\pi}\, Q\, \alpha^2 \quad \text{that is } s = \pi r^2 Q,$$

for the sphere, and more generally: s = SQ where S is the area of the geometric cross section.

Volume Scattering Function, Total Scattering Coefficient

The sum of the differential cross sections, relative to θ, of N particles contained in the unit volume constitutes the volume scattering function. When the particles under consideration are spherical, and when in addition they are of identical radius r, one may write:

$$\beta(\theta) = N\,s(\theta) = N\,\pi r^2\, q(\theta)\,, \qquad \beta(\theta) = N\frac{\lambda^2}{8\pi^2}\left(i_1(\theta) + i_2(\theta)\right)$$

N has dimensions of L^{-3}, β has dimensions of L^{-1}, and the unit will be $m^{-1} sterad^{-1}$.

This is the ratio of the flux scattered in direction θ per unit of solid angle to the incident flux, the volume scattered being unity. Extension of the integral to the entire space yields the total scattering coefficient b:

$$b = \iint_{4\pi} \beta(\theta)\, d\Omega = 2\pi\int_0^{\pi}\beta(\theta)\sin\theta\, d\theta\,, \quad (b = N\pi r^2 Q \text{ for spherical particles})$$

the ratio of the total scattered flux to the incident flux on a

unit volume; the dimensions are L^{-1}, the unit m^{-1}. If the spherical particles are not of uniform size, the result will be:

$$\beta(\theta) = \int_0^\infty n(r)\,\pi r^2\,Q_\theta(r)\,dr \text{ , with } \int_0^\infty n(r)\,dr = N \quad \text{and} \quad b = \int_0^\infty n(r)\,\pi r^2\,Q(r)\,dr \text{ .}$$

Phase Function and Normalized Volume Function

The phase function is also a dimensionless quantity defined by: $P(\theta) = 4\pi \frac{Q(\theta)}{Q} = 2\,\frac{i_1(\theta) + i_2(\theta)}{a^2}$. One also defines: $P_1(\theta) = \frac{4\,i_1}{Q\,a^2}$ and $P_2(\theta) = \frac{4\,i_2}{Q\,a^2}$. For a single particle: $P(\theta) = 4\pi\frac{\beta(\theta)}{s}$ for a scattering volume: $P(\theta) = 4\pi\frac{\beta(\theta)}{b}$; and in all cases:

$$\iint^{4\pi} P(\theta) \equiv 4\pi \text{ .}$$

It is more convenient to use the normalized volume function defined by $\bar{\beta}(\theta) = \frac{P(\theta)}{4\pi} = \frac{\beta(\theta)}{b}$, ; as a result:

$$\iint^{4\pi} \bar{\beta}(\theta)\,d\Omega \equiv 1 \text{ , } \bar{\beta}_1(\theta) = \frac{i_1}{\pi\,Q\,a^2} \quad \text{and} \quad \bar{\beta}_2(\theta) = \frac{i_2}{\pi\,Q\,a^2}$$

$$\bar{\beta}(\theta) = \frac{1}{2}\,(\bar{\beta}_1(\theta) + \bar{\beta}_2(\theta))$$

Note on Polarization

All the preceding formulas correspond to cases in which the incident wave is natural; the more general case where the state of polarization of the incident wave is random has been examined earlier (Section 1.2). In this case, four intensity functions rather than two are useful in describing the phenomenon of scattering (by isotropic spheres):

/65

$$i_1 = S_1 S_1^*$$
$$i_2 = S_2 S_2^*$$
$$i_3 = 1/2\,(S_1 S_2^* + S_2 S_1^*) = \mathrm{Re}\,(S_1 S_2^*)$$
$$i_4 = i/2\,(S_1 S_2^* - S_2 S_1^*) = -\mathrm{Im}\,(S_1 S_2^*) \text{ .}$$

Formulas relating to the intensity and not the phase of the scattered wave which make use only of i_1 and i_2 remain unchanged: this is the case for $q(\theta)$, $s(\theta)$, $\beta(\theta)$ and their integrals. However, using the same formulas it is quite possible to define, for example, β_1, β_2, β_3 and β_4 with $\beta = (1/2)(\beta_1 + \beta_2)$. Indeed, some investigators define and use four normalized functions $P_1(\theta)/4\pi \ldots P_4(\theta)/4\pi$. As has been stated (Section 1.2), the equation for the rate of polarization is different in this general case.

LIST OF PRINCIPAL SYMBOLS USED

The following list includes symbols which do not correspond to the magnitudes defined above. The sections and equations (in Part 2) in which these symbols appear for the first time are indicated in parentheses.

α	Particle size parameters	(2.2)
a_n, b_n	Mie coefficients	(2.2, 2.4)
a_{ij}	Scattering matrix coefficients	(1.8)
A_i, A_i^*	Complex amplitudes. The asterisks indicate complex conjugates	(1.9, 1.11)
A_1, A_2, B_1, B_2	Parameters in log normal or exponential laws of distribution	(3.11, 3.12)
d	Diameter	
E_ℓ, E_r	Electric field components $\vec{E}$	(1.1)
ψ_n, χ_n, ζ_n	Ricatti-Bessel and Ricatti-Hankel functions	(2.4 to 2.8)
$F(\theta)$	Angular distribution function (Rayleigh-Gans)	(2.21)
$F'(\theta)$	Distribution function (diffraction)	(2.24)
$F(d)$, $F(\alpha)$, $F(\rho)$	Particle distribution function	(Section 3.1, Part 2)

G(U)	Gans function	(2.22)
H_n, J_n, Y_n	Hankel function of order n, Bessel functions of first and second types of order n	
i_T	$(1/2)(i_1 + i_2)$ -- cf. Definitions	(Section 2.2.1, Part 2)
I, Q, U, V or I_1, I_2, U, V	Stokes parameter	(1.2, 1.11)
k	Wave number $(= 2\pi/\lambda)$	(Section 2.1, Part 2)
λ	Wavelength	
Λ	Lorentz-Lorenz term: $(n^2 - 1)/(n^2 + 2)$	(2.15)
m	Relative index of particle in relation to medium in Part 2	(Section 2.1)
m	Exponent of Junge law of distribution beginning with Section 3.2 (Part 2)	
n	Order of terms in series	(2.2) /66
n	Relative index (cf. "m" above) beginning with Section 2.2 (Part 2)	
N	Total number of particles per unit volume	(Part 2, Section 3.1.1 and Part 3, Section 3.4)
nm, μm	Nanometer and micrometer	
p and $p(\theta)$	Rate of polarization	(Part 1, Sections r and 1.7)
p	Gradient of curves $i_T(\theta)\alpha^{-4}$	(Part 2, Section 3.2.1)
P_n	Legendre polynomial of order n	(2.3)

Q	Efficiency factors for absorption, scattering, attenuation	(2.25 to 2.28)
$\bar{Q}$	Mean efficiency factor for scattering	(3.2)
r	Ratio of scattering of sample to scattering by benzene	(Part 1, Section 4.2)
$R_p(\theta)$	Characteristic ratio of scattering by particles	(Part 1, Section 4.7)
ρ	Parameter equal to $2\alpha \lvert n - 1 \rvert$	(2.19)
S_1, S_2	Amplitude functions (complex)	(2.1)
S and V	Surface area of geometric cross sections and volumes of particles	(Part 3, Section 3.4.2)
θ	Scattering angle	

APPENDIX 2: COMPUTATION PROCEDURE AND ADAPTATION TO COMPUTER

1. Calculation of Individual Indicatrices by Mie Theory

1.1. Equations Used

The equations (2.2) furnished by Mie theory have shown that the complex amplitudes of the scattered wave $S_1(\alpha,m,\theta)$ and $S_2(\alpha,m,\theta)$ are expressed in the form of series which at each order combine:

-- the Mie coefficients a_n and b_n dependent on the relative size α and the relative index m by way of Ricatti-Bessel and Ricatti-Hankel functions of order n (2.4).

-- the functions π_n and τ_n, dependent solely on the scattering angle θ, by way of functions containing the Legendre polynomials of order n occurring in the argument $\cos\theta$ (2.3).

It is possible to generate these functions with the use of recursive formulas, after setting the corresponding values at the first orders. This computation diagram is similar to that recommended by R. Penndorf and B. Goldberg (1956) and by D. Deirmendjian et al. (1961). Recently (1969) the latter investigator has again taken up a detailed description of the case of a complex index of refraction. Another computational procedure using the logarithmic derivatives of the Ricatti-Bessel functions (see, for example, G.W. Kattawar and G.N. Plass, 1967) may also be used.

Coefficients a_n and b_n: Recurrence for Ricatti-Bessel and Ricatti-Hankel Functions

In conformity with (2.5), (2.7) and (2.9), the functions ψ_n and ζ_n, which along with their derivative are involved in coefficents a_n and b_n, are expressed by:

$$\psi_n(x) = \left(\frac{\pi x}{2}\right)^{1/2} J_{n+1/2}(x) \quad , \qquad \zeta_n(x) = \psi_n(x) + i\ \chi_n(x) \quad ,$$

with $\chi_n(x) = -\left(\frac{\pi x}{2}\right)^{1/2} Y_{n+1/2}(x)$.

One assumes: $\psi_n(x) = S_n(x)$ and $\chi_n(x) = C_n(x)$.

Initially, these functions will be expressed solely by Bessel functions of the first type, using the equation:

$$Y_{n+1/2}(x) = (-1)^{n+1} J_{-(n+1/2)}(x)$$

between functions of the first type J and the second type Y; thus $S_n(x)$ and $C_n(x)$ will be written:

$$S_n(x) = \left(\frac{\pi x}{2}\right)^{1/2} J_{n+1/2}(x) \qquad C_n(x) = (-1)^n \left(\frac{\pi x}{2}\right)^{1/2} J_{-(n+1/2)}(x) .$$

For functions of the first type, the following recursive equation holds for three successive orders:

$$2\frac{n}{x} J_n = J_{n-1} + J_{n+1} \qquad \text{or} \qquad J_n = 2\frac{n-1}{x} J_{n-1} - J_{n-2}$$

Substituting n + 1/2 for n:

$$J_{n+1/2} = 2\frac{n-1/2}{x} J_{n-1/2} - J_{n-3/2} \qquad \text{or again} \qquad S_n(x) = \frac{2n-1}{x} S_{n-1}(x) - S_{n-2}(x) \qquad \text{(II.1A)}$$

Substituting -(n + 1/2) for n:

$$J_{-n-1/2} = 2\frac{-n-3/2}{x} J_{-n-3/2} - J_{-n-5/2}$$

that is:

$$(-1)^n C_n(x) = 2\frac{-n-3/2}{x} (-1)^{n+1} C_{n+1} - (-1)^{n+2} C_{n+2}$$

Setting aside two orders:

$$C_n(x) = \frac{2n-1}{x} C_{n-1}(x) - C_{n-2}(x) \qquad \text{(II.1B)}$$

an equation identical to that established for S_n.

The calculations may be performed after values have been set for the first two orders, that is:

$$S_o(x) = (\pi x/2)^{1/2} J_{1/2}(x) = \sin x \qquad C_o(x) = (\pi x/2)^{1/2} J_{-1/2}(x) = \cos x$$

$$S_1(x) = (\pi x/2)^{1/2} J_{3/2}(x) = \frac{\sin x}{x} - \cos x \qquad C_1(x) = -(\pi x/2)^{1/2} J_{-2/3}(x) = \frac{\cos x}{x} + \sin x \qquad \text{(II.2)}$$

The derivatives ψ' and ζ', that is, S' and S' + iC', are also involved in the expressions for a_n and b_n. There is a recursive equation linking the derivative of the Bessel function of order n to the functions of order n and n - 1 themselves:

$$x J'_n(x) = -n J_n(x) + x J_{n-1}(x)$$

which, applied directly to S_n and C_n, yields the equations:

$$S'_n(x) = -\frac{n}{x} S_n(x) + S_{n-1} \qquad C'_n(x) = -\frac{n}{x} C_n(x) + C_{n-1} \qquad \text{(II.3)}$$

Finally, a_n will be expressed by means of the functions S_n, C_n and their first derivative in the form:

$$a_n = \frac{S'_n(m\alpha) S_n(\alpha) - m S_n(m\alpha) S'_n(\alpha)}{S'_n(m\alpha)\,(S_n(\alpha) + i C_n(\alpha)) - m S_n(m\alpha)\,(S'_n(\alpha) + i C'_n(\alpha))}$$

All the terms in this equation may be calculated by means of the preceding formulas. (An analogous equation is used to find b_n.) If m is real, all the functions pertain to real arguments, and in computing a_n the real part and the imaginary part may be separated; one assumes:

$$p = S'(m\alpha) S(\alpha) - m S(m\alpha) S'(\alpha) \qquad q = S'(m\alpha) C(\alpha) - m S(m\alpha) C'(\alpha) , \qquad \text{(II.4)}$$

making it possible to state that:

$$a_n = \frac{p}{p + iq} ,$$

and consequently:

$$\mathrm{Re}\{a_n\} = \frac{1}{1 + p^2/q^2} \qquad \text{and} \qquad \mathrm{im}\{a_n\} = \frac{-p/q}{1 + p^2/q^2} . \qquad \text{(II.5)}$$

As has been seen, the result is that the image of any a_n (or any b_n) within the complex plane falls on a circle with a radius of 1/2 centered on the point im = 0, Re = 0.5 (cf. Fig. II.1). This is an important point in that it furnishes a simple means of checking all numerical calculations. Another practical result is related to the adoption of the convergence criterion for the series of a_n or b_n functions: when these numbers become small at a sufficiently high order, the circle being in the osculating plane of the parabola, the result necessarily is:

$$\text{im}\{a_n\} \sim \{\text{Re}\{a_n\}\}^{1/2} .$$

Assuming that convergence has been attained when the terms a_n or b_n become less than 10^{-7}, for example (this is the value which has been chosen) amounts to applying this condition solely to the imaginary parts, the real part here being on the order of 10^{-14}.

Functions π_n and τ_n: Recurrence of Legendre Polynomials in Derivatives

Eqs. (2.3) may be stated more explicitly in another way by linking π_n to τ_n:

$$\pi_n(\cos\theta) = \frac{1}{\sin\theta} P'_n(\cos\theta) = \frac{d P_n(\cos\theta)}{d\cos\theta} ;$$

or by assuming:

$$x = \cos\theta \quad , \quad \pi_n(x) = P'_n(x) , \tag{II.6}$$

The result is:

$$\tau_n(\cos\theta) = \frac{d}{d\theta} P'_n(\cos\theta) , \qquad \text{that is:} \quad \tau_n(\cos\theta) = \frac{d}{d\theta}\left(\pi_n(\cos\theta) \cdot \sin\theta\right) ,$$

$$\tau_n(\cos\theta) = \frac{d\,\pi_n(\cos\theta)}{d\theta} \sin\theta + \cos\theta\ \pi_n(\cos\theta) ,$$

$$\tau_n(\cos\theta) = -\frac{d\,\pi_n(\cos\theta)}{d\cos\theta} \sin^2\theta + \cos\theta\,\pi_n(\cos\theta) ,$$

that is: $$\tau_n(x) = x\ \pi_n(x) - (1 - x^2)\ \pi'_n(x) \tag{II.7}$$

where is τ_n is given solely as a function of π_n and its derivative π'_n in relation to the argument $x = \cos\theta$.

In order to calculate Eq. (2.6), $P'_n(x)$ must be expressed as a function of the lower orders. Between three successive orders, the following recursive equation applies to the Legendre polynomials:

$$(n+1)\, P_{n+1}(x) - (2n+1)\, x\, P_n(x) + n\, P_{n-1}(x) = 0 \ ,$$

deriving:

$$(n+1)\, P'_{n+1}(x) - (2n+1)\, P_n(x) - (2n+1)\, x\, P'_n(x) + n\, P'_{n-1}(x) = 0 \ .$$

Now, the following equation links the polynomial and its derivative:

$$x\, P'_n(x) - P'_{n-1}(x) = n\, P_n(x)$$

making it possible to eliminate P_n from both equations; consequently:

$$n\, P'_{n+1}(x) - (2n+1)\, x\, P'_n(x) + (n+1)\, P'_{n-1}(x) = 0 \ ,$$

setting aside one order (n substituted for n + 1), the recursive equation for π_n may be written:

$$\pi_n(x) = \frac{1}{n-1}\left[(2n-1)\, x\, \pi_{n-1}(x) - n\, \pi_{n-2}(x)\right] \ , \qquad \text{(II.8)}$$

which makes it possible to compute $\pi_n(x)$ on the basis of the values for the two previous orders.

In an analogous manner, a recursive equation is found for τ_n which contains π_n and functions of the immediately preceding order π_{n-1} and τ_{n-1}:

$$\tau_n(x) = \left[\tau_{n-1}(x) + \pi_n(x)\right]x + (nx^2 - n + 1)\, \pi_{n-1}(x) \ . \qquad \text{(II.9)}$$

Using these equations (2.7) and (2.8), functions π_n and τ_n may be calculated for any given order, once the initial values for the two first orders have been set (cf. 2.9 A and 2.9 B, which give these values).

1.2. Organization of Calculations

The initially assumed givens are:

-- [words missing in original] extreme values for the scattering angle θ and the step chosen $\Delta\theta$ (for example: 0 (2) 180).

-- [words missing] variable of values for the size parameter $\alpha_1, \alpha_2 \ldots$ between which the step $\Delta\alpha$ has a value of [words missing].

-- [words missing] index of refraction m, which may be incremented by Δm, as many times as determined at the beginning [? -- words missing].

-- [words missing] a_n and b_n.

-- [words missing] which must be computed in the first place, since it is these factors which determine [words missing] series and set the order to be reached.

The index of refraction m and the size parameter α being given, the values for functions S and C are computed for the first two orders using the formulas established (2.2) a priori, and their derivatives S' and C' are derived from these formulas by means of Eqs. (2.3). The real and imaginary parts of a_n and b_n are calculated by constructing Eqs. (2.4) and (2.5) and are stored by the computer.

After one order has been set aside, S, C, S' and C' are cal-

culated once again, this time using the recursive equations (2.1A), (2.1B) and (2.3), and this loop is completed by calculating and storing the new values a_{n+1} and b_{n+1}. The cycle is repeated as many times as necessary so that convergence will be obtained to the degree of precision set in advance. It was assumed that convergence was adequate when the terms a_n and b_n generated became less than 10^{-7}. As has been shown, it was necessary to impose this condition only on the imaginary part. In addition it might be noted that it was necessary to apply it only to $I_m(a_n)$, since numerically it appears that b_n is always less than a_n, more precisely, on the order of magnitude of a_{n+1}.

When this condition has been met, there is no further return to the beginning of the loop and the first part of the calculations is completed. At this point the store contains:

-- the maximum order reached, that is, N.

-- successive N values for

-- the sum $\sum_{1}^{N} (2n+1)\ \mathrm{Re}\,(a_n+b_n)$ which has been gradually accumulated and will serve for calculation of $S(0)\alpha^{-2}$ and the efficiency factor Q.

Calculation of Values for Angles

An initial value is assigned to θ (0° or 180°, for example) and the argument $x = \cos\theta$ is computed, as well as the first two orders for π and τ, using the initial formulas established. The values for a_n and b_n of the same order again are involved, making it possible to compute the real and imaginary parts of:

$$(a_n\ \pi_n(x) + b_n\ \tau_n(x))\ \frac{2n+1}{n(n+1)} \quad \text{and of:} \quad (a_n\ \tau_n(x) + b_n\ \pi_n(x))\ \frac{2n+1}{n(n+1)}\ .$$

The same calculus is performed N times, with the sole difference that in these loops, π_n and τ_n are generated by means of the recursive equations (2.6) and (2.7). When the calculations

have been completed the store will have accumulated:

$$\sum_{1}^{N} \frac{2n+1}{n(n+1)} \left(\mathrm{Re}\{a_n\}\,\pi_n + \mathrm{Re}\{b_n\}\,\tau_n\right) = \mathrm{Re}\{S_1(\theta)\} \quad ,$$

$$\sum_{1}^{N} \frac{2n+1}{n(n+1)} \left(\mathrm{im}\{a_n\}\,\pi_n + \mathrm{im}\{b_n\}\,\tau_n = \mathrm{Im}\{S_1(\theta)\}\right) \quad ,$$

and the analogous expressions:

$$\mathrm{Re}\{S_2(\theta)\}\ ,\ \mathrm{im}\{S_2(\theta)\}\ .$$

The intensity functions $i_1(\theta)$ and $i_2(\theta)$ for this angle θ are then computed by finding the square of the moduli:

$$i_1(\theta) = \left(\mathrm{Re}\{S_1(\theta)\}\right)^2 + \left(\mathrm{im}\{S_1(\theta)\}\right)^2$$
$$i_2 \cdots\cdots S_2 \qquad\qquad S_2 \quad .$$

Also computed at this stage are $i_T = 1/2(i_1 + i_2)$, the polarization $p = i_1 - i_2/i_1 + i_2$ and the phase functions

$P_1(\theta)/4\pi = \dfrac{i_1}{\pi\, Q\, \alpha^2}$ and $P_2(\theta)/4\pi$. (Functions P_3 and P_4 were not computed.) Examples of indicatrices calculated in this way are shown in the graphs below.

Catenation

The angle θ is then incremented by $\Delta\theta$, and the second part of the calculations is performed by integration, while the results from the first part (coefficients a_n and b_n) are brought into play as needed. When all the scattering angles have been examined, the calculations for a given particle have been completed and the results are read out from the stores. Depending on the options, which are not mutually exclusive, they may be transferred to magnetic tape, punch cards, or a list, or they may be given in the form of graphs.

The program increments the size parameter α by $\Delta\alpha$ (determined

in advance), and the entire calculus is performed again from the beginning (new a_n and b_n coefficients); this is repeated as many times as necessary to attain the preset maximum value for α.

When this series of cases has been processed, it is possible to use another loop overlaying the initial parameters to set a new value for parameter α, and, other things being equal ($\Delta\alpha$, $\Delta\theta$, maximum and minimum values for α and θ), to increment the index. Depending on the initial data furnished, this classical structure makes it possible to catenate the computations for as many cases as desired.

Precision

The truncation criterion for series a_n and b_n used here (10^{-7}) is that recommended by Penndorf and Goldberg (1956, 1960), and also used by Dermendjian, Clasen and Viezee (1961). (In cases where the index is complex it is converted into $a_n a_n^* + b_n b_n^* < 10^{-14}$.) The value of the criterion determines the degree of precision which may be expected for the $i(\theta)$ function values and those derived from them. This precision is six significant figures, no matter what the absolute value of the number may be. It is not possible to predict the degree of precision with absolute certainty by numerical analysis, since the speed of convergence for the uncomputed terms is a priori not predictable; thus the results must be compared with other published results, or the calculations must be checked by changing the value of the criterion (a procedure which has also been used). In this way the stated degree of precision may be confirmed.

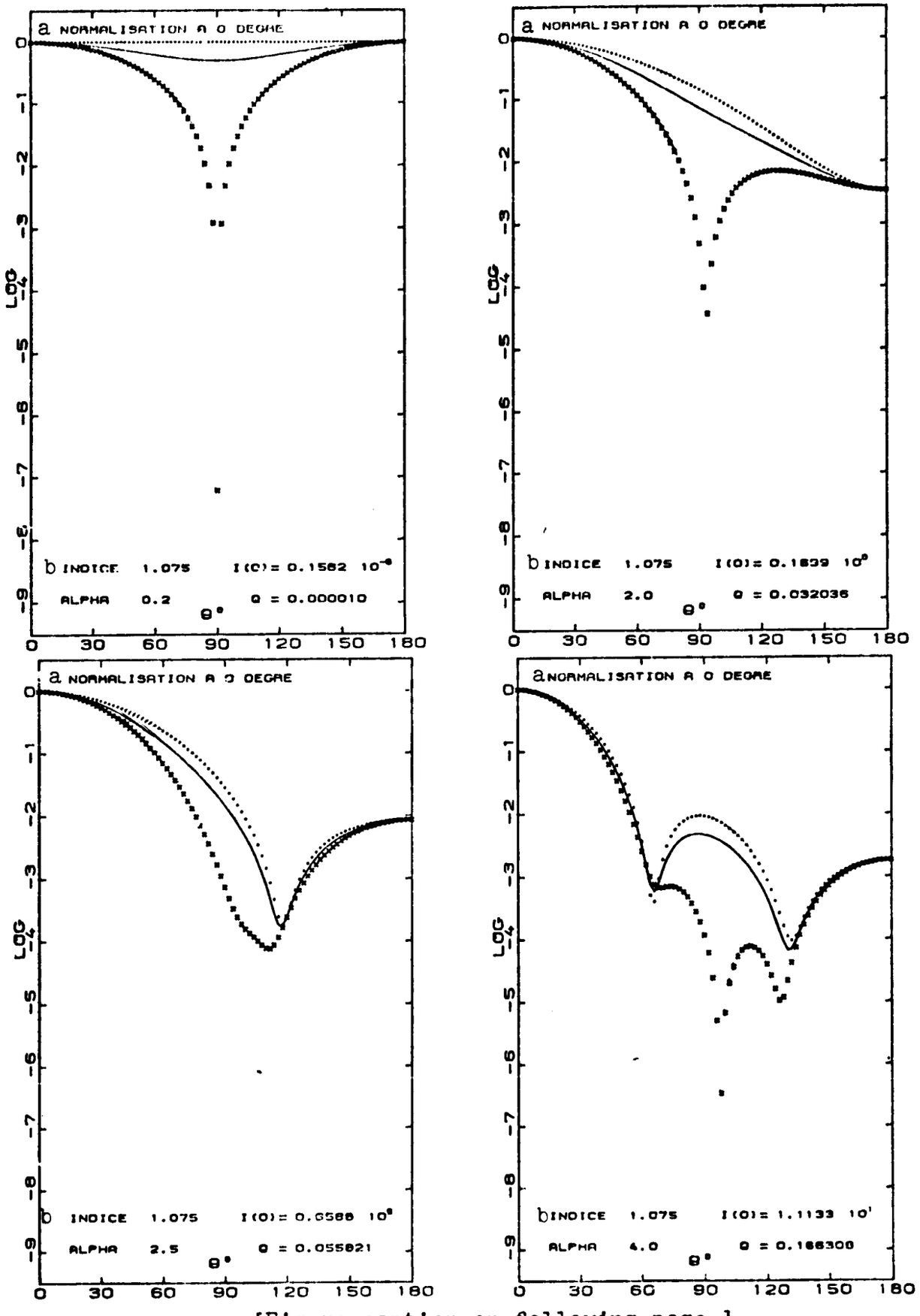

[Figure caption on following page.]

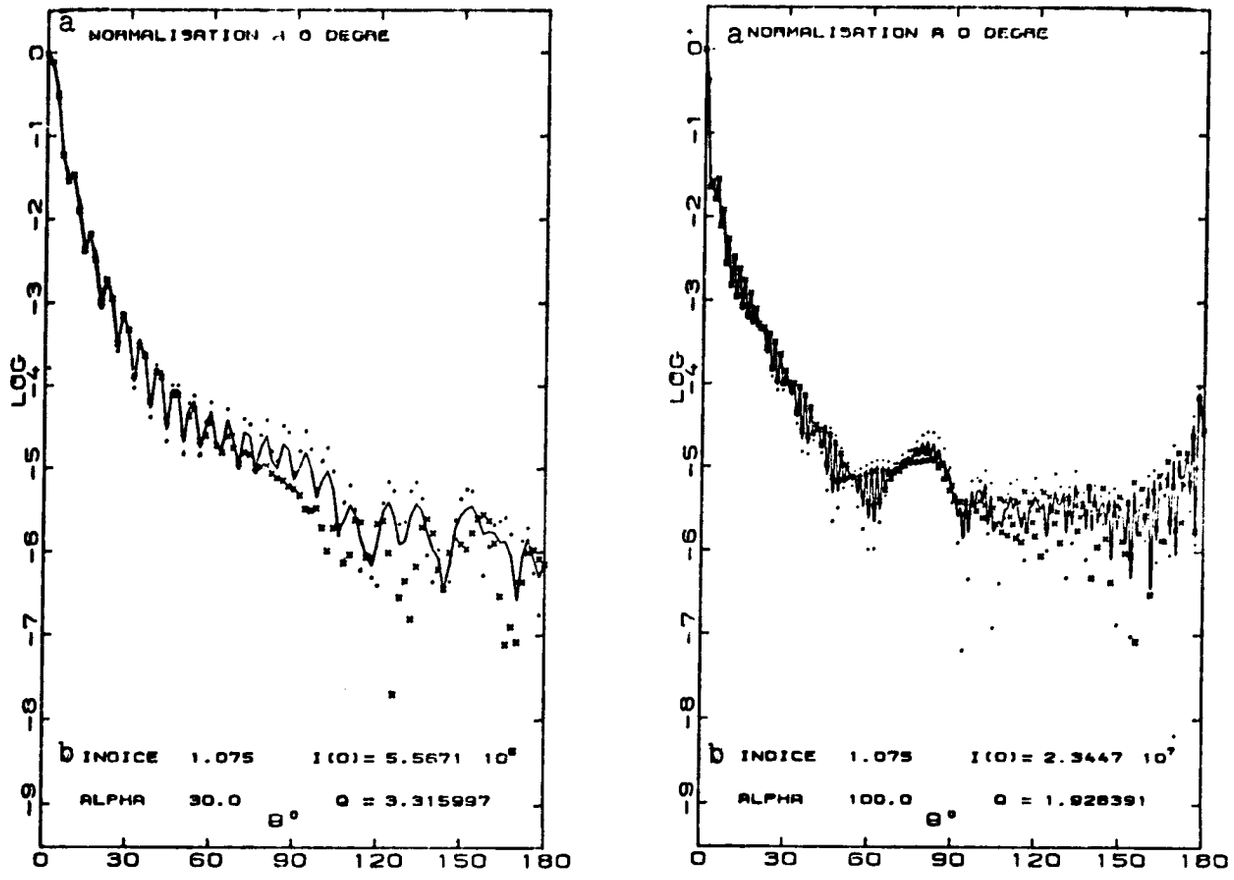

Examples of scattering indicatrices computed for a relative index of refraction of 1.075 and for the indicated α parameter values. These figures serve as an illustration of the expansions given in Sections 2.1.2 (Variations in Indicatrices), 2.2.3 (Rayleigh-Gans Range) and 2.2.5 (Reflection-Refraction). The data are normalized to 0° in order to plot the indicatrix (log ordinate scale) and the value $i(0°)$ at this angle is indicated as well as the efficiency factor Q. The two polarized components $i_1(\theta)$ and $i_2(\theta)$ are represented by dots and crosses, respectively, and the curve corresponds to the total intensity $i_p(\ ) = (1/2)\ i_T(\theta) = (1/2)[i_1(\theta) + i_2(\theta)]$.

Key: a. Normalized to 0°.
b. Index.

Series a_n and b_n converge more slowly as α becomes higher. For all the cases treated (index less than 1.15), an approximate

empirical equation was found to hold true: $N \simeq 1.07\ \alpha + 10$, linking α to the number of orders N necessary to satisfy the criterion $< 10^{-7}$. An equation of this type has further been proposed to limit a priori the number of recursions to be performed (Penndorf); it is impossible for this equation to be generally applicable since the value for the index also comes into play.

It is necessary to calculate the Mie coefficients a_n and b_n using double precision (17 siginificant figures). Without entering into detail on this numerical aspect, this is due to the fact that in recursions for computation of S'_n and C'_n, subtractions must be performed which result in the occurrence of numerically (but not mathematically) indeterminate functions; when the terms generated differ only beginning with the eighth significant figure, it is impossible to compute their differences by single precision (in this case the store for each number consists of eight decimal places). This results in the necessity for division by zero, which cannot be performed, and the program goes into an infinite loop without ever satisfying the convergence criterion. Double precision computation, which must be used when $\alpha > 20$ or 25, removes this difficulty, although it does increase the computation time by a factor of approximately four. Dermendjian has recently emphasized the necessity for this precaution (1969).

2. Computation for Polydispersed Systems

2.1. Organization of Computations

There is no special difficulty involved in performing these computations. They may be organized in several ways; the most frequently used method may be briefly summarized as follows.

The integrals of type (3,2) and (3.3) (Part 2) yielding

$\bar{\beta}_1(\theta)$ and $\bar{\beta}_2(\theta)$ are, of course, replaced by weighted summations of terms corresponding to the 60 previously computed individual indicatrices; this amounts to the statement that $d\alpha$ is not constant, but rather is small when it corresponds to classes of particle size which are plentifully represented and increases, on the other hand, as the size of the particles increases and their number decreases. The weighting term $C(\alpha)$ is computed on the basis of the law of distribution used (Junge law, etc.). It thus becomes necessary to calculate summations such as:

(1) $\sum_{k=1}^{61} i_{kj}(\theta,\alpha) \cdot C_k(\alpha)$, (numerator from 3.3)

(2) $\sum_{k=1}^{61} \alpha^2 \cdot Q(\alpha)\, C_k(\alpha)$, (denominator from 3.3), with $j = 1$ or 2.

(3) $\sum_{k=1}^{61} \alpha^2 \cdot C_k(\alpha)$

The summations are performed progressively and simultaneously for the 91 angles considered, ranging from 0° to 180°, in steps of 2° (expression 1 above) and also for the other two expressions (2 and 3). Discrete α values correspond to the 60 values for k. After the term C_k, of the order k, has first been computed by means of the law of distribution, the 182 values for $i_{kj}(\theta)$, that for Q and that for α corresponding to the same order k are once again obtained and multiplied by C_k, then summed with the analogous values computed for the previous orders, in 184 stores corresponding to the 184 sums to be performed.

Subsequently the operations predicted by (3.2) and (3.3) (Part 2) are performed, as well as the additional computations:

$$\bar{\beta}(\theta) = \frac{1}{2}\left(\bar{\beta}_1(\theta) + \bar{\beta}_2(\theta)\right) \qquad \text{and} \qquad p(\theta) = \frac{\bar{\beta}_1(\theta) - \bar{\beta}_2(\theta)}{\bar{\beta}(\theta)}$$

Optional outputs make it possible to review partial results corresponding to low truncation (minimum k ≥ 1), high truncation (maximum k < 61), or both at once.

Automatic reinitiation changing the distribution parameters makes it possible to process all the necessary cases.

2.2. Computations Within the Lower Limit Law $\alpha_m = 0.2$

In this case use of the Rayleigh theory is justified (cf. 2.2.2, Part 2); this theory is shown in Table 1 below, where a comparison is made of computations of i_T by Mie theory and by Rayleigh theory, for $\alpha = 0.2$ and $\theta = 0°$ (as an example). Under these conditions the intensity functions are written (cf. Eq. (2.15), Section 2.2.2. and Eq. (2.31), Section 2.2.10):

$$i_1(\theta) = \alpha^6 \Lambda^2 , \quad i_2 = \alpha^6 \Lambda^2 \cos^2\theta \quad \text{and} \quad Q = (8/3)\ \alpha^4 \Lambda^2$$

The integrals may be rigorously calculated from the arbitrary size 0 up to 0.2, in order to evaluate the maximum error, when the distribution is expressed by a power law (or an exponential law). The expressions:

$$\Lambda^2 \int_0^{0,2} \alpha^6 \left|\frac{1}{\cos^2\theta}\right| \alpha^{-m}\, d\alpha \quad \text{and} \quad (8/3)\,\Lambda^2 \int_0^{0,2} \alpha^4 \cdot \alpha^2 \cdot \alpha^{-m}\, d\alpha ,$$

corresponding to (1) and (2) are computed. With the exception of the factors, the resultant value is: $\frac{1}{7-m} \left|\alpha^{7-m}\right|_0^{0,2}$

which has a finite value if $m > 7$ (cf. Part 2, Section 3.2.2). As Table 1 shows, these quantities are always negligible in comparison to those computed between 0.2 and 200. (It was assumed for these computations that there was a particle corresponding to $\alpha = 1$ and that the exponent m of distribution was 3.9.)

TABLE 1

a Indice	i_T (0°) ($\alpha = 0,2$) Rayleigh	Mie	Q(α) ($\alpha = 0,2$) Rayleigh	Mie	$\int_0^{0,2} i(0)\alpha^{-m}d\alpha$	$\int_{0,2}^{200} i(0)\alpha^{-m}d\alpha$	$\int_0^{0,2} / \int_{0,2}^{200}$
					m = 3,9		%
1,02	0,1130 10^{-7}	0,1131 10^{-7}	0,75 10^{-6}	1,0 10^{-6}	0,0102 10^{-4}	0,162	0,006
1,05	0,6986 "	0,7001 "	4,66 "	5,0 "	0,0744 "	0,369	0,02
1,075	1,5567 "	1,5619 "	10,31 "	10,0 "	0,165 "	0,534	0,03

Key: a. Index

TABLE 2

a Exposant	$\int_0^{100}$	$\int_{100}^{\infty}$
-3,6	93,0	7,0 %
-3,8	97,4	2,6 %
-4,0	99,0	1,0 %
-4,5	99,35	0,65 %
b Gausso log.	90 % c pour	$\int_0^{5,5}$
Expon.	90 % c pour	$\int_0^{8,1}$

Key: a. Exponent
b. Gaussian-log
c. For

2.3. Computations Beyond Upper Limit

This problem is presented in Part 2 (Section 3.2.3). Using the factor ρ rather than α, and assuming Q to be constant and equal to 2 if $\rho > 100$, integration of $Q(\rho)\rho^{2-m}$ from 100 to ∞ is immediately calculable and yields the asymptotic values sought. One thus obtains the ratios of a few exponential values to the total value given in Table 2, expressed as a percentage; this table also shows the values for ρ corresponding to 90% of the total scattering with the log-normal and exponential distributions considered.

REFERENCES

1. Bauer, D., and Morel, A., "Etude aux petits angles de l'indicatrice de diffusion des eaux de mer," Ann. Geophys. 23/1, 109 (1967).

2. Bauer, D., and Ivanoff, A., "Description d'un diffusiomètre "intégrateur," Cah. Océanogr. 23/9, 827 (1971).

3. Beardsley, G.F., Jr., "Mueller scattering matrix of sea water," J. Opt. Soc. Am. 58/1, 52 (1968).

4. Beardsley, G.F., Pak, H., Carder, K., and Lundgren, B., "Light scattering and suspended particles in the Eastern Equatorial Pacific Ocean," J. Geophys. Res. 75/15, 2837 (1970).

5. Briggs, R.O., and Hatchett, G.L., "Technique for improving underwater visibility with video equipment," Ocean Sci. Engin. 1, 1234 (1965).

6. Brown, O.B., and Gordon, H.R., "Tables of Mie scattering functions for low index particles suspended in water," Univ. of Miami Dept. of Phys. Report, ref. MIAPH-OP, 715 pp. (1972).

7. Brun-Cottan, J.C., "Etude de la granulométrie des particules. Mesures effectuees avec un Coulter Counter," Cah. Océanogr. 23/2, 193 (1971).

8. Burt, W.V., "Interpretation of spectro-photometer readings on Chesapeake Bay waters," J. Mar. Res. 14/1, 33 (1955).

9. Burt, W.V., "A light scattering diagram," J. Mar. Res. 15/1, 5 (1956).

10. Carder, K.L., Beardsley, G.F., Jr., and Pak, H., "Particle size distribution in the eastern equatorial Pacific," J. Geophys. Res. 76, 5070 (1971).

11. Carder, K.L., Domlinson, R.D., and Beardsley, G.F., "A technique for the estimation of indices of refraction of marine phytoplankters," Limnol. Oceanogr. 17/6, 833 (1972).

12. Cohen, G., and Eisenberg, H., "Light scattering of water, deuterium oxide, and other pure liquids," J. Chem. Phys. 43/3, 914 (1965).

13. Copin, C., and Copin, G., "Chemical analysis of suspended particulate matter collected in the northeast Atlantic," Deep Sea Res. 19, 445 (1972).

14. Copin, C., and Copin, G., "Etude chimique des particules en suspension dans l'eau de mer en Méditerranée occidentale," J. Thalass. Jugoslav. (1973) (forthcoming).

15. Debye, P., Ann. Physik 30, 59 (1909).

16. Deirmendjian, D., Clasen, R., and Viezee, W., "Mie scattering with complex index of refraction," J. Opt. Soc. Am. 51/6, 620 (1961).

17. Deirmendjian, D., "Scattering and polarization properties of polydispersed suspensions with partial absorption," in Electromagnetic Scattering, edited by Milton Kerker, Pergamon Press, 1963, pp. 171-189.

18. Deirmendjian, D., Electromagnetic Scattering on Spherical Polydispersions, American Elsevier Publishing Co., Inc., 1969, 290 pp.

19. Duntley, S.Q., "Light in the sea," J. Opt. Soc. Am. 53, 214 (1963).

20. Gilbert, G.D., Pernicka, J.C., "Improvement of underwater visibility by reduction of backscatter with a circular polarization technique," SPIE, Underwater Photo-Optics Seminar Proceedings, Santa Barbara, California, 1966.

21. Gordon, D.C., "Some studies on the distribution and composition of particulate organic carbon in the Atlantic Ocean," Deep Sea Res. 17, 233 (1970).

22. Gordon, H.R., and Brown, O.B., "A theoretical model of light scattering by Sargasso Sea particulates," Limnol. Oceanogr. 17/6, 826 (1972).

23. Harris, J.E., "Characterization of suspended matter in the Gulf of Mexico. I. Spatial distribution," Deep Sea Res. 19/10, 712 (1972).

24. Hinzpeter, H., "Messungen der Streufunktion der Polarisation des Meerwassers," Kieler Meeresforsch. 28/1, 36 (1962).

25. Hobson, L.A., "The seasonal and vertical distribution of suspended particulate matter in an area of the Northeast Pacific Ocean," Limnol. Oceanogr. 12/4, 642 (1967).

26. Hodkinson, J.R., "Light scattering and extinction by irregular particles larger than the wavelength," in Electromagnetic Scattering, edited by Milton Kerker, Pergamon Press, 1963.

27. Holland, A.C., and Gagne, G., "The scattering of polarized

light by polydispersed systems of irregular particles," Appl. Opt. 9/5, 1113 (1970).

28. Hulburt, E.O., "Optics of distilled and natural waters," J. Opt. Soc. Am. 35, 698 (1945).

29. Ivanoff, A., "Quelques résultats concernant les propriétés diffusantes des eaux de mer," U.G.G.I. Monograph 10, 45-51 (1961).

30. Ivanoff, A., and Morel, A., "Terminologie concernant l'optique océanographique," Cah. Océanogr. 22/5, 457 (1970).

31. Ivanoff, A., "Introduction à l'océanographie (Introduction to Oceanography), Vol. I, Paris, Vuibert Publishing, 208 pp.

32. Jerlov, N.G., "Particle distribution in the ocean," Rep. Swed. Deep Sea Expedition 3, 73 (1953).

33. Jerlov, N.G., "Optical measurements in the Eastern North Atlantic," Medd. Oceanogr. Inst. Göteborg 38/11, 4 (1961).

34. Jerlov, N.G., "Optical oceanography," Oceanogr. Mar. Biol. Ann. Rev. 1, 89 (1963).

35. Jerlov, N.G., Optical Oceanography, Amsterdam, Elsevier, 1968, 194 pp.

36. Junge, C.E., Air Chemistry and Radioactivity, New York, Academic Press, 1963, 382 pp.

37. Kattawar, G.W., and Plass, G.N., "Electromagnetic scattering from absorbing spheres," Appl. Opt. 6/8, 1377 (1967).

38. Kinney, P.J., Loder, T.C., and Groves, J., "Particulate and dissolved organic matter in the Amerasian Basin of the Arctic Ocean," Limnol. Oceanogr. 16/1, 132 (1971).

39. Kozlianinov, M.V., "Nouvel instrument pour la mesure des propriétés optiques des eaux de mer," Trud. Inst. Okeanol. Akad. Nauk. SSSR 25, 134 (1957).

40. Kullenberg, G., "Scattering of light by Sargasso Sea water," Deep Sea Res. 15/4, 423 (1968).

41. Kullenberg, G., "Light scattering in the central Baltic," Copenhagen Univ., Inst. Phys. Oceanogr., Rep. No. 5 (1969).

42. Kullenberg, G., "Observations of light scattering in different water masses," Electromagnetics of the Sea, AGARD Conf. Proceed. No. 77, Paris (1970).

43. Kullenberg, G., and Olsen, N.B., "A comparison between observed and computed light scattering functions," Copenhagen Univ., Inst. Phys. Oceanogr., Rep. No. 19 (1972).

44. Lisitsin, A., and Bogdanov, Y., "Granulométrie et composition de la matière en suspension dans l'océan Pacifique (en russe)," Oceanogr. Res. Coll. 18, 53 (1968).

45. Mankovsky, V.I., Semenikkine, V.M., and Neuimin, O.G., "Diffusiomètre marin," Akad. Nauk. Ukr. SSR, Inst. Hydrophys. Mar. 2/48, 171 (1970).

46. Mankovski, V.I., "Relations entre coefficient total et coefficients angulaires de diffusion," Akad. Nauk. Ukr. SSR, Mar. Hydrophys. Inst. 6/65, 145 (1971).

47. Mie, G., "Beiträge zur optik trüber Medien speziell kolloidalen Metallösungen," Ann. Physik. 25, 377 (1908).

48. Morel, A., "Interprétation des variations de la forme de l'indicatrice de diffusion de la lumière par les eaux de mer," Ann. Geophys. 21/2, 281 (1965).

49. Morel, A., "Etude expérimentale de la diffusion de la lumière par l'eau, les solutions de chlorure de sodium et l'eau de mer optiquement pures," J. Chim. Phys. 10, 1359 (1966).

50. Morel, A., "Etude à diverses longueurs d'onde de l'indicatrice de diffusion pour les eaux de mer," Proc. Verb. 10, AISPO/IUGG, 14th Gen. Ass., Berne, 1967, pp. 204-205.

51. Morel, A., "Note au sujet des constantes de diffusion de la lumière pour l'eau et l'eau de mer optiquement pures," Cah. Océanogr. 20/2, 157 (1968 a).

52. Morel, A., "Relations entre coefficients angulaires et coefficient total de diffusion de la lumière pour les eaux de mer," Cah. Océanogr. 20/4, 291 (1968 b).

53. Morel, A., "Examen des résultats expérimentaux concernant la diffusion de la lumière par les eaux de mer," Electromagnetics of the Sea, AGARD Conf. Proceed. No. 77, Paris, 1970.

54. Morel, A., "Application de la théorie de Mie au calcul de l'indicatrice de diffusion de la lumière pour les eaux de mer," C.R. Acad. Sci. 274, 1387 (1972 a).

55. Morel, A., "Au sujet de l'emploi du coefficient total de diffusion pour évaluer la teneur des eaux de mer en particules

en suspension," C.R. Acad. Sci. 247, 1447 (1972 b).

56. Morel, A., "Indicatrices de diffusion theoriques calculees par la theorie de Mie appliquee a des systemes polydisperses de particules," Villefranche-sur-Mer Oceanographic Research Center Report No. 10 (1973).

57. Morel, A., "Optical properties of pure water and pure seawater," in Optical Aspects of Oceanography, Academic Press (forthcoming).

58. Morrison, R.E., "Experimental studies on the optical properties of sea water," J. Geophys. Res. 75/3, 612 (1970 a).

59. Morrison, R.E., "Characteristics of the optical volume scattering function of sea water," J. Oceanogr., Soc. Japan 26/2, 101 (1970 b).

60. Nyffeler, F., "Etude de la diffusion de la lumière a diverses longueurs d'onde à l'aide de sources classiques et de sources laser," Paris, Third Cycle Thesis, 1969, 83 pp.

61. Nyffeler, F., "Etude de la diffusion de la lumiere aux petits angles par l'eau de mer," Electromagnetics of the Sea, AGARD Conf. Proceed. No. 77 (1970).

62. Otchakovski, Y.E., "Comparaison des indicatrices mesurées et calculées pour l'eau de mer," Trud. Inst. Okeanol. Akad. Nauk. SSSR 77, 125 (1965 a).

63. Otchakovski, Y.E., "Relations entre coefficient d'extinction et matière en suspension dans la mer," Trud. Inst. Okeanol. Akad. Nauk. SSSR 77, 35 (1965 b).

64. Pak, H., Zaneveld, J.R., and Beardsley, G.F., Jr., "Mie scattering by suspended clay particles," J. Geophys. Res. 76/21, 5065 (1971).

65. Penndorf, R., and Goldberg, B.,"Geophysical Research Papers," Air Force Cambridge Research Center, Rep. 45, 3, Bedford, Mass., 1956.

66. Penndorf, R., "Geophysical Research Papers," Air Force Cambridge Research Center, Rep. RAD-TR 60-10, Bedford, Mass., 1960.

67. Perrin, F., "Polarization of light scatter by isotropic opalescent media," J. Chem. Phys. 10, 415 (1942).

68. Perrin, F., and Abragam, A., "Polarisation de la lumière diffusée par les particules sphériques," J. Phys. et Rad.

12/2, 69 (1951).

69. Petzold, T.J., "Volume scattering functions for selected ocean waters. Visibility," San Diego, California, SIA Technical Report Ref. 72-78, 1972, 79 pp.

70. Physical Oceanography Research Team, "Results of Observations Made in 1964, 1965, 1966 and 1967," Cah. Océanogr. 21, Suppl. 2, 193 (1969).

71. Pickard, G.L., and Giovando, L.F., "Some observations of turbidity in British Columbia inlets," Limnol. Oceanogr. 5, 162 (1960).

72. Preisendorfer, R.W., "Radiative transfer on discrete space," in Pure and Applied Mathematics, Vol. 74, Pergamon Press, 1965, 462 pp.

73. Prieur, L., and Morel, A., "Etude théorique du régime asymptotique, relations entre caractéristiques optiques et coefficient d'extinction," Cah. Océanogr. 23/1, 35 (1971).

74. Reese, J.W., and Tucker, S.P., "Light measurements off the San Diego coast," N.U.C. Technical Publication No. 203, 1970, 37 pp.

75. Riley, G.A., "Particulate organic matter in sea water," Adv. Mar. Biol. 8, 1 (1970).

76. Sasaki, T., Okami, N., Oshiba, G., and Watanabe, S., "Angular distribution of scattered light in deep sea water," Rec. Oceanogr. Works. Jap. 5/2, 1 (1960).

77. Sasaki, T., "Angular distribution of scattered light in deep sea water," Proc. Verb. 10, 203, AISPO/IUGG, 14th Gen. Ass., Berne, 1967.

78. Sasaki, T., Okami, N., and Matsumura, S., "Scattering functions for deep sea water of the Kuroshio," La mer 6/3, 165 (1968).

79. Sheldon, R.W., and Parsons, T.R., "A continuous size spectrum for particulate matter in the sea," J. Fish. Res. Bd. Canada 24, 909 (1967).

80. Sheldon, R.W., and Sutcliffe, W.H., Jr., "Retention of marine particles by screens and filters," Limnol. Oceanogr. 14/3, 441 (1969).

81. Sheldon, R.W., Prakash, A., and Sutcliffe, W.H., Jr., "The

size distribution of particles in the ocean," Limnol. Oceanogr. 17/3, 327 (1972).

82. Spilhaus, A.F., "Observations of light scattering in sea water," Limnol. Oceanogr. 13, 418 (1968).

83. Stratton, J.A., and Houghton, H.G., "A theoretical investigation of the transmission of light through fog," Phys. Rev. 38, 159 (1931).

84. Tyler, J.E., "Scattering properties of distilled and natural waters," Limnol. Oceanogr. 6, 451 (1961).

85. Van de Hulst, H.C., Light Scattering by Small Particles, John Wiley & Sons, Inc., 1957, 470 pp.

86. Wells, H.G., and Todd, M.N., "Loss of optical resolution in sea water by multiple small angle scattering," Electromagnetics of the Sea, AGARD Conf. Proceed. No. 77, Paris, 1970.

87. Williams, J., "Optical properties of the sea," United States Naval Inst. Oceanogr. Series, 1970, 123 pp.

88. Yentsch, C.S., "A non-extractive method for the quantitative estimation of chlorophyll in algal cultures," Nature 179, 1302 (1957).

89. Zaneveld, J.R.V., and Pak, H., "Method for the determination of of the index of refraction of particles suspended in the ocean," J. Opt. Soc. Am. 63/3, 321 (1973).